KTH Chemical Science and Engineering

Novel Porous Films from Functional and Biocompatible Linear-Dendritic Hybrids

Marie V. Walter

KTH Royal Institute of Technology
School of Chemical Science and Engineering
Dept of Fibre and Polymer Technology

Akademisk avhandling

Som med tillstånd av Kungliga Tekniska Högskolan i Stockholm framlägges till offentlig granskning för avläggande av teknisk doktorsexamen fredagen den 19:e april 2013, kl 10:00 i sal F3, Lindstedtsvägen 26, KTH, Stockholm. Avhandlingen försvaras på engelska. Fakultetsopponent: Professor Steve P. Rannard från University of Liverpool (UK).

Stockholm 2013

"If we knew what it was we were doing, it would not be called research, would it?"
Albert Einstein

TRITA-CHE-Report 2013:15
ISSN 1654-1081
ISBN 978-91-7501-691-7

ABSTRACT

In the last decades, the fabrication of ordered nano- and microporous structures has attracted increasing interest due to their specific properties and multiple possible applications in electronics, as templates or in the biological field. The development of such materials has been favored by the introduction of the simple breath-figure templating method in the 1990's. In order to fully exploit the potential of these porous materials, the use of advanced functional molecules as precursors is essential. One suitable class of molecules is the well-defined linear-dendritic hybrids (LD hybrids) family. The structural variations, multiple end-groups and possible amphiphilicity of these molecules are significant advantages that could lead to highly sophisticated functional materials with potential usage in biology. Therefore, this project was directed towards the synthesis of advanced LD hybrids and the evaluation of their ability to form ordered functional porous films.

A degradation and toxicity study was initially conducted on polyester-based 2,2-bis(methylol)propionic acid (bis-MPA) dendrimers under physiological conditions to support the potential usage of these molecules for biological purposes. The materials were found to undergo a relatively fast depolymerization process at pH 7.5. Moreover, the initial dendrimer and its decomposition products were proven to be non-toxic for immune competent cells, allowing for the utilization of these molecules for biological applications.

A linear-dendritic-linear hybrid library was successfully synthesized from biocompatible poly(ethylene glycol) (PEG), poly(ε-caprolactone) (PCL) and bis-MPA building blocks using a combination of ring-opening polymerization (ROP)and copper(I)-catalyzed azide-alkyne cycloaddition (CuAAC). The materials, consisting of one long PEG block connected to the focal point of the dendron and several PCL arms attached at its periphery, were used to construct ordered porous films using the breath figure method. The polymeric architecture strongly affected the ordering of the films with a more regular morphology obtained from a more flexible polymer. Changing the semi-crystalline PCL to amorphous polylactide (PLA) also permitted the formation of porous arrays. Interestingly, films obtained from inverted structures possessing one long PCL block and several short PEG chains, also presented a regular morphology. Moreover they could be activated to exhibit multiple surface hydroxyl groups.

To increase the number of orthogonal synthetic methodologies available for the preparation of advanced macromolecules, high molecular weight dendritic macrothiols were synthesized. These molecules were efficiently coupled to a number of core molecules via thiol-ene coupling, generating a comprehensive library of dendritic materials. This approach represents an attractive alternative to the commonly used, but potentially toxic, CuAAC.

Exploiting the obtained results, a final LD hybrid was synthesized from atom transfer radical polymerization (ATRP) of 2-hydroxyethyl methacrylate (HEMA) derivatives and thiol-ene coupling (TEC) with macrothiols. This macromolecule was successfully utilized to form functional ordered porous arrays and the availability of peripheral alkyne functional groups was demonstrated by efficient coupling with fluorescent Rhodamine-B. The HEMA-backbone allowed for the introduction of cross-linkable azide groups that were used to significantly improve the thermal stability of the films from 50 °C to 200 °C. These materials have the potential to be used in applications such as catalysis, in medicine and as sensors.

SAMMANFATTNING

Under de senaste decennierna har intresset för ordnade nano- och mikroporösa strukturer ökat då dessa strukturer har specifika egenskaper och därmed kan användas i en rad olika applikationer, bland annat inom elektronik och biotekniska tillämpningar. Introduktionen av ”breath figure” metoden i slutet av nittonhundratalet har underlättat utvecklingen av dessa material. För att maximalt dra nytta av dessa strukturer, är det nödvändigt att använda funktionella molekyler som startmaterial. Linjära-dendritiska (LD) hybrider är lämpliga startmaterial eftersom de kan byggas i olika kombinationer, har många ändgrupper och kan vara amfifila. Därmed kommer detta arbete att fokusera på syntes av multifunktionella LD hybrider från biokompatibla byggstenar samt analys av porösa filmer framställda av dessa material.

I hela studien används 2,2-bis(metylol)propionsyra (bis-MPA) som dendritisk byggsten. Därför utvärderades dess nedbrytning och toxicitet under fysiologiska förhållanden. Vid pH 7.5 depolymeriserar materialen snabbt och monomerer frigörs. Varken dendronen eller monomeren uppvisade någon toxisk aktivitet mot makrofager *in vitro* vilket möjliggör användning inom biologiska områden.

Linjära-dendritiska-linjära hybrider syntetiserades framgångsrikt från biokompatibla poly(etylenglykol) (PEG), poly(ε-kaprolakton) (PCL) och bis-MPA via ringöppningspolymerisation och koppar(I)-katalyserad azid-alkyn cykloadditionskemi (CuAAC). Biblioteket som byggdes upp bestod av dendroner från första till fjärde generationen, funktionaliserade med en PEG kedja i kärnan samt PCL av olika längder i periferin så att samtliga molekyler skulle ha en liknande molekylvikt. Dessa material användes för att framställa porösa filmer. Filmernas porositet visade sig vara starkt beroende av polymerens arkitektur: den mest flexibla hybriden, som innehöll en dendron av tredje generationen, formade välordnade filmer. Isoporösa filmer kunde också framställas genom att byta ut delkristallin PCL mot amorf poly(laktid). För att vidare studera effekten av arkitekturen, byggdes en inverterad struktur med en dendron av tredje generationen funktionaliserad med en lång PCL kedja i kärnan och korta PEG kedjor i änden. Denna hybrid gav också upphov till välordnade filmer med hydroxylgrupper tillgängliga för vidare modifieringar.

Dendritiska tioler med hög molekylvikt syntetiserades därefter för att kunna framställa mer avancerade strukturer genom att öka antalet ortogonala byggstenar. Dessa makrotioler kopplades framgångsrikt till olika allyl-funktionella kärnor via tiol-ene kemi (TEC) och ett komplett bibliotek av dendritiska polymerer erhölls. Denna strategi är ett intressant alternativ till det potentiellt toxiska CuAAC.

Slutligen syntetiserades en alkyn-funktionell LD hybrid via atom transfer radical polymerisation (ATRP) från ett 2-hydroxyethyl metakrylat (HEMA) derivat och TEC koppling med en makrotiol. Porösa filmer bildades framgångsrikt av detta material och alkyngrupperna kunde lätt modifieras via CuAAC med en azid-funktionell fluorescerande rhodamine-B. Efter funktionaliseringen av HEMAs sidogrupper med azider samt tvärbindning av filmerna med UV, erhölls material som var stabila upp till 200 ^{0}C . Dessa funktionella material kan användas i många olika applikationer, bland annat inom katalys, medicin eller som sensorer.

LIST OF PAPERS

This thesis is a summary of the following papers:

I. "Stability and biocompatibility of a library of polyester dendrimers in comparison to polyamidoamine dendrimers", Neus Feliu, Marie V. Walter, Maria I. Montañez, Andrea Kunzmann, Anders Hult, Andreas Nyström, Michael Malkoch and Bengt Fadeel, *Biomaterials*, **2012**, 33, 1970-1981.

II. "Linear dendritic polymeric amphiphiles with intrinsic biocompatibility: synthesis and characterization to fabrication of micelles and honeycomb membranes", Pontus Lundberg, Marie V. Walter, Maria I. Montañez, Daniel Hult, Anders Hult, Andreas Nyström and Michael Malkoch, *Polymer Chemistry*, **2011**, 2, 394-402.

III. "A one component methodology for the fabrication of honeycomb films from biocompatible amphiphilic block copolymer hybrids: a linear-dendritic-linear twist", Marie V. Walter, Pontus Lundberg, Daniel Hult, Anders Hult and Michael Malkoch, *Polymer chemistry*, **2013**, DOI: 10.1039/c3py00053b.

IV. "Novel macrothiols for the synthesis of a structurally comprehensive dendritic library using thiol-ene click chemistry", Marie V. Walter, Pontus Lundberg, Anders Hult and Michael Malkoch, *Journal of Polymer Science: Part A. Polymer Chemistry*, **2011**, 49, 2992-2995.

V. "Thermally stable and functional honeycomb films from linear-dendritic hybrids derived from HEMA and bis-MPA", Marie V. Walter, Oliver C. J. Andrén, Hjalmar Brismar and Michael Malkoch, *manuscript*.

My contribution to the appended papers:

I. Part of the experimental work (degradation study) and part of the preparation of the manuscript.

II. Part of the experimental work (honeycomb films) and part of the preparation of the manuscript.

III. Almost all the experimental work and most of the preparation of the manuscript.

IV. Almost all the experimental work and most of the preparation of the manuscript.

V. Almost all the experimental work and most of the preparation of the manuscript.

Other publications not included in this thesis:

VI. "Accelerated growth of dendrimers via thiol-ene and esterification reactions", Maria I. Montañez, Luis M Campos, Per Antoni, Yvonne Hed, Marie V. Walter, Brandon T. Krull, Anzar Khan, Anders Hult, Craig J. Hawker and Michael Malkoch, *Macromolecules*, **2010**, 43, 6004-6013.

VII. "Hybrid one-dimensional nanostructures: one-pot preparation of nanoparticle chains via directed self-assembly of in situ synthesized discrete nanoparticles", Marie V. Walter, Nicolas Cheval, Olimpia Liszka, Michael Malkoch and Amir Fahmi, *Langmuir*, **2012**, 28, 5947-5955.

VIII. "Simplifying the synthesis of dendrimers: accelerated approaches", Marie V. Walter and Michael Malkoch, *Chemical Society Reviews*, **2012**, 41, 4593-4609.

IX. Marie V. Walter and Michael Malkoch (**2012**). "*Accelerated synthesis of dendrimers*". In A. dieter Schlüter, Craig J. Hawker and Junji Sakamoto, Synthesis of polymers: New structures and methods (vol 2, pp. 1027-1055). Weinheim: Wiley-VCH.

X. "Multifunctional polyethylene glycol: synthesis, characterization and potential applications of dendritic-linear-dendritic block copolymer hybrids", Oliver C. J. Andrén, Marie V. Walter, Ting Yang, Anders Hult and Michael Malkoch. Submitted to *Macromolecules*.

ABBREVIATIONS

AFM	Atomic Force Microscopy
Alk	Alkyne
All	Allyl
ATRA	Atom Transfer Radical Addition
ATRP	Atom Transfer Radical Polymerization
BF	Breath Figure
Bipy	2,2'-Bipyridyl
Bis-MPA	2,2-Bis(methylol)propionic acid
CA	Contact Angle
CaH_2	Calcium hydride
$CHCl_3$	Chloroform
Cu(I)Cl	Copper(I) Chloride
$Cu(II)Cl_2$	Copper(II) Chloride
$Cu(II)SO_4$	Copper(II) sulfate
$Cu(PPh_3)_3Br$	Tris(triphenylphosphine)copper(I) bromide
CuAAC	Copper(I) Catalyzed Azide-Alkyne Cycloaddition
DCC	N,N'-Dicyclohexylcarbodiimide
DCM	Dichloromethane
DIPEA	N,N-Diisopropylethylamine
$Đ_m$	Molar mass dispersity
DMAP	4-(Dimethylamino)pyridine
DMF	Dimethylformamide
DMPA	2,2-Dimethoxyphenyl acetophenone
DMSO	Dimethylsulfoxide
DOWEX®	Acidic resin
DP	Degree of Polymerization
DSC	Differential Scanning Calorimetry
DTT	Dithiothreitol
EDTA	Ethylenediaminetetraacetic acid
EtOAc	Ethyl acetate
FE-SEM	Field Emission Scanning Electron Microscopy
Gn	Dendron of generation "n"
HEMA	2-Hydroxyethyl methacrylate
HMDM	Human Monocyte-Derived Macrophages
HO-EBiB	Hydroxyethyl 2'-bromoisobutyrate
k_{act}	Rate constant of activation
k_{deact}	Rate constant of deactivation
k_p	Rate constant of propagation
k_t	Rate constant of termination
LA	Lactide
LD	Linear-Dendritic
LDL	Linear-Dendritic-Linear
LPS	Lipopolysaccharide
MALDI-TOF MS	Matrix-Assisted Laser Desorption/Ionization Time of Flight Mass Spectrometry
MeOH	Methanol
$MgSO_4$	Magnesium sulfate

M_n	Number average molecular weight
MTT	3-(4,5-Dimethylthiazol-2-yl)-2,5-diphenyltetrazolium bromide
N_a	Avogadro number
Na_2CO_3	Sodium carbonate
NaAsc	Sodium ascorbate
$NaHSO_4$	Sodium hydrogen sulfate
NaOH	Sodium hydroxide
NMP	Nitroxide Mediated Polymerization
NMR	Nuclear Magnetic Resonance
PAMAM	Poly(Amidoamine)
PBS	Phosphate Buffered Saline
PCL	Poly(ε-caprolactone)
PEG	Poly(ethylene glycol)
PLA	Poly(lactide)
PPI	Poly(propylene imine)
p-TSA	*p*-toluenesulfonic acid
RAFT	Reversible Addition-Fragmentation Chain-Transfer
RDRP	Reversible-Deactivation Radical Polymerization
R_g	Radius of gyration
RH	Relative Humidity
ROP	Ring-Opening Polymerization
SEC	Size Exclusion Chromatography
$Sn(Oct)_2$	Tin(II)-2-ethylhexanoate
STS	Staurosporine
TBAB	Tetrabutylammonium bromide
TEA	Triethylamine
TEC	Thiol-Ene Coupling
TEG	Tetraethylene glycol
T_g	Glass transition temperature
THF	Tetrahydrofuran
THP	Tetrahydropyranyl
T_m	Melting temperature
TMP	Trimethylolpropane
UV	Ultra Violet
γ	Interfacial tension
ΔH_m	Enthalpy of melting
ε-CL	ε-Caprolactone
ρ	Density

TABLE OF CONTENT

1. PURPOSE OF THE STUDY

With the fast development of nanotechnology, the preparation of advanced functional materials has attracted significant attention from the scientific community. A typical example is the preparation of micro- and nanoporous functional films using the simple breath figure method. Due to their specific properties, these films have numerous potential applications for example in electronics or in the biological field for cell culturing or scaffolding. To fulfill the requirements of such applications, the synthesis of always more sophisticated macromolecules is essential. Therefore, scientists are continuously presenting new classes of materials. One significant breakthrough was the introduction of dendritic polymers and linear-dendritic (LD) hybrids, which possess unique properties. The endless possibilities of combining different linear and dendritic fragments and the facile introduction of amphiphilicity into these macromolecules are significant advantages of these structures. Moreover, considering the multiple end-groups present on the dendritic block together with the tunable amphiphilic character of the molecules, LD hybrids are foreseen as excellent candidates for the fabrication of highly functional porous films via the water-templated breath figure (BF) method.

The general purpose of this study was to synthesize highly functional and stable porous films that could potentially be used for biological applications. Therefore the synthesis of biocompatible macromolecules possessing multiple functional groups as well as moieties allowing for cross-linking, and thus improved stability, of the films was explored. To reach this final goal, several investigations needed to be conducted. In order to permit the synthesis of biocompatible materials, thorough investigation of the biodegradability and toxicity of the building blocks was a prerequisite. Therefore the first study was devoted to an investigation of the degradation profile and *in vitro* toxicity of bis-MPA dendrimers. In parallel, to efficiently tailor the film properties, acquiring a deeper knowledge of the effect of LD hybrid architecture on the formation of ordered porous arrays was essential. Consequently, a comprehensive study was conducted to explore the effect of the dendritic linker, coupling chemistry and physical properties of the hybrids on pore formation. Another investigation was dedicated to the development of new high molecular weight dendritic thiols and their ability to couple to various core molecules via UV-initiated thiol-ene coupling chemistry. This study was performed to provide a facile synthetic methodology, available to access advanced macromolecules in various solvent conditions, as an alternative to the copper(I)-catalyzed azide-alkyne cycloaddition. Finally the aim of the last study was to exploit the previously acquired knowledge to design functional LD hybrids and use them to develop stable and highly functional porous films.

2. INTRODUCTION

2.1 POLYMERS

Natural polymers are present on earth since the appearance of life. In fact, they can be found in many living organisms, for example in the form of DNA, cellulose, collagen, silk or natural rubber. In the 18th century, natural polymers started to be synthetically modified but it is only in 1909 that the first fully synthetic polymer was commercialized under the name of Bakelite (thermosetting phenol formaldehyde resin).[1] Since then the polymer industry has been continuously growing and synthetic polymers are today essential components in our everyday life.

The name polymer is derived from the Greek words *πολύς* ("polus", meaning part) and *μέρος* ("meros", meaning units) and can be translated as "many parts". A polymer is therefore simply the assembly of many units or monomers together into a large molecule. The monomers can be covalently linked to each other in different ways resulting in either linear or branched architectures (Figure 2-1). Moreover different monomers can be combined in a single molecule forming block copolymers, alternating copolymers or random copolymers. Both the composition and the architecture of the polymer strongly affect the properties of the molecule. Therefore tailoring these two parameters is essential to access advanced structures with desired properties such as response to an external stimuli, conductivity or luminescence. While linear or randomly branched polymers are exploited industrially, block copolymers, stars or perfectly branched structures are particularly interesting for fundamental research because of their specific properties.

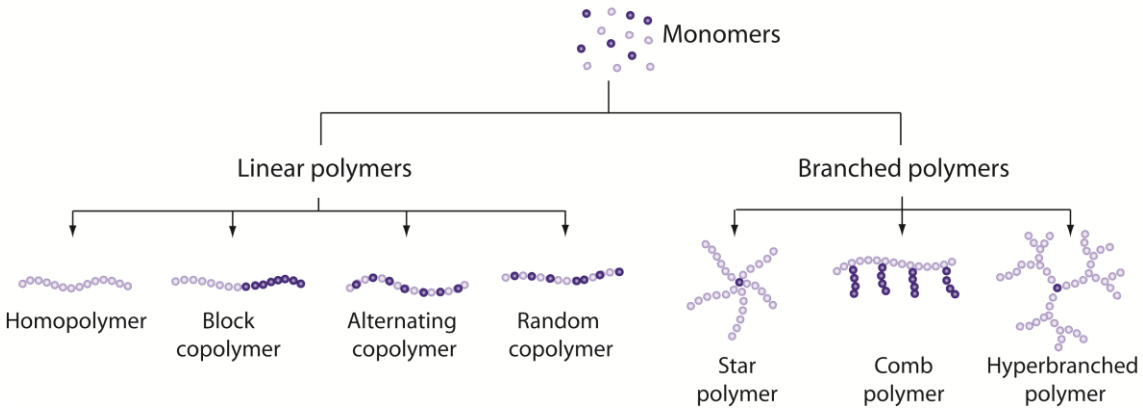

Figure 2-1. Illustration of different polymer architectures and compositions.

2.2 DENDRIMERS

2.2.1 Definition

Dendritic polymers are one of the latest additions to the polymer family. The name dendrimer comes from the greek word "δένδρον" (pronounced "dendron") meaning tree and reflects the highly branched structure of this group of polymers. Dendritic polymers can be divided into monodisperse and polydisperse frameworks (Figure 2-2). Among dendritic polymers, dendrimers and dendrons are particularly interesting structures because of their structural perfection and high number of functional end-groups. In contrast to the other sub-classes of the dendritic family which present molar mass dispersities ($Đ_m$) in the range of 1.1 to 10, dendrimers and dendrons have a perfectly uniform structure and can be isolated as monodisperse compounds.[2]

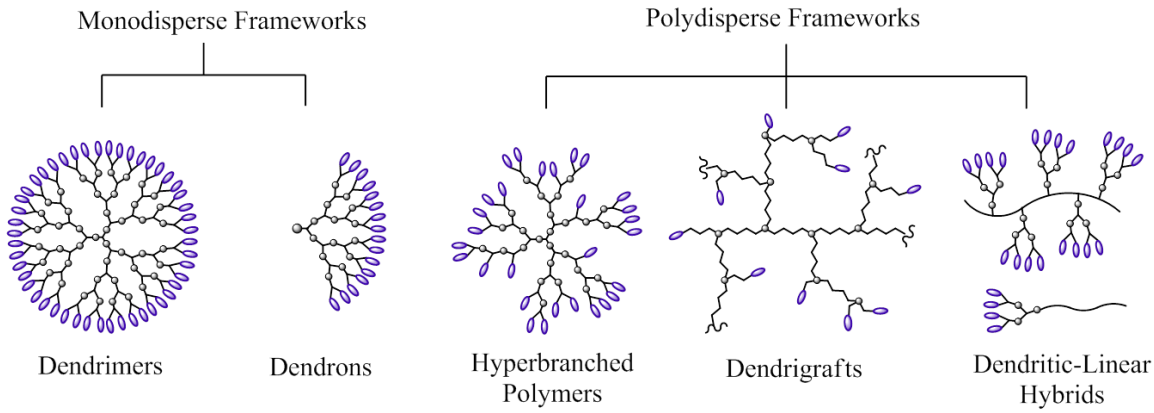

Figure 2-2. The dendritic polymer family.

Dendrimers consist of interconnected multifunctional AB*n* monomers where A and B are two different functionalities and *n* is equal or higher than 2 (Figure 2-3). The three-dimensional structure of a dendrimer is centered on a multifunctional moiety; the core of the dendrimer. Typically, the core possesses 3 or 4 functionalities. The monomers are attached in perfect layers around the core, each layer being called a generation. The same structure is found in dendrons, which are wedges of dendrimers. The external layer of the dendrimer is decorated with activated groups available for further reaction. Traditionally, the inner part of the dendrimer was dormant, but new methods have emerged to synthesize dendrimers with internal functionalities.[3,4]

2.2.2 Synthesis

The first synthesis of a dendritic material was reported in 1978 by Vögtle *et al.* who synthesized a branched polypropylene-amine structure.[5] Their "cascade molecule" was generated by repetitive monomer addition and activation of the branched molecule. Even though the achieved structure was of low molecular weight, this work is today acknowledged as the starting point for research in the dendritic polymer field.

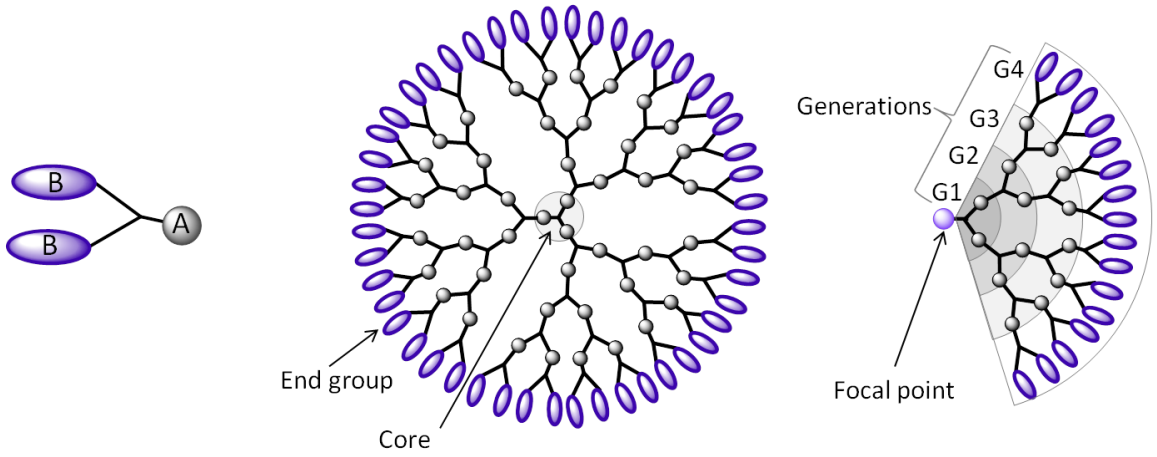

Figure 2-3. Schematic view of a generation four dendrimer and its architectural components.

In 1985, two parallel studies were published by Tomalia *et al.*[6] and Newcome *et al.*[7] who reported the synthesis of poly(amidoamine) (PAMAM) dendrimers and poly(etheramide) arborols respectively. The strategy used in these works, called divergent growth approach, is today one of the most used synthetic pathways towards commercial dendrimers. It initiates dendrimer growth from a multifunctional core and continues outward by repetition of monomer addition and activation steps. The external B functionalities of the monomer are initially deactivated during monomer addition and thereafter activated to enable further growth (Figure 2-4).

Later in the 1990's, the convergent method, which relies on the construction of perfectly branched dendrons that are, in a final step, coupled to a multifunctional core, was introduced by Hawker and Frechet.[8]

To obtain a flawless structure, good control over each reaction step as well as efficient chemical reactions and purification steps are necessary, making dendrimer synthesis using a divergent or convergent approach tedious and time consuming. Therefore, other methods such as the double stage convergent growth, the double exponential growth or the orthogonal growth have been developed more recently to facilitate dendrimer synthesis.[9]

Independently of the employed synthetic strategy, dendrimer growth is restricted by a steric limit known as the De Gennes dense packing. In fact, the number of monomer units increases exponentially with dendrimer growth while the available volume grows at a more slowly pace. Therefore, dendrimers adopt a more globular conformation with increasing generation.[10]

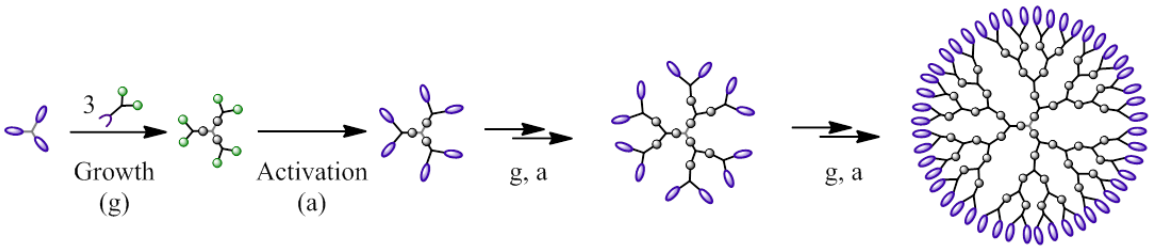

Figure 2-4. Schematic representation of the divergent growth of a generation four dendrimer.

Today, several types of dendrimers have been synthesized and are widely used in fundamental research. These include the commercially available PAMAMs (Dendritech®[11] and Dendritic Nanotechnologies[12]), 2,2,-bis(methylol) propionic acid (Bis-MPA) (Polymer Factory[13]) and poly(propylene imine) (PPI) (Symo-Chem BV[14]) dendrimers. Other well-established structures are the poly(benzylether), arborols and phosphorus dendrimers.

2.2.3 Linear-dendritic hybrid materials

The high number of end-groups and specific properties of dendrimers have been combined with linear polymers to create a new class of materials, the linear-dendritic hybrids (Figure 2-2). Depending on the relative position of the linear and dendritic blocks, a variety of architectures can be achieved such as LD, LDL, DLD, $(LD)_n$, L_nD where L symbolizes a linear block and D a dendritic structure (Figure 2-5). To preserve the advantages inherent to the monodisperse character of the dendron or dendrimer, efficient coupling chemistries as well as controlled polymerization techniques are required. An unlimited variety of well-defined architectures can thereby be achieved with tailored properties. This approach represents an elegant way towards the synthesis of amphiphilic macromolecules. Nowadays, linear-dendritic hybrids have shown promises for applications as nanoreactors, in catalysis, and in the biomedical field.[15-17]

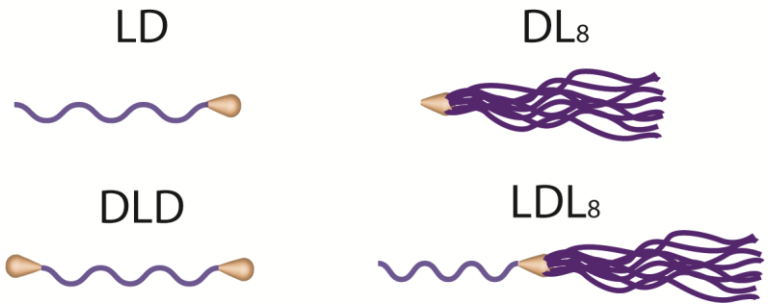

Figure 2-5. Examples of typical linear-dendritic hybrid structures (not to scale).

2.2.4 Biological applications and toxicity of dendrimers

The compact structure of dendrimers gives rise to specific properties such as low intrinsic viscosity and improved solubility as compared to linear analogs of identical molecular

weights. These properties originate from the limited entanglement of the polymer chains. Moreover, their globular structure and inherent cavities can be exploited to encapsulate molecules, leading to applications in light-harvesting, catalysis or drug delivery.[18, 19]

To exploit the specific properties of dendrimers, biological purposes, such as nanomedicine or cancer therapy, are particularly suitable since the relatively high cost of these advanced molecules does not represent an obstacle for such specific applications. Therefore, several studies have been conducted on the subject using the commercially available PAMAM, PPI and bis-MPA structures.[19-22] However a critical requirement for biological usage is the biocompatibility of the system. While PPIs and PAMAMs are cytotoxic[23], bis-MPA dendrimers have proven to be non-toxic and non-invasive[24, 25] and hence are excellent candidates for biomedical applications.

2.3 CLICK-CHEMISTRY AND EFFICIENT COUPLING REACTIONS

2.3.1 Click chemistry

The concept of click chemistry was introduced in 2001 by Sharpless and coworkers[26] and has had substantial impact in many fields, as revealed by the high number of reviews published on the subject.[27-31] In order for a reaction to be classified as "click", a number of criteria need to be fulfilled such such as being highly efficient, wide in scope, tolerant to other functional groups and forming stable compounds with no or few bi-products. These requirements can be achieved because of a high thermodynamic driving force, usually greater than 20 kcal/mol, associated with click reactions. Therefore click reactions were also described as being "spring-loaded for a single trajectory" since they process rapidly towards a single product.

While Sharpless originally envisioned applications of click chemistry for the synthesis of biologically active molecules, the concept has also had a significant impact in the field of polymer science.[32] Actually in polymer chemistry, the efficiency of click reactions, the lack of byproducts and the simple purification by precipitation have presented strong advantages for the synthesis of advanced macromolecular architectures which would not have been achievable with classic chemical reactions. However, the requirements of click chemistry have been revised when applied to polymer synthesis and conjugation reactions.[33] For instance, in polymer-polymer conjugations, equimolarity is of critical importance since the separation of polymers of similar structures is difficult to perform. Moreover, the starting materials must be readily available or easily synthesized and the reaction must proceed under simple reaction conditions, ideally in the presence of oxygen and water.

Nowadays, a number of reactions has been classified as "click reactions", as initially described by Sharpless. These include i) the cycloaddition of unsaturated species, especially 1,3-dipolar cycloaddition reactions but also Diels-Alder transformations, ii) nucleophilic substitution chemistry, particularly ring-opening reactions of strained heterocyclic electrophiles, iii) carbonyl chemistry of the "non-aldol" type and iv) addition to carbon-

carbon multiple bonds, especially oxidative cases such as epoxidation but also Michael addition of Nu-H reactants.[26]

2.3.2 Copper(I)-catalyzed azide-alkyne cycloaddition (CuAAC)

The non-catalyzed azide-alkyne reaction was already introduced in 1893 when the first synthesis of 1,2,3-triazoles from diethyl acetylenedicarboxylate and phenyl azide was presented by Michael *et al.*[34] This reaction, also known as the Huisgen reaction because of the wide study performed by Huisgen *et al.* on 1,3 dipolar cycloadditions in the middle of the 20th century[35], produces a mixture of 1,4 and 1,5 disubstituted products (Scheme 2-1). Later in 2002, two parallel studies of Fokin and Sharpless[36] and Meldal *et al.*[37] reported the first synthesis of a selective 1,4-disubstituted triazole using copper (I) catalyst for the azide-alkyne cycloaddition. This reaction is now usually referred to as the copper(I)-catalyzed azide-alkyne cycloaddition (CuAAC).

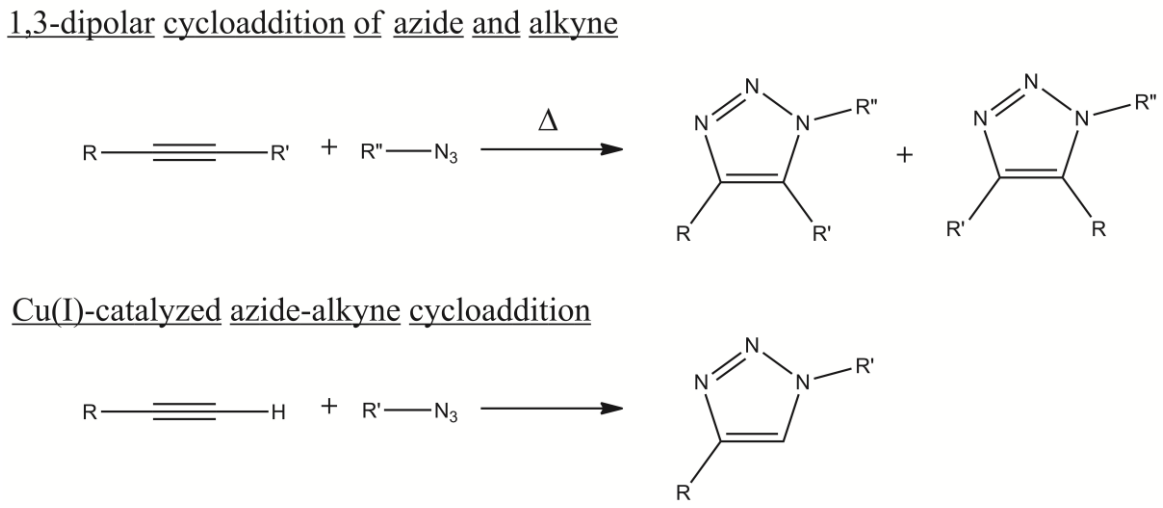

Scheme 2-1. Overview of the thermal 1,3-cycloaddition and CuAAC reactions.[38]

The reaction mechanism was proposed by Fokin and Finn in 2007 (Scheme 2-2).[39] A large variety of copper catalysts can be used for this type of reaction provided that Cu(I) is generated. To facilitate the reaction, the concentration of Cu(I) catalyst must be kept at its maximum. The catalyst can originate from a Cu(II) pre-catalyst together with a reducing agent, from a Cu(I) catalyst associated with a base or amine ligand and a reducing agent or from a Cu(0) compound (such as a wire), the surface of which forms the required Cu(I) catalyst. Since the toxicity of copper can be an obstacle for biological applications, copper-free variations such as stain-promoted alkyne-azide cycloaddition have been developed.[40, 41] For a more detailed overview of the catalytic systems used in CuAAC, the reader is encouraged to read one of the many reviews published on the subject.[38, 42-44] Today, the CuAAC is by far the most used of the click reactions and it has been proven to be highly suitable for polymer synthesis.[45]

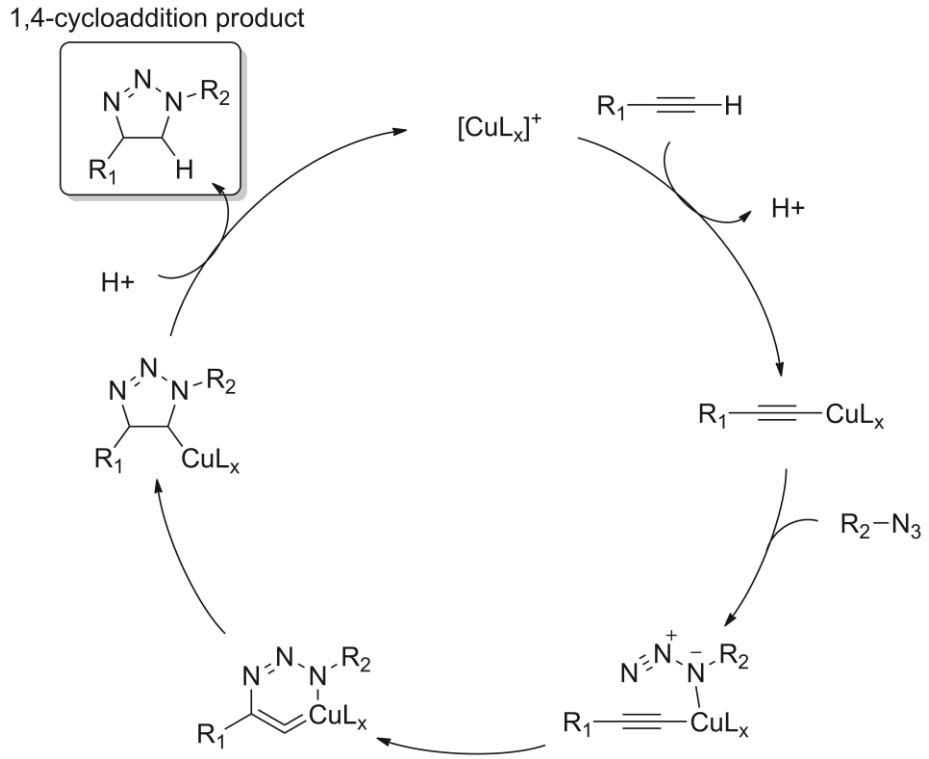

Scheme 2-2. Overview of the mechanism of the CuAAC reaction.[39]

2.3.3 Thiol-ene coupling chemistry (TEC)

Thiol-ene chemistry was first reported by Posner *et al.* in 1905[46] who showed that thiols and enes can react spontaneously or in the presence of an acid. Later, in 1926 it was discovered that allyl mercaptan spontaneously gels upon heating, and this report is considered to be the first example of a thiol-ene polymerization reaction.[47] Attention was then focused on two particular thiol-ene reactions, namely the thiol-ene free-radical addition to electron rich/electron poor carbon-carbon double bonds and the catalyzed Michael addition of thiols to electron deficient carbon-carbon double bonds.[48]

Free-radical thiol-ene chemistry was largely exploited in the last century at an industrial scale, mostly for the production of cross-linked systems. However, this type of chemistry suffered from bad odor of the initiating thiol monomers, yellowing of the product (mostly due to remaining residues of initiator) and rapid weathering. The consecutive introduction of cheap acrylate-based systems led to the abandonment of this system.

The revival of this chemistry is mainly related to the development of new photoinitiators and the incorporation of thiol monomers in acrylic systems to lower oxygen inhibition and improve the final network properties.[49] Due to its high efficiency, the term "click" was recently applied to the thiol-ene reaction and a lot of research work has been devoted to this type of chemistry.[50]

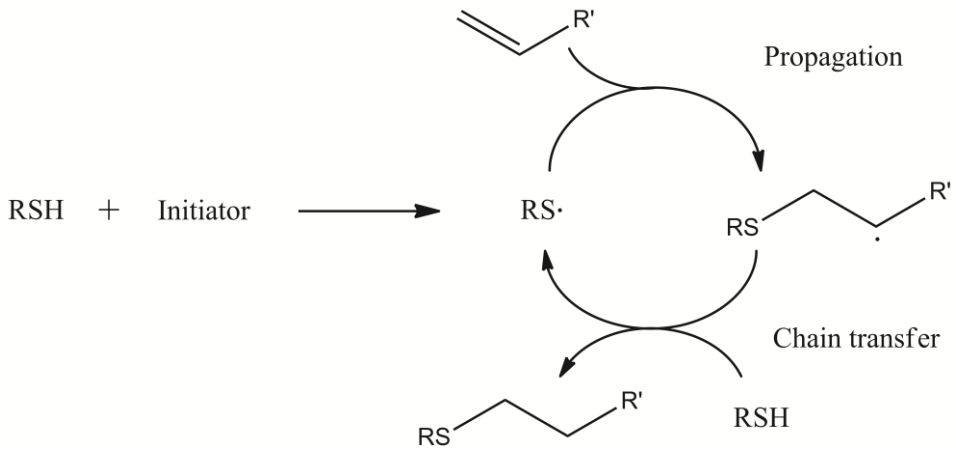

Scheme 2-3. The idealized free-radical thiol-ene reaction.

In general, thiol-ene polymerization is a step growth process involving two steps: addition of the thiyl radical to the carbon-carbon double bond (propagation) and hydrogen abstraction from a thiol group by a carbon-centered radical to regenerate a thyil radical (chain transfer) (Scheme 2-3). The thiol-Michael addition, which undergoes an anionic chain process, follows a similar mechanism with the radicals being replaced by their anionic counterparts.[48] A clear advantage of the thiol-ene coupling reaction in comparison to other classical free-radical polymerizations is the low sensitivity towards oxygen inhibition. The peroxy radicals formed by reaction of a carbon-centered propagating radical with molecular oxygen is able to abstract a thiol hydrogen thus reforming a thiyl radical susceptible to continue the main propagation (Scheme 2-4). However, the final products are different and removal of oxygen prior to reaction is preferred when a well-defined structure is desired.

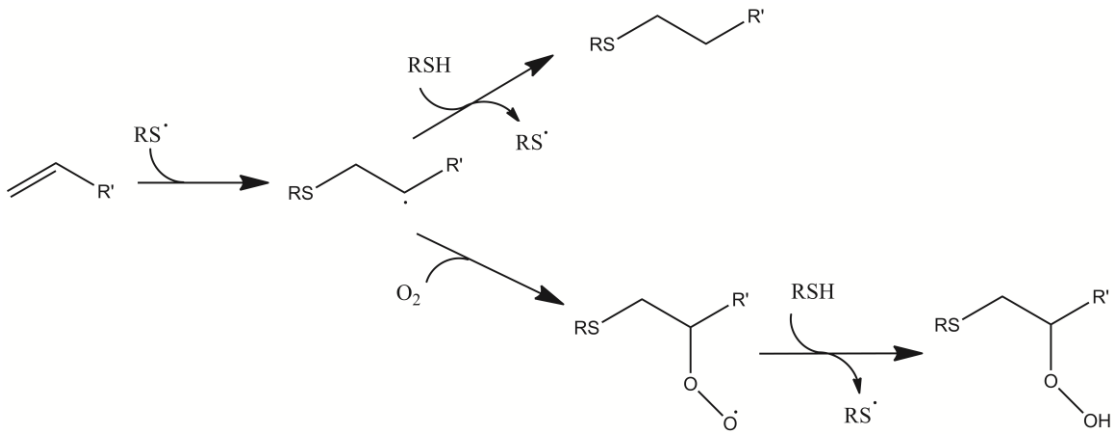

Scheme 2-4. Hydrogen abstraction vs. oxygen-scavenging routes for the free-radical thiol-ene reaction.

The reaction rate is greatly influenced by the structure of the ene involved. Generally, the reactivity of the ene decreases with decreasing electron density of the carbon-carbon double bond. Norbornene, methacrylate, styrene and conjugated dienes are special cases affected by other factors.[49] One significant side reaction in the free-radical thiol-ene system is the homopolymerization of the ene but by appropriately choosing the ene monomer, the thiol-ene reaction can be favored (Figure 2-6).[48, 51] The thiol-Michael addition reaction involves electron-deficient enes such as (meth)acrylates, maleimides, α,β-unsaturated ketones or acrylonitriles and can be catalyzed by strong bases, metals, organometallics or Lewis acids.

Today, the thiol-ene coupling (TEC) has been shown to be suitable for the synthesis of sophisticated macromolecules and polymers.[9, 29, 30, 32] The absence of toxic transition metal catalyst as well as the development of new catalyst-free TEC reactions represent a clear advantage of TEC for biological applications.[52, 53]

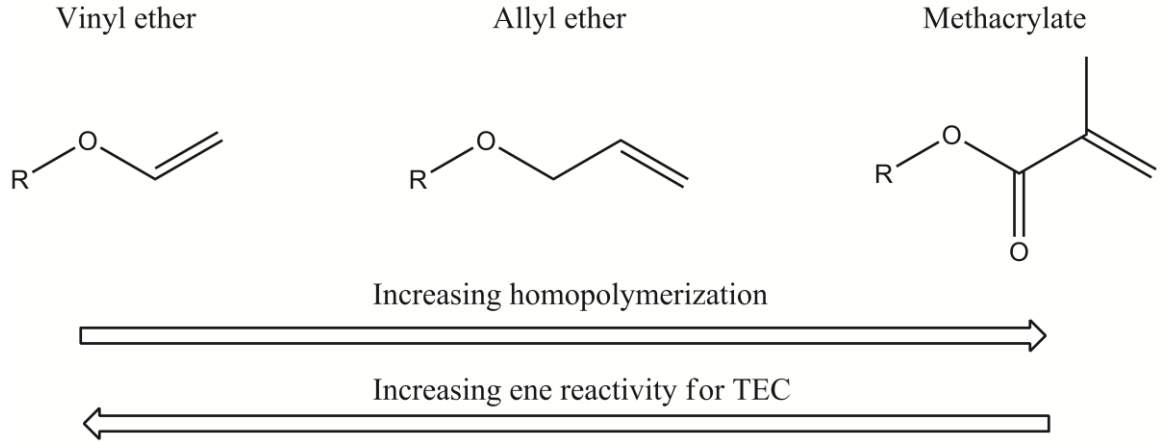

Figure 2-6. Ene monomer reactivity and degree of homopolymerization of the ene monomers.

2.4 CONTROLLED POLYMERIZATION TECHNIQUES

The synthesis of well-defined macromolecules not only requires the use of efficient coupling chemistries but also necessitates good control over polymer chain length and dispersity. This requirement can be fulfilled by the use of controlled polymerization techniques such as ring-opening polymerization (ROP)[54] and reversible-deactivation radical polymerization (RDRP)[55]. The family of RDRP includes nitroxide mediated polymerization (NMP),[56-58] atom transfer radical polymerization (ATRP)[59] and reversible addition fragmentation chain transfer (RAFT)[60, 61] polymerization. From this family, ATRP is the most studied system due to its versatility, compatibility with a wide range of monomers and the commercial availability of different ligands.

2.4.1 Ring-Opening Polymerization of cyclic esters (ROP)

ROP is a useful polymerization technique applicable to a variety of cyclic monomers including lactones, lactides, cyclic carbonates, siloxanes and ethers. While aliphatic polyesters can be synthesized either by traditional polycondensation of alcohols and acids or by ROP of cyclic esters, high molecular weight polyesters are most efficiently synthesized by ROP of lactones or lactides. ROP can proceed through different mechanisms (anionic, cationic, coordination, activated monomer, activated chain end or polymerization in disperse media)[54, 62] among which the coordination-insertion polymerization using tin(II)-2-ethylhexanoate (or tin octoate), $Sn(Oct)_2$, as catalyst is the most common. Advantages of $Sn(Oct)_2$ reside in its high efficiency, relatively low toxicity (approved by the Food and Drug Administration) and commercial availability.[63]

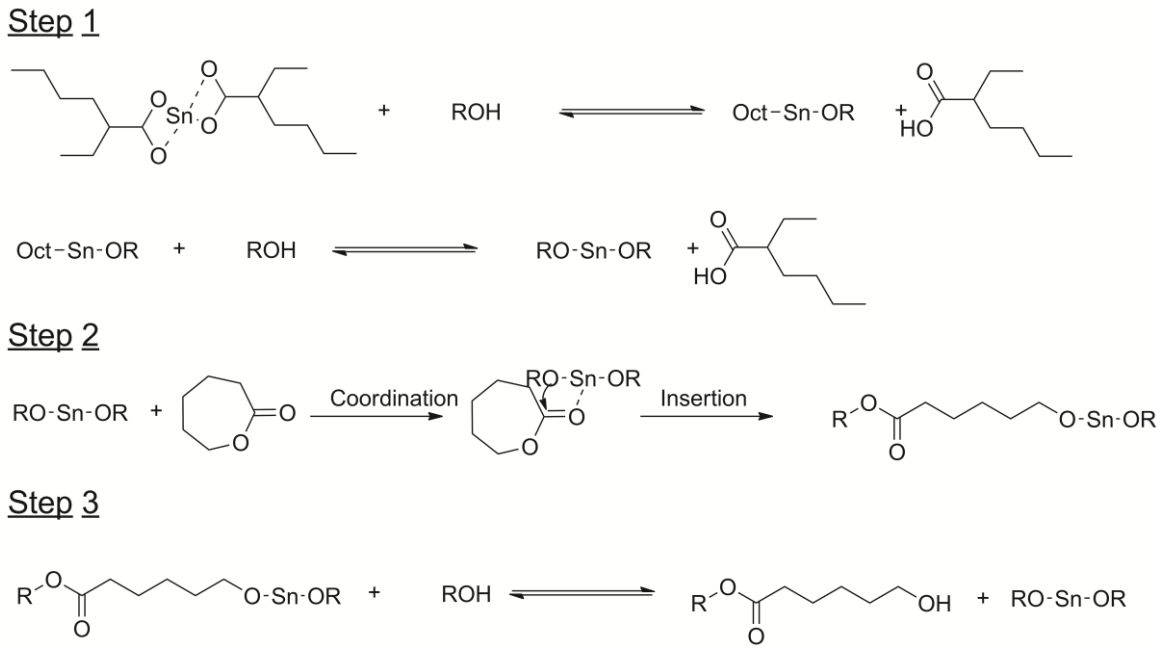

Scheme 2-5. Coordination-insertion mechanism for ROP of ε-caprolactone with an alcohol as co-initiator (ROH). Step 1 shows the formation of the active catalyst, step 2 describes the initiation and step 3 illustrates the equilibrium between activated and deactivated chain-ends.

The coordination-insertion mechanism proposed for the polymerization of ε-caprolactone starts by the formation of an initiator from $Sn(Oct)_2$ and a co-initiator (usually an alcohol or amine). The active initiator opens and inserts the cyclic ester monomer hence forming the polymeric chain. Possible side reactions are transesterifications, macrocyclizations or esterifications with octanoic acid.[54] A significant drawback of this mechanism is the difficulty to completely remove the tin catalyst considering. Therefore, other synthetic methods involving organic catalysts or enzymes are being thoroughly investigated.[64]

From the family of cyclic esters, lactide (LA) and ε-caprolactone (CL) are highly used monomers, the main reasons being their biocompatibility and biodegradability which makes

their polymeric derivatives suitable for biological applications.[65] ROP is also an efficient tool for the synthesis of advanced macromolecules such as amphiphilic polymers or dendritic-linear hybrids.[17, 66]

2.4.2 Atom Transfer Radical Polymerization (ATRP)

The first reports on ATRP were published in 1995 by parallel studies from Kato *et al.*,[67] Wang and Matyjaszewski[68] and Percec and Barboiu[69]. However the chemistry underlying the ATRP, known as atom transfer radical addition (ATRA), was already introduced in the 1940's.[70] In conventional radical polymerizations, the continuous initiation, the fast radical propagation and the occurrence of termination reactions result in broad dispersities and absence of control over the nature of the end-groups. In ATRP, the termination reactions are significantly suppressed and mainly initiation and propagation take place. In order to control the propagation, a fast initiation is necessary to ensure that all chains start propagating simultaneously. Suppression of termination reactions is achieved by creating a dynamic equilibrium between active and dormant species, while shifting the equilibrium towards the dormant side (Scheme 2-6). By doing so, the concentration of active radicals is lowered and thus the probability of termination reactions strongly reduced. Consequently, the living character of the end-groups can be preserved.[59]

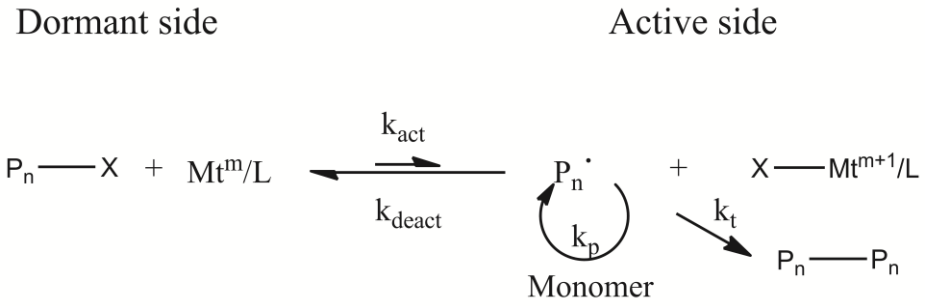

Scheme 2-6. ATRP equilibrium. $P_n^{\bullet}$ is the propagating radical, Mt^m is the transition metal catalyst at the oxidation state m, L is the ligand and X an halogen atom. k_{act}, k_{deact}, k_p and k_t represent the rate constants of activation, deactivation, propagation and termination respectively.

ATRP is a versatile polymerization method. This technique has been applied to the polymerization of several monomers such as styrenics, acrylates, methacrylates, acrylamides, methacrylamides and acrylonitriles. It is also tolerant to various functional groups including epoxides, cyanides, amines and hydroxyls. Moreover ATRP can be performed in both bulk and solution, using either organic or aqueous media. However, even though ATRP is a commonly used polymerization method, it suffers from several drawbacks. Firstly, the relatively high amount of transition metal catalyst required for the polymerization can result in coloring and toxicity of the synthesized polymeric material. Secondly, ATRP is highly sensitive to oxygen and thorough deoxygenation of the system is necessary, complicating the synthetic procedure. Nevertheless, the high versatility of ATRP towards monomer structures

and its tolerance to various solvents and functional groups make this system a suitable tool for the synthesis of diverse molecules. Additionally, the living character of the end-groups allows for further polymerization or functionalizations and permits the preparation of advanced macromolecular architectures such as block or star polymers.[71, 72]

2.5 HONEYCOMB FILMS

2.5.1 Breath figure method

Nano- and microporous structures with long-range ordering have for long attracted scientific interest due to their numerous possible applications in optics,[73, 74] catalysis,[75] sensors[76-78] or life science[79-81]. A myriad of techniques have been introduced for their preparation such as colloidal crystal templating, microphase separation of copolymers or biotemplating. However all these methods require the removal of the template to access the porous structure. A significant breakthrough in the field was the introduction of the breath figure (BF) method in 1994 by François and coworkers.[82] BF is a template-free method in which pores are generated from the condensation of water droplets on a cold surface.[83, 84] The method originates from observations of Aitken who reported already in 1893 the formation of water droplets on solid surfaces, a concept that was further investigated by Rayleigh in the beginning of the 19th century[85, 86]. Later Knobler and Beysens noticed that BFs could also form on paraffin oil and they observed that an hexagonal pattern was generated with droplets separated by a thin film of oil.[87-89]

The "breath figure" method, whose name originates from the mode of generation of these arrays of droplets, can produce ordered arrays of pores over large areas (4-50 mm^2) with pore sizes in the nanometer to micrometer range. This simple and inexpensive method can today be applied to a multitude of systems including synthetic polymers, grafted cellulose fibers[90] or gold nanoparticles[91].

2.5.2 Mechanism of the BF formation

Although this phenomenon has been known for a long time, its detailed mechanism is still not well understood. The mechanism accepted today was suggested by Srinivasarao and is based on formation and consecutive "crystallization" of BFs.[92] In a first step, a hydrophobic polymer is dissolved in a volatile organic solvent, generally non miscible with water, and the solution is drop cast on a solid substrate under humid atmosphere (relative humidity, RH, above 50 %). Upon evaporation of the solvent, the temperature of the surface of the solution drops down to -6 to 0 °C[92] resulting in nucleation of water droplets all over the surface. The droplets grow in size and self-arrange into arrays of hexagonally packed droplets. Simultaneously, the polymer precipitates at the water/organic solvent interface, stabilizing the droplets and preventing coalescence. After complete evaporation of the organic solvent and the water, an array of ordered pores is obtained (Figure 2-7).[83]

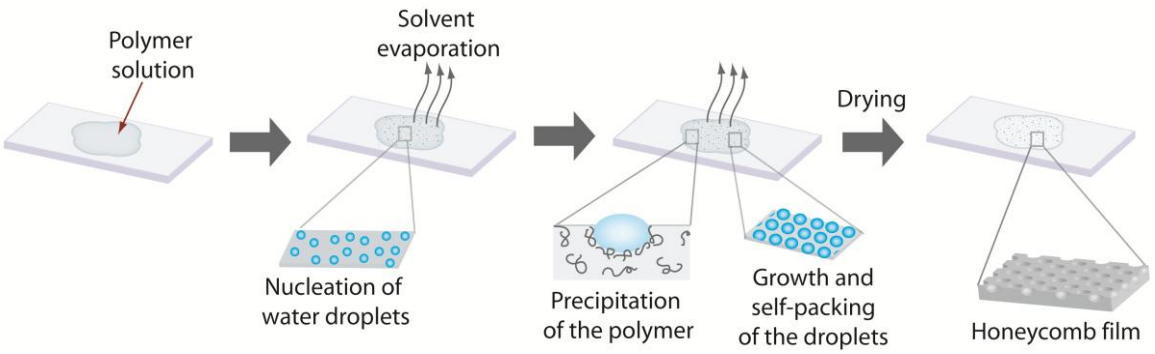

Figure 2-7. Formation of a honeycomb film by the BF method**.**

In the dried films, the pores are often interconnected suggesting that coalescence must have occurred in the final stage of the film formation. Moreover, several layers of pores can sometimes be observed caused by diffusion of the water droplets into the organic solution. Which mechanism is responsible for the hexagonal arrangement of droplets is still not clearly established but Marangoni convection and thermocapillary forces have been suggested to explain this phenomenon.[83]

2.5.3 Stability of the films

Due to the nature of the film formation process, which only relies on precipitation around a dynamic template, the porous films are easily damaged by heat or solvent, limiting their possible use in a number of applications. To overcome this drawback, two main approaches have been suggested, namely blending and cross-linking. [93, 94] The blending process consists in adding a linear polymer to star polymers of identical structure to improve the strength of the film. For example Stenzel-Rosenbaum *et al.* showed that by adding up to 20 wt % of linear polystyrene to a solution of polystyrene stars, less brittle films were obtained.[95] The other approach, capitalizes on cross-linking via UV irradiation, thermal treatment or chemical reaction to improve both the thermal and solvent stability of the films. One example is the UV irradiation of polystyrene films performed by Li *et al.* which resulted in an improved resistance towards various organic solvents as well as temperatures up to 250 °C.[96]

2.5.4 Polymer architecture

In their introductory work, François *et al.* reported the formation of breath figures from polystyrene stars and polyparaphenylene-block-polystyrene cast under moist air flow from carbon disulfide.[82] Today the library of architectures known to form BF while cast under appropriate conditions has been extended to include linear,[92, 96, 97] hyperbranched[98, 99] and rod-coil block polymers[100-103]. Although it was originally thought that linear polystyrene was inappropriate for the formation of BFs due to slow precipitation at the solvent/water interface,[101, 104, 105] it has now been demonstrated that ordered films can be obtained from this material when cast under optimized conditions.[106] However, in comparison to more favorable systems such as branched or star polymers, linear polymers require a fine-tuning of

the casting conditions. To overcome this drawback, surfactants can be added to the polymeric solution to stabilize the droplets and favor the formation of films.[94, 107]

Changes at the molecular level such as number of arms for a star polymer or nature of the end-groups are critical parameters to control the size and shape of the pores. At constant molecular weight, increasing the number of arms of polystyrene stars from 5 to 18 results in a significant decrease in pore size from 800 nm to 250 nm.[108] Other studies have revealed that by changing the end-groups of polystyrene stars from hydroxyl to perfluoroalkyl, the shape of the pores was changing from spherical to cylindrical.[109]

2.5.5 Parameters governing the film properties

Initial studies on the BF method have revealed that variables such as humidity, solvent, air flow, temperature, substrate, concentration of the solution, polymer architecture and type of polymer are crucial to control the quality of the film. By tailoring the casting parameters, the pore size can be tuned between 200 nm and 20 μm.[92]

In general the structural properties of the film such as pore size and regularity are dependent on kinetics of solvent evaporation and water condensation. Several studies have been performed on the growth of the droplets and showed that the droplets grow slowly in the beginning and that after 3 seconds a stable regime with $R \propto t^{0.35}$ is reached where R represents the radius of the droplet.[87-89, 110] In order to obtain large pores, a high humidity and long evaporation time are thus necessary. On the opposite, a fast evaporation rate will favor the formation of small pores. This kinetic control is typically valid for stars or comb polymers. As such control can be obtained through variation of several parameters such as humidity, solvent, air flow, temperature or concentration of the solution, it leads to the formation of ordered arrays under a broad window of casting conditions. Humidity is probably the most important factor and a relative humidity level above 50 % is necessary to create favorable condensation. In general the pore size increases almost linearly with increasing humidity.[111] On the contrary, increasing the air flow or the polymer concentration results in a decrease in pore size.[92]

2.5.6 Amphiphilic polymers

Amphiphilic polymers represent a special case in the formation of BFs. For this kind of systems, the formation of ordered porous array is a thermodynamically driven process in which the hydrophilic to hydrophobic balance and associated interfacial tension are critical parameters. The amphiphilic polymer chains act as interfacial active compounds and the strong interaction of the hydrophilic segment with water strongly affects the regularity of the films. While the introduction of polar end-groups or short hydrophilic segments favors the formation of regular arrays of pores, long hydrophilic blocks might induce coalescence of water droplets thereby preventing the formation of an ordered porous array. These systems require a fine-tuning of the casting conditions and well-ordered films are more difficult to obtain than with a kinetic-dependent system.

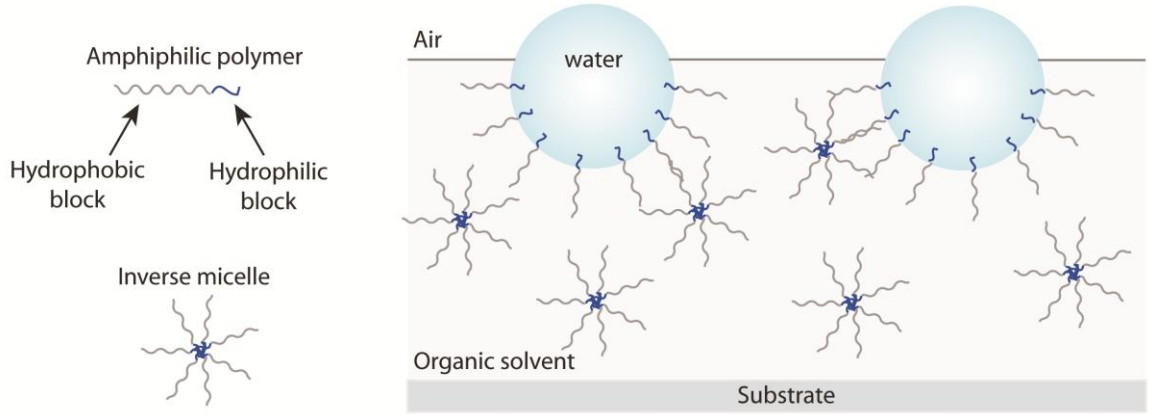

Figure 2-8. Schematic representation of the formation of inverse micelles and the arrangement of amphiphilic polymers at the water/organic solution interface during film casting.

Nevertheless, amphiphilic structures are of particular interest for applications requiring functionalization of the pores. These block copolymers are prone to form inverse micelles when dissolved in a non polar organic solvent. When water condenses on the surface of the solution, these inverse micelles start interacting with water and the polymer rearranges around the water droplets. Such mechanism leads to an enrichment of the pores in hydrophilic functionalities (Figure 2-8).[112-115]

2.5.7 Applications

Due to their specific morphology, honeycomb films are potential candidates for a myriad of applications including photoelectric conversion, sensors or catalysis.[94] Moreover the simple and fast preparation process of these films render them attractive as template for other kinds of structural materials. The combination of a hydrophobic polymer matrix with surface roughness and the presence of air within the pores gives rise to highly hydrophobic films that could, after optimization of their optical properties (transparency), be suitable for coatings of substrates such as windows.[94] Finally, honeycomb films are interesting for biological applications such as cell culture scaffolds since their morphology and mechanical properties can favor cell attachment and proliferation.[93, 94]

3. EXPERIMENTAL

3.1 DEFINITIONS

Throughout the thesis, the hydroxyl functional dendrimer of generation four based on a TMP core will be noted TMP-G4-OH.

The LDL hybrids materials will be referred to as Alk-G*n*-PCL_x after ROP of PCL with a DP of *x* from a generation *n* alkyne functional dendron and PEG_{2k}-G*n*-PCL_x after CuAAC reaction with a PEG of molecular weight 2 000 g/mol. The materials synthesized via TEC reaction will be noted PEG_{2k}-S-Gn-PCL_x. The macromolecule obtained from ROP of lactide will be noted PEG_{2k}-G3-PLA_{30}. The inverted LDL will be denoted PCL_{240}-G3-TEG-THP and PCL_{240}-G3-TEG-OH respectively before and after deprotection of the THP group.

Dendrimers built from a disulfide core will be noted S_2-$(Gn\text{-}Ac)_2$ or S_2-$(Gn\text{-}OH)_2$ and the macrothiols will be referred to as HS-G*n*-Ac and HS-G*n*-OH as acetonide (Ac) and hydroxyl (OH) functionalized and with G*n* indicating a dendron of generation *n*.

The LDs based on the HEMA-benzylidene monomer will be referred to as poly(HEMA-$Bz)_{22k}$-G2-TEG-Alk where 22k is the molecular weight (22 000 g/mol) of the linear poly(HEMA-Bz) block, G2 is a dendritic linker of generation two, TEG stands for tetraethylene glycol and Alk represents the terminal alkyne groups. The random polymer based on HEMA-Benzylidene and HEMA-azide monomers will be noted poly(HEMA-Bz-*ran*-HEMA-N_3).

3.2 MATERIALS

Bis-MPA was kindly donated by Perstorp. TMP, hydroxyl functional bis-MPA dendrimers of generation 4 and alkyne functional dendrons were provided by Polymer Factory. ε-caprolactone (Acros Organics) was distilled over CaH_2 and stored over molecular sieves (4 Å) under argon (g). Tin (II)-2-ethylhexanoate (95%) ($SnOct_2$) was dried using molecular sieves (4 Å) in a solution of dry toluene prior to use. The extractions were performed using a 10 wt% $NaHSO_4$ aqueous solution as acidic water phase and a 10 wt % Na_2CO_3 aqueous solution as basic water phase. Flash chromatography was performed using silica gel for column chromatography, ultra pure, 40-60 μm, 60A from Acros organics.

Benzylidene-protected 2,2-bis(methylol)propionic acid anhydride (benzylidene-protected bis-MPA anhydride) and 6-azidohexanoic anhydride were synthesized according to previously published procedures.[116, 117] PEG-N_3 was synthesized as reported earlier.[118]

All other starting materials were purchased from commercial sources (Sigma-Aldrich, Chemtronica or VWR) and used as received.

3.3 INSTRUMENTATION

MALDI-TOF MS spectrum acquisitions were conducted on a Bruker UltraFlex MALDI-TOF MS with SCOUT-MTP Ion Source (Bruker Daltonics, Bremen) equipped with a N_2-laser (337nm), a gridless ion source and reflector design. The instrument was calibrated using SpheriCal™ calibrants purchased from Polymer Factory Sweden AB. A THF solution of DHB/HABA (10 mg/mL) dopped with sodium trifluoroacetate was used as matrix. The software FlexAnalysis Bruker Daltonics, Bremen, version 2.2 was used for spectra analysis.

^{1}H NMR and ^{13}C NMR experiments were performed on a Bruker Avance NMR instrument. ^{1}H NMR spectra were acquired at 400 MHz and ^{13}C NMR spectra were acquired at 100 MHz. The residual solvent peak was used as internal standard.

SEC using **THF** (1.0 mL min^{-1}) as the mobile phase was performed at 35 °C using a Viscotec TDA model 301 equipped with two T5000 columns, a VE 5200 GPC autosampler, a VE 1121 GPC solvent pump, and a VE 5710 GPC degasser (all from Viscotec/Malvern.). A calibration method was created using narrow linear polystyrenes standards. Corrections for flow rate fluctuations were made using toluene as an internal standard. Viscotec OmniSEC 4.0 software was used to process data.

SEC using **DMF** as mobile phase (0.2 mL min^{-1} with 0.01 M LiBr) was conducted at 50 °C on a TOSOH EcoSEC HLC-8320GPC system equipped with an EcoSEC RI detector and three columns (PSS PFG 5 μm; Microguard, 100 Å, and 300 Å) from PSS GmbH. A conventional calibration method was created using narrow linear poly(methyl methacrylate) standards. Toluene was used as an internal standard for correction of flow rate fluctuation. The data were processed with the software PSS WinGPC Unity version 7.2.

SEC using **$CHCl_3$** as mobile phase (1 ml min^{-1}, 30 °C) was performed on a Verotech PL-GPC 50 Plus system equipped with a PL-RI detector and two PLgel 10 μm mixed D (300 x 7.5 mm) columns from Varian. The calibration was created using polystyrene standards.

UV light irradiation (macrothiols, paper 4) was carried out with a Hamamatsu L5662 equipped with a L 6722 Hg-Xe lamp. The intensity was 20-60 mW cm^{-2}, measured with a Hamamatsu C6080-03 light power meter, calibrated for 365 nm. UV light irradiation (poly(HEMA-Bz)-G2-OH,paper 5) was conducted using a UVP Black-Ray® B-100AP High Intensity UV Lamp at a wavelength of 365 nm.

DSC measurements were conducted on a Mettler Toledo DSC. Heating and cooling rate were set to 10 °C min^{-1}.

Contact angle and **interfacial tension** measurements were performed on a KSV Instrument CAM 200 equipped with a Basler A602f camera. All measurements were conducted at 25 °C under 50 % RH. Values of interfacial tension were acquired using the pendant drop method.

Optical microscopy was conducted on a Leica DM IRM optical microscope.

FE-SEM images of gold (LDL hybrids, paper 3) or platinum (LD hybrids, paper 5) sputtered samples were acquired on a Hitachi S-4300 FE-SEM.

AFM topographic images were recorded on a CSM Instrument Atom Force Microscope in tapping mode. The images were analyzed using the free software Gwyddion 2.12.

Confocal fluorescence microscopy was performed using a Zeiss LSM5 Pascal microscope equipped with a 63x/1.4 NA oil immersion objective. Rhodamine-B fluorescence was excited at 543 nm and emission was detected with a long pass 570 nm filter.

3.4 POLYMER SYNTHESIS

This section describes some of the typical synthetic procedures used in this thesis. Detailed experimental setups, procedures and characterization data can be found in the appended papers and in their supplementary information.

3.4.1 Synthesis of PEG-Gn-PCL LDL hybrids

A library of LDL hybrids was synthesized via ROP of ε-CL and CuAAC reaction (Figure 3-1). Typical examples of synthetic protocols used for the ROP and CuAAC reactions of the PEG_{2k}-Gn-PCL_x materials are given below.

3.4.1.1 ROP of ε-CL and LA initiated from bis-MPA dendrons.

Hydroxyl terminated bis-MPA dendrons of generation 1 to 4 functionalized with an acetylene moiety at the focal point and propargyl alcohol were used as macroinitiators for the ROP of CL and LA. The reactions were performed using $Sn(Oct)_2$ as catalyst in toluene at 110 °C. The targeted DPs were calculated to be reached at 75 % monomer conversion.

A typical procedure is given as example: a flame dried round bottom flask was equipped with a stir bar and charged with alk-G3-OH (475 mg, 0.55 mmol). The flask was sealed with a septum and 1 ml of dry toluene was added to the system. The flask was heated to 110 °C and toluene was removed by vacuum. The flask was filled with argon gas and ε-CL (19.4 ml,

175.20 mmol) and toluene (20 ml) were added to the system. After complete dissolution of the initiator, $Sn(Oct)_2$ (0.44 ml of a 1 mmol/ml solution in toluene, 0.44 mmol) was introduced in the flask and the progress of the reaction was followed by ^1H NMR. Once a monomer conversion of 75 % was reached, the vessel was removed from the oil bath, diluted with DCM and precipitated in MeOH. The white precipitation was collected and dried under vacuum.

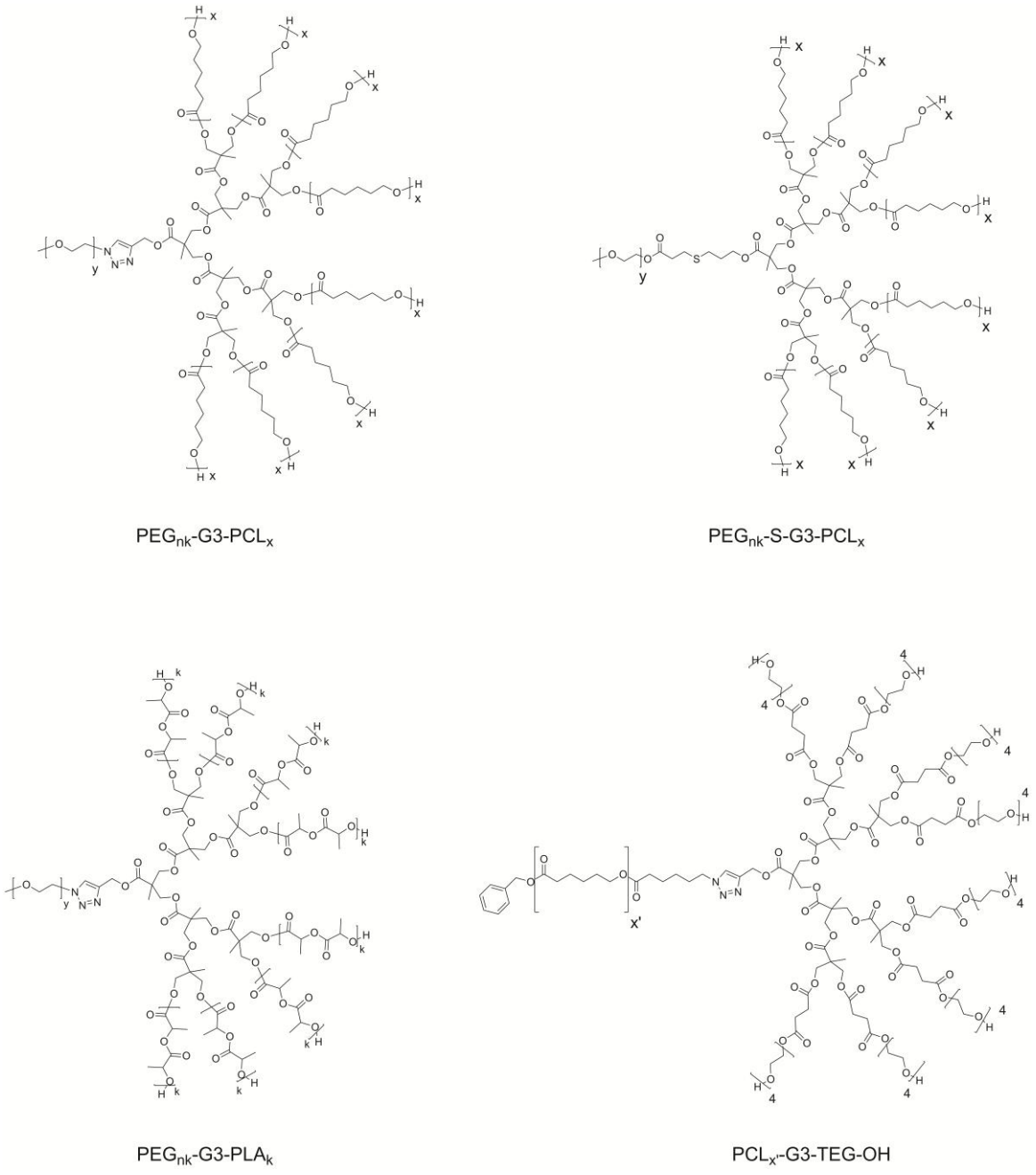

Figure 3-1. Schematic representation of a PEG_{nk}-G3-PCL_x, a PEG_{nk}-S-G3-PCL_x, a PEG_{nk}-G3-PLA_k and an inverted $PCL_{x'}$-G3-TEG-OH LDL hybrids.

3.4.1.2 Synthesis of PEG-Gn-PCL LDL hybrids by CuAAC reaction

Coupling of the alkyne functional bis-MPA-PCL dendrons to the azide terminated PEG was conducted using DIPEA and $Cu(PPh_3)_3Br$ in a [alkyne]:[azide]:[DIPEA]:[$Cu(PPh_3)_3Br$] feed ratio of 1:5:5:1.

Generally, PEG_{2k}-N_3 (322 mg, 0.16 mmol) and alk-G3-PCL30 (1 g, 0.031 mmol) were dissolved in THF. DIPEA (20 mg, 0.15 mmol) and $Cu(PPh_3)_3Br$ (28 mg, 0.030 mmol) were added to the system. The vessel was sealed with a septum and heated to 60 °C over night. The reaction was followed by ^1H NMR and when full conversion of the alkyne groups was observed, the product was precipitated in MeOH. The white filtrate was collected and dried under vacuum.

3.4.1.3 Synthesis of PEG-S-Gn-PCL LDL hybrids by TEC reaction

The thiol-ene reaction for the synthesis of the LDL had an allyl to thiol feed ratio of 1:10. All-G3-PCL_{30} (500 mg, 0.02 mmol) and HS-PEG_{2k} (354 mg, 0.2 mmol) were dissolved in 1 ml unstabilized THF. A catalytic amount of DMPA was added to the vial and the solution was exposed to UV for 1h. The product was precipitated in cold MeOH and isolated as a white powder.

3.4.2 Synthesis of macrothiols

Bis-MPA dendrons functionalized with a thiol moiety at the focal point were synthesized by successive dendrimer growth from a di-hydroxyl functional disulfide core followed by cleavage of the disulfide bond (Figure 3-2). Typical synthetic procedures for the anhydride coupling, ketal deprotection and disulfide cleavage reactions are described below.

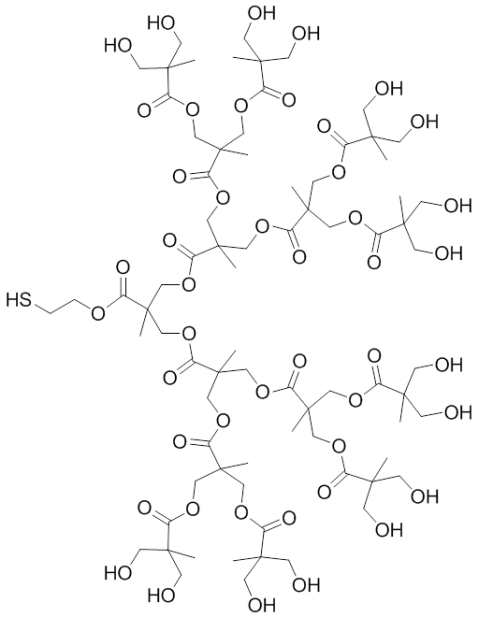

Figure 3-2. Schematic structure of a macrothiol of generation 4, HS-G4-OH.

3.4.2.1 Dendrimer growth via anhydride coupling

The procedure used for the synthesis of the acetonide protected dendrimer of first generation is given as example. A round bottom flask equipped with a stir bar was charged with 2,2-dihydroxyethyl disulfide (20 g, 130 mmol), 4-(dimethylamino)pyridine (DMAP) (3.17 g, 26 mmol), pyridine (63 mL) and DCM (180 mL). Acetonide-protected bis-MPA anhydride (128 g, 390 mmol) was added to the reaction vessel and the solution was stirred over night. The progress of the reaction was monitored by ^{13}C NMR spectroscopy. When full substitution of the hydroxyl groups was observed, the residual anhydride was quenched with water over night. The solution was extracted 5 times with $NaHSO_4$ and twice with Na_2CO_3. The organic phase was dried on $MgSO_4$, filtered and the solvent was evaporated. The product was purified by column chromatography in EtOAc/heptane 10/90.

3.4.2.2 Dendrimer activation via ketal deprotection

Removal of the acetonide protecting group was conducted using an acidic catalyst resin such as DOWEX® 50W-X2 in methanol. The procedure followed for the synthesis of the activated dendrimer of first generation is shown here as example. S_2-(G1-Ac)$_2$ (13 g, 28 mmol), methanol (100 mL) and DOWEX® (13 g) were added to a round bottom flask under stirring. The progress of the reaction was followed by MALDI-TOF MS, ^1H NMR and ^{13}C NMR. The acidic resin was filtered off and the filtrate was concentrated by evaporation of the solvent.

3.4.2.3 Formation of macrothiols by cleavage of the disulfide bond

Cleavage of the disulfide linkage was performed using DTT and TEA in DCM in a [disulfide]:[DTT]:[TEA] feed ratio of 1:2:4.The protocol followed for the synthesis of the acetonide protected macrothiol of first generation is given here as example. S_2-(G1-Ac)$_2$ (10 g, 21.4 mmol), dichloromethane (100 mL), DTT (6.6 g, 42.8 mmol) and TEA (12 mL, 85.6 mmol) were added to a round bottom flask. The solution was then flushed with argon for 20 min. The progress of the reaction was monitored by ^1H NMR spectroscopy and MALDI-TOF spectroscopy. When full cleavage was achieved, the solution was extracted twice with $NaHSO_4$. The organic phase was dried on $MgSO_4$, filtered and the solvent was evaporated. The obtained crude product was purified by column chromatography in EtOAc/Heptane 10/90.

3.4.3 TEC reactions for coupling of macrothiols

Macrothiols were coupled to various polymeric cores via TEC reaction. The procedure used for the coupling to a triallyl functional core is given as example. HS-G3-Ac (252 mg, 0.024 mmol) and triazine-triallyl (10 mg, 0.040 mmol) were dissolved in unstabilized THF. DMPA (3 mg, 0,002 mmol) was added to the system and the vessel was closed with a septum and purged with argon for 5 min. The solution was irradiated by UV (365 nm) for 30 min. The product was purified by column chromatography in EtOAc/Heptane.

3.4.4 Polymerization of HEMA by ATRP

The general polymerizations of HEMA-Bz were performed using HO-EBiB, 2,2'-bipyridyl, Cu(I)Cl and $Cu(II)Cl_2$ in anisole at 50 °C with a [HEMA-Bz]/[HO-eBIB]/[Cu(I)Cl]/[$Cu(II)Cl_2$]/[Bipy] feed ratio equal to 2*DPtarget:1:1:0.1:2. The polymerization of HEMA was conducted in a water/MeOH 50/50 system at 0°C using eBIB, 2,2'-bipyridyl, Cu(I)Cl and $Cu(II)Cl_2$ with a [HEMA-Bz]/[HO-eBIB]/[Cu(I)Cl]/[$Cu(II)Cl_2$]/[Bipy] feed ratio equal to 1.25*DPtarget:1:1:0.15:2.

A typical procedure for the synthesis of poly(HEMA-Bz)$_{22k}$-OH is given in example. To a round bottom flask were added HEMA-Bz (12 g, 36 mmol), HO-EBiB (42 mg, 0.2 mmol), 2,2'-bipyridyl (62 mg, 0.4 mmol) and anisole (12 ml). The flask was sealed with a rubber septum and degassed for 5 min under vacuum followed by 5 min of argon flushing. The flask was opened and Cu(I)Cl (20 mg, 0.2 mmol) and Cu(II)Cl2 (3 mg, 0.02 mmol) were quickly added to the vessel. The flask was sealed again, degassed by two cycles of 5 min vacuum followed by 5 min argon, and immersed in a thermostated oil bath at 50 °C. The progress of the reaction was monitored by ^{1}H NMR and when a monomer conversion of 50 % was reached, the reaction solution was exposed to air and diluted with DCM. The solution was passed through a neutral aluminum oxide column to remove the copper. The solvent was evaporated and the polymer was precipitated twice from THF to cold MeOH. The product was collected as a white powder and dried under vacuum.

3.4.5 Miscellaneous

The synthesis of other small molecules used in this thesis is presented in Scheme 3-1.

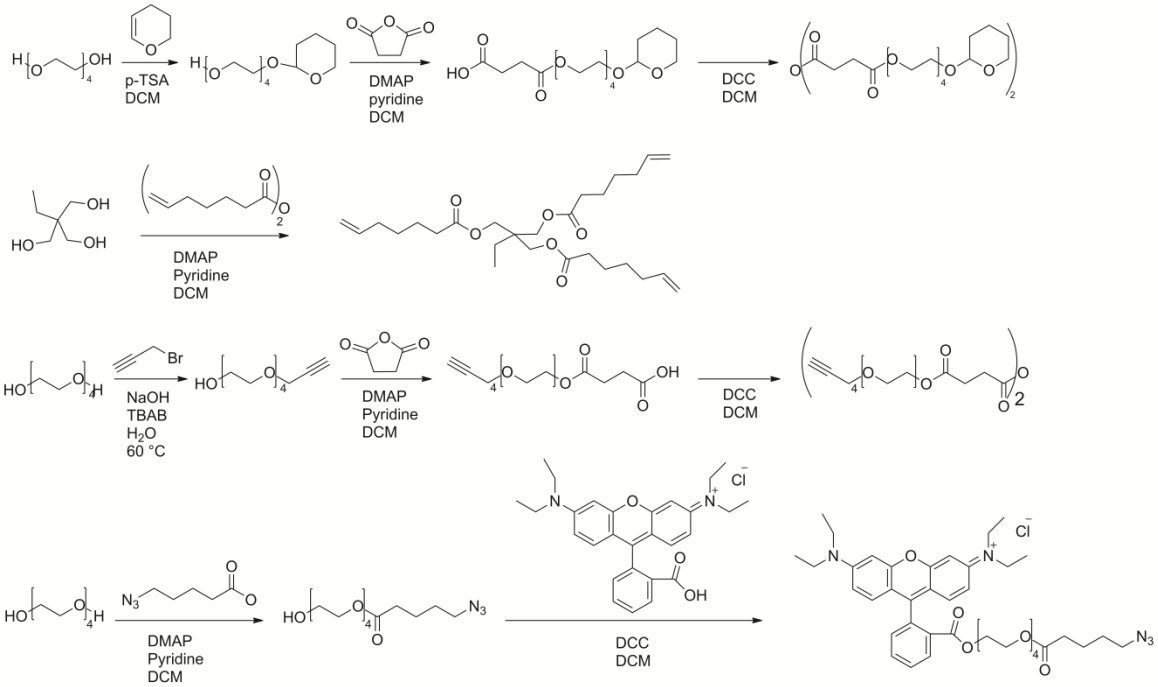

Scheme 3-1. Overview of the synthesis of THP-protected TEG anhydride, triallyl functional TMP, Alkyne-functional TEG anhydride and azide functional Rhodamine-B.

3.5 DEGRADATION STUDY

The degradation of Bis-MPA dendrimers was evaluated at different temperatures and different pHs. TMP-G4-OH was dissolved in phosphate-citrate buffers of constant ionic strength (I = 0.15 M) at different pHs (4.5, 5.5, 6.5, 7.5). The solutions were heated to 37 °C and aliquots were taken at specific time intervals and analyzed by MALDI-TOF MS.

3.6 TOXICITY

Mitochondrial function of human monocyte-derived macrophages (HMDM) exposed to dendrimers was determined using MTT assay. Cells were exposed to dendrimers at different doses (0.5 to 100 μM) for up to 48 h. The supernatant was then removed and, after washing with PBS, 100 μl of MTT solution (0.5 mg/ml) was added and incubated for 3h at 37 °C. 50 μl of DMSO were added to dissolve the formed formazan crystals and MTT conversion was quantified by measuring the absorbance at 570 nm. Results are expressed as % of mitochondrial activity analyzed using cells from at least three healthy blood donors.

3.7 HONEYCOMB FILM FORMATION

Ordered porous films were obtained via the BF method by casting a polymer solution under humid atmosphere. The typical procedure used for casting of the LDLs is given here as example. The LDL was dissolved in benzene at a concentration of 1 mg/ml and 50 μl of the solution were cast on a glass substrate (the substrate was washed with ethanol before use). The solution was allowed to evaporate at room temperature (20 °C) in a closed humid chamber (≈ 95 % RH). After complete solvent evaporation, a white film was left on the substrate for assesment.

3.8 LABELLING OF HONEYCOMB FILMS WITH RHODAMINE-B

Honeycomb films cast on glass substrate were labeled with Rhodamine-B before confocal fluorescence microscopy analysis. The cast film was placed in a glass vial. Rhodamine-B (100 μl of a 4 mg/ml solution in water), NaAsc (20 μl of a 2 mg/ml solution in water), Cu(II)SO_4 (14 μl of a 1 mg/ml solution in water) and water (2.76 ml) were added to the vial. The vial was protected from light and placed on a shaking table (250 rpm) for 2 h. The film was rinced and leached in deionized water for 30 min. After drying, 50 μl of aqueous non-fluorescing mounting medium (Shandon Immu-Mount) and a cover slip were placed on the film.

4. RESULTS AND DISCUSSION

Bis-MPA dendrimers have attracted interest in various fields and particularly for biological applications. Based on a polyester scaffold, they are often claimed to be biodegradable even though no thorough study has been performed on the subject. Therefore the establishment of the degradation profile of bis-MPA dendrimers under physiological conditions together with a toxicity study of the degradation products was of significant importance. Due to their commercial availability and multiple functional hydroxyl groups, bis-MPA dendrons are also appealing for the synthesis of advanced branched macromolecules. Their terminal hydroxyl groups can easily be reacted to incorporate various types of polymers or bioactive compounds, enabling the synthesis of a myriad of sophisticated macromolecules. With their polyester backbone bis-MPA dendrons and dendrimers have been suggested as suitable candidates for the synthesis of amphiphilic LDs with targeted applications in drug delivery.[66] Amphiphilic LD hybrids can self-assemble into micelles under appropriate conditions.[66] Apart from micelle formation, amphiphilic LDs are envisioned to be suitable for the formation of ordered porous films via the BF method. Due to their well-defined structure, LDL could be exploited to acquire a better understanding of the effect of the macromolecular architecture on the film formation. Alternatively, dendritic wedges could be used to introduce multifunctionality inside the pores of the film.

4.1 DEGRADATION AND TOXICITY STUDY OF BIS-MPA DENDRIMERS

Initial studies from Parrott *et al.*on the toxicity of bis-MPA dendrimers on rats revealed that high generation bis-MPA dendrimers were rapidly removed from the blood-stream via the kidneys and did not accumulate in any organs, suggesting good biocompatibility.[119] However, a more thorough study of the subject was still lacking. In fact, a better understanding of the interactions of these materials with relevant biological systems is a prerequisite for the development of new types of nano-carriers for biomedical applications. Therefore the degradation profile of a fourth generation dendrimer as a function of time and pH as well as the toxicity of its structural components for immune-competent cells were investigated. The composition of the TMP-G4-OH dendrimer and its structural components are presented in Figure 4-1.

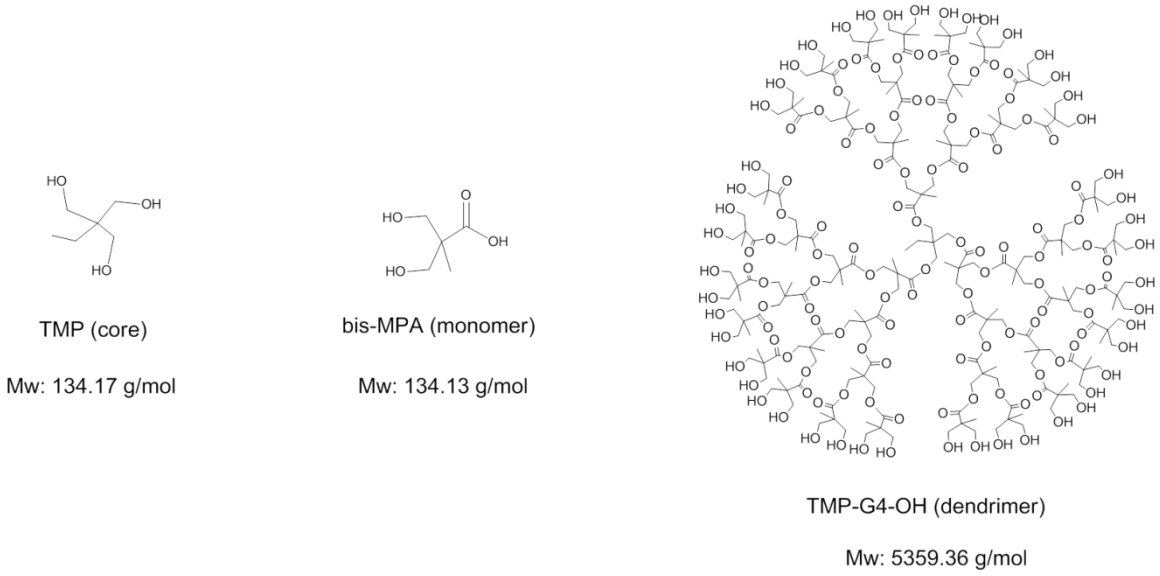

Figure 4-1. Schematic representation of a fourth generation bis-MPA dendrimer and its structural components.

4.1.1 Degradation under physiological conditions.

In order to be classified as biocompatible, dendrimers should present a fast renal elimination rate or degradation into non-toxic products followed by excretion[120]. Due to their polyester scaffold, bis-MPA dendrimers are expected to undergo hydrolysis in aqueous environment, the rate of degradation being pH dependent. The degradation study was therefore conducted at pH 4.5, 5.5, 6.5 and 7.5, which are representative of diverse parts of

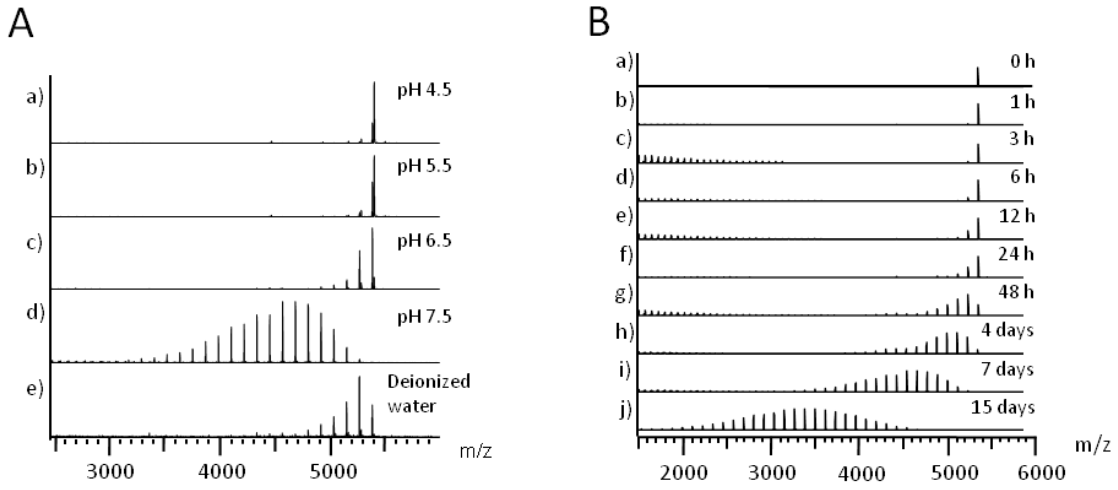

Figure 4-2. MALDI-TOF MS evaluation of the stability of a fourth generation bis-MPA dendrimer at 37 °C at different pHs and times. A) Stability at different pHs after 7 days at pH 4.5 (a), pH 5.5 (b), pH 6.5 (c), pH 7.5 (d) and in deionized water (e). B) Stability at pH 7.5 evaluated at different times 0h (a), 1h (b), 3h (c), 6h (d), 12h (e), 24h (f), 48h (g), 4 days (h), 7 days (i) and 15 days (j).

the body. The temperature was set to 37 °C and the concentration and ionic strength of the solution were kept constant at 100 μM and 0.15 M, respectively. The degradation of the fourth generation dendrimer was followed by MALDI-TOF MS, observing changes from the initial molecular weight of 5365 g/mol (Figure 4-2). Variations in pH show that the dendrimer degrades faster at alkaline pH than in acidic pH (Figure 4-2A). For comparison, degradation in deionized water (pH 7.4) was recorded. The faster degradation at higher pH is caused by hydrolysis of the ester bond under alkaline condition. To better understand the degradation mechanism, the degradation of the dendrimer at pH 7.5 was followed over 15 days (Figure 4-2B). After 6 h, the first signs of degradation were observed as one monomer was hydrolyzed from the structure. Once the first monomer has been cleaved, the access to the internal ester bonds is facilitated and the degradation processes faster. No peak corresponding to high molecular weight dendrons could be observed by MALDI-TOF MS indicating that the degradation progresses from the periphery towards the core, releasing monomer after monomer, following a depolymerization process.

4.1.2 Toxicity study

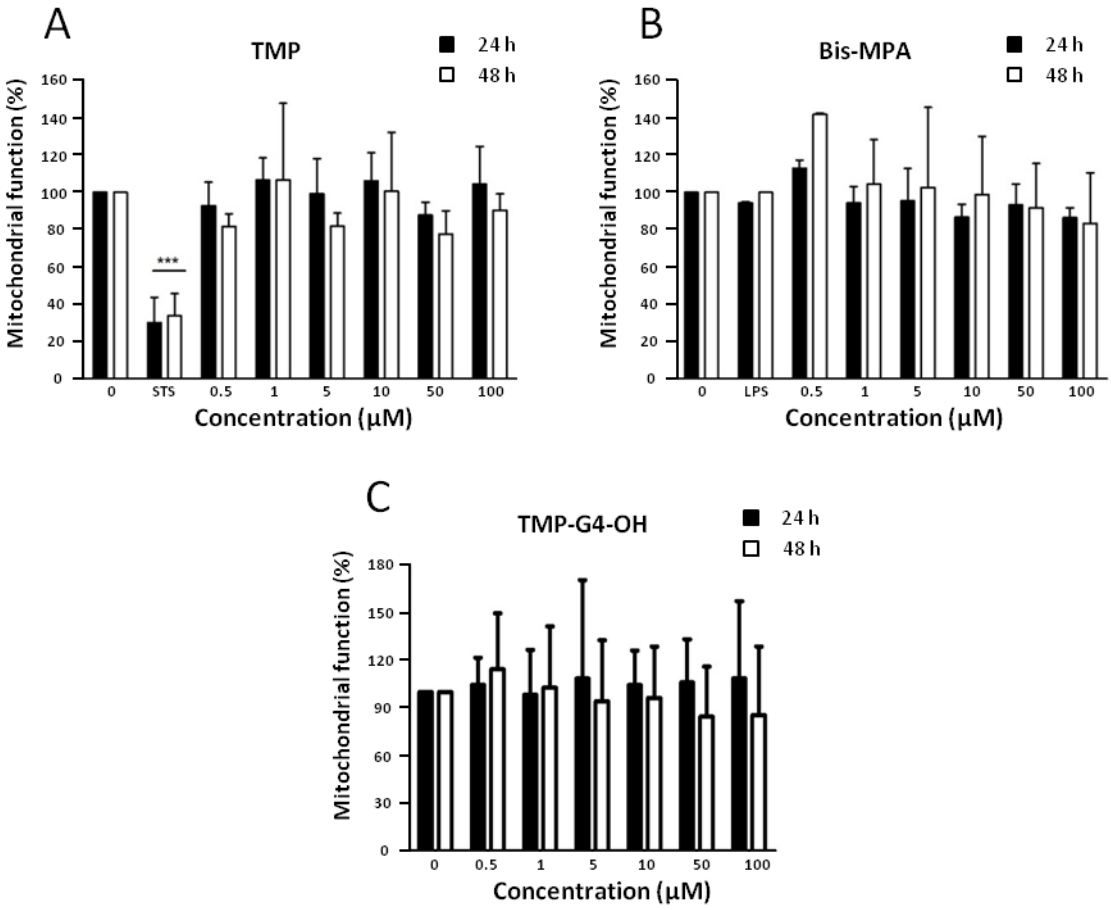

Figure 4-3. *In vitro* biocompatibility of TMP-G4-OH dendrimer and its structural fragment TMP and bis-MPA. Mitochondrial function was assessed by MTT assay upon exposure of HMDM to TMP (A), bis-MPA (B) and TMP-G4-OH dendrimer (C) for 24 h (black) and 48 h (white). STS was used as a positive control and LPS was included in panel B for comparison.

According to the results obtained from the degradation study, once a dendrimer is placed in physiological conditions, bis-MPA monomers, and eventually the TMP core, are released. Therefore, information regarding the toxicity of the dendrimer as well as its structural components is of significant importance. The effect of the dendrimer and its fragments on the viability of primary human monocyte-derived macrophages (HMDM) was evaluated by MTT assay. Since macrophages play a significant role in clearing foreign substances from the blood circulation, the assessment of the effect of dendrimers on monocyte-derived macrophages is highly relevant. No evidence of a decreased mitochondrial function was observed after 48h (Figure 4-3). For comparison, the effect of a well-known cytotoxic compound, SDS, was measured and show a clear decrease in mitochondrial function already after 24h (Figure 4-3 A). Other *in vitro* studies confirmed the good biocompatibility of these polyester dendrimers (paper I).

4.2 Synthesis of LDL hybrids and Formation of honeycomb films

Recently, the emergence of the concept of click chemistry has amplified the range of well-defined macromolecules that could be synthesized, the only limitation being researcher imagination. Of particular interest was the development of a new class of materials, the dendritic-linear hybrids. These materials possess a perfectly branched structure and can easily be tuned to present an amphiphilic character. Thus, the use of these monodisperse branched structures was envisioned to provide a deeper understanding of the parameters governing the pore formation in the BF method. Moreover, the introduction of branching units was expected to favor the formation of ordered films from otherwise challenging polymers such as semi-crystalline PCL.

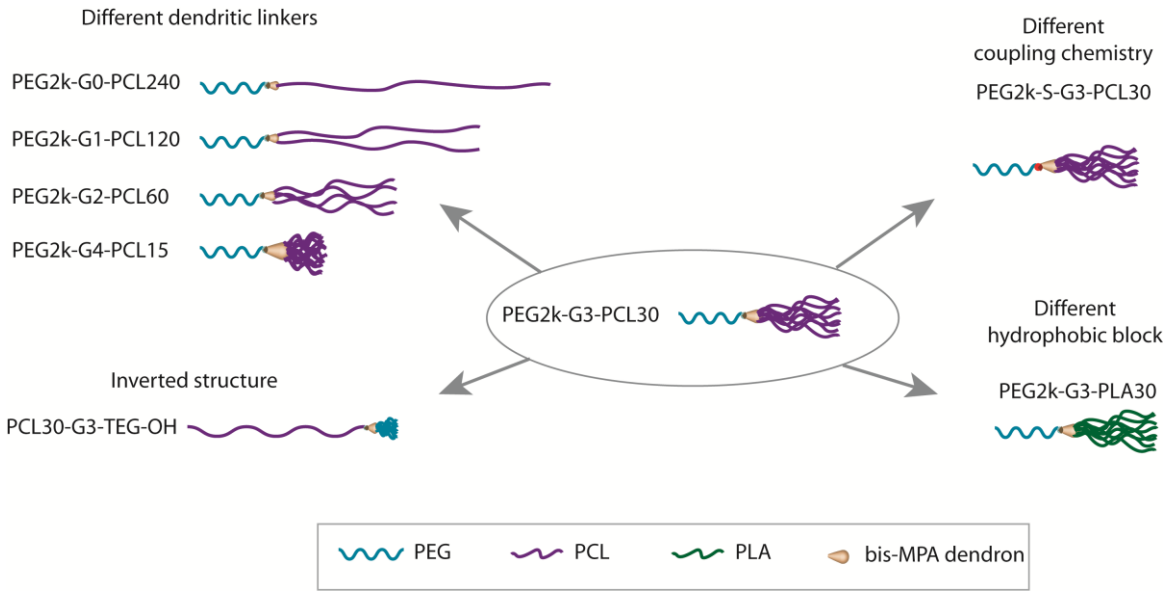

Figure 4-4. Schematic overview of the LDL library synthesized via ROP and efficient coupling reactions.

As a result, a library of amphiphilic LDL was designed and the effect of their macromolecular features on the films characteristics was investigated. This was achieved by synthesizing a comprehensive library of LDL hybrids having a constant total molecular weight but different branching. The hydrophilic to lipophilic balance was kept constant throughout the whole study. Since honeycomb films are envisioned to be used in applications such as cell scaffolding and cell culturing, the use of biocompatible polymers was preferred. For that reason bis-MPA was selected as dendritic linker while amphiphilicity was introduced in the structure by combining hydrophilic PEG with hydrophobic PCL or PLA, all the building blocks being biocompatible and/or biodegradable. (Figure 4-4).

4.2.1 PEG_{2k}-G*n*-PCL_x LDL hybrids

4.2.1.1 LDL synthesis via ROP of ε-Cl and CuAAC chemistry

Bis-MPA dendrons of generation one to four having an alkyne group at the focal point and terminated by hydroxyl groups were used as macroinitiators for the ROP of ε-CL. The library of material was constructed aiming at a constant total molecular weight of PCL. Hence, a G4 dendron will bear 16 PCL chains with a DP of 15 each while a G1 dendron has two linear chains with a DP of 120 each. For comparison, a linear analogue was synthesized from propargyl alcohol with a DP of CL of 240. The ROP of ε-CL was performed at 110 °C with $Sn(Oct)_2$ as catalyst and the reactions were conducted until a monomer conversion of 75 % was reached (Figure 4-5A). Amphiphilicity was introduced in the structure by coupling an azide functional PEG of 2000 g/mol to the alkyne moiety of the molecules via CuAAC chemistry. Excess of azide (up to 5 eq) was required to reach full conversion. The unreacted PEG could easily be removed by precipitation in methanol. While the lower generations (G0-G2) of the DLs only required 24-72 h and 40 °C to be completely substituted, the high generation DLs necessitated up to 5 days and 60 °C. ^{1}H-NMR spectra of Alk-G3-PCL30 and PEG2k-G3-PCL30 are presented in Figure 4-5B and C respectively. As observed on the spectra, the shift of the proton in alpha position of the alkyne bond from 4.71 ppm to 5.25 ppm (signal *h*) confirms that full substitution was achieved. Moreover the strong signal at 3.6 ppm (signal *l,m*) corresponding to the PEG backbone and the appearance of the triazole proton after CuAAC reaction at 7.79 ppm (signal *i*) prove that PEG has been successfully incorporated into the molecule. All the materials show low dispersity, between 1.03 and 1.30, both before and after CuAAC reaction (Table 4-1). Since traces of residual copper could be a concern for biological applications, the LDLs were precipitated in a $MeOH/H_2O$ (50/50) solution containing 1 % EDTA and the products were collected as white powders. DSC performed on the materials (Table 4-1) revealed that all the LDLs are semi-crystalline and that T_m was only slightly affected by changes in DP or dendron generation between G0 and G3. A slight drop in T_m and ΔH_m is observed for the fourth generation material caused by the relatively low DP of the PCL.

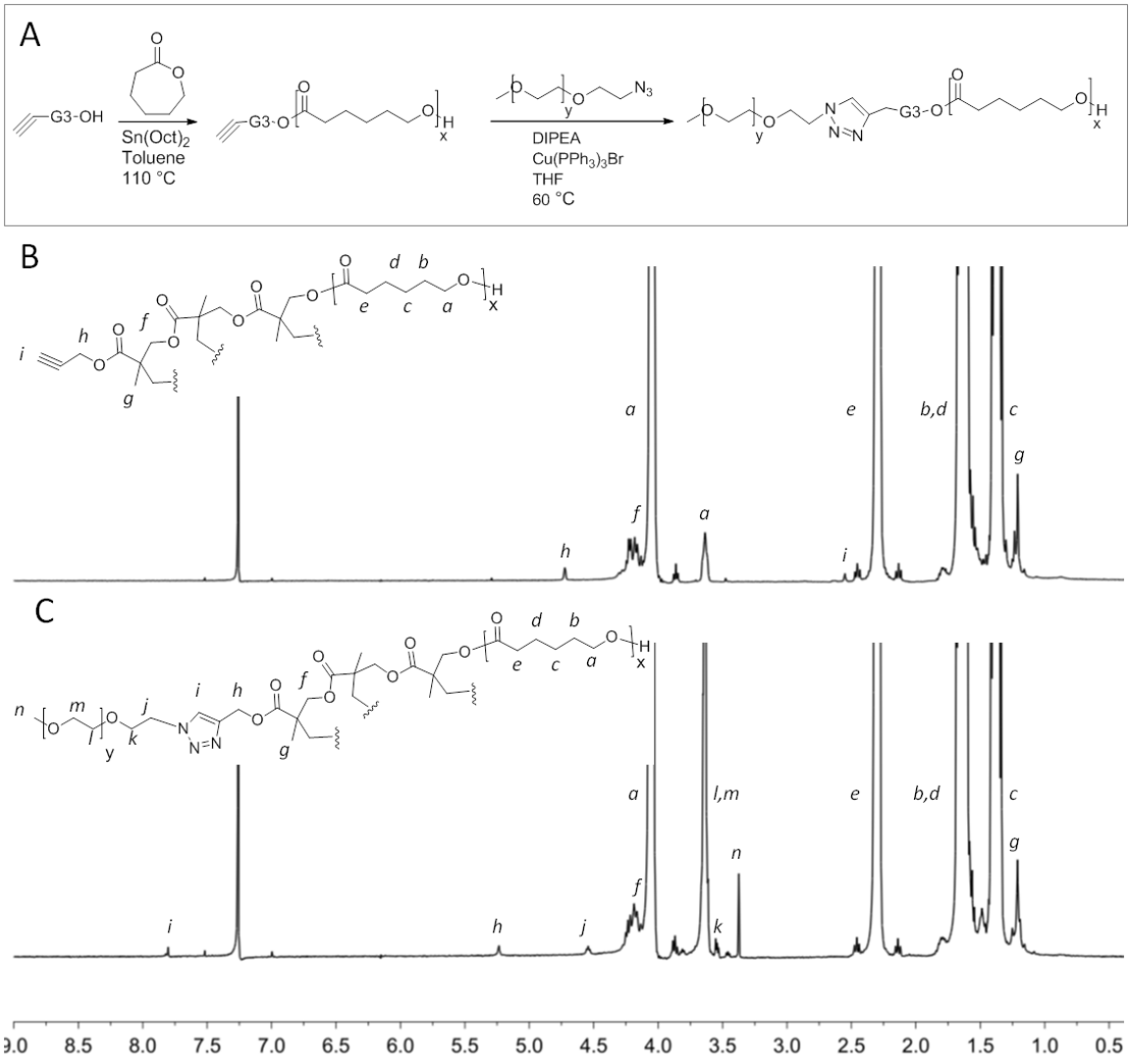

Figure 4-5. Synthesis of the PEG-Gn-PCL LDL via ROP of ε-CL and CuAAC reaction (A). ^{1}H-NMR spectra of the alk-G3-PCL_{30} (B) and PEG_{2k}-G3-PCL_{30} materials (C) in $CDCl_3$

4.2.1.2 Formation of honeycomb films

The library of materials was used to generate honeycomb films via the BF method. Films were cast from the LDL materials in benzene (50 μl of a 1 mg/ml solution) on glass substrate under 95 % relative humidity. Observation of the films by optical microscopy and SEM revealed the influence of the dendritic linker on the formation of ordered arrays (Figure 4-6). With increasing generation of the dendritic linker, the ordering of the films improved, a well-ordered morphology being achieved for the PEG_{2k}-G3-PCL_{30} LDL having 8 branches. For both the linear PEG_{2k}-G0-PCL_{240} and the branched PEG_{2k}-G1-PCL_{120}, small wall cavities are present in between the larger pores. Closer examination of the film cast from the PEG_{2k}-G3-PCL_{30} hybrid exposed a well-ordered structure with a monolayer of large open pores ≈ 2.5 μm in diameter (Figure 4-7 A and B). Investigation of the topography of the films by AFM revealed a wall thicknes of 200 nm and a pore depth of 150 nm (Figure 4-7C).

Table 4-1. Characterization of synthesized materials.

Sample	No. arms	$M_{n,\ theo}$ (g/mol)	M_n [a] (g/mol)	$Đ_m$ [a]	R_g [b] (nm)	T_m [c] (°C)	ΔH_m [c] (J/g)	γ [d] (mN/m)	CA_{flat} [e] (°)	$CA_{isoporous}$ [e] (°)	ϱ [f] (g/ml)
Alk-G0-PCL_{240}	1	27452	26400	1.21	5.8						
Alk-G1-PCL_{120}	2	27568	31300	1.13	6.2						
Alk-G2-PCL_{60}	4	27800	41100	1.13	7.1						
Alk-G3-PCL_{30}	8	28265	39300	1.11	6.8						
Alk-G4-PCL_{15}	16	29194	36300	1.06	6.3						
PEG_{2k}-G0-PCL_{240}	1	29452	26700	1.10	6.0	56.0	58.9	17.2 ± 0.4	75 ± 3	83 ± 11	0.054
PEG_{2k}-G1-PCL_{120}	2	29568	30800	1.03	6.8	54.5	51.9	19.1 ± 0.2	70 ± 1	86 ± 10	0.037
PEG_{2k}-G2-PCL_{60}	4	29800	36400	1.30	6.7	54.5	59.9	22.3 ± 0.4	77 ± 1	121 ± 5	0.039
PEG_{2k}-G3-PCL_{30}	8	30265	35400	1.08	7.0	52.9	58.3	19.1 ±0.1	73 ± 1	119 ± 3	0.035
PEG_{2k}-G4-PCL_{15}	16	31194	34000	1.03	6.3	47.8	43.9	15.8 ±0.2	73 ± 2	86 ± 4	0.049
PEG_{2k}-S-G3-PCL_{30}	8	30371	40600	1.07	/	52.2	56.1	18.6 ± 0.2	71 ± 6	110 ± 6	/
PEG_{2k}-G3-PLA_{30}	8	37505	37900*	1.04*	/	/	/	25.9 ± 0.1	79 ± 3	113 ± 6	/
PCL_{240}-G3-TEG-THP	8	31262	36500 *	1.24	/	55.3	51.1	25.7 ± 0.2	80 ± 2	95 ± 7	/

[a] Determined from THF SEC using conventional calibration. [b] Determined from THF SEC using triple detection. [c] Determined using DSC. [d] Determined from pendant drop experiment. The standard deviation was based on five measurements. [e] Measured on isoporous films. The standard deviation was based on five measurements. [f] Calculated from results obtained from THF SEC. * Determined from $CHCl_3$ SEC.

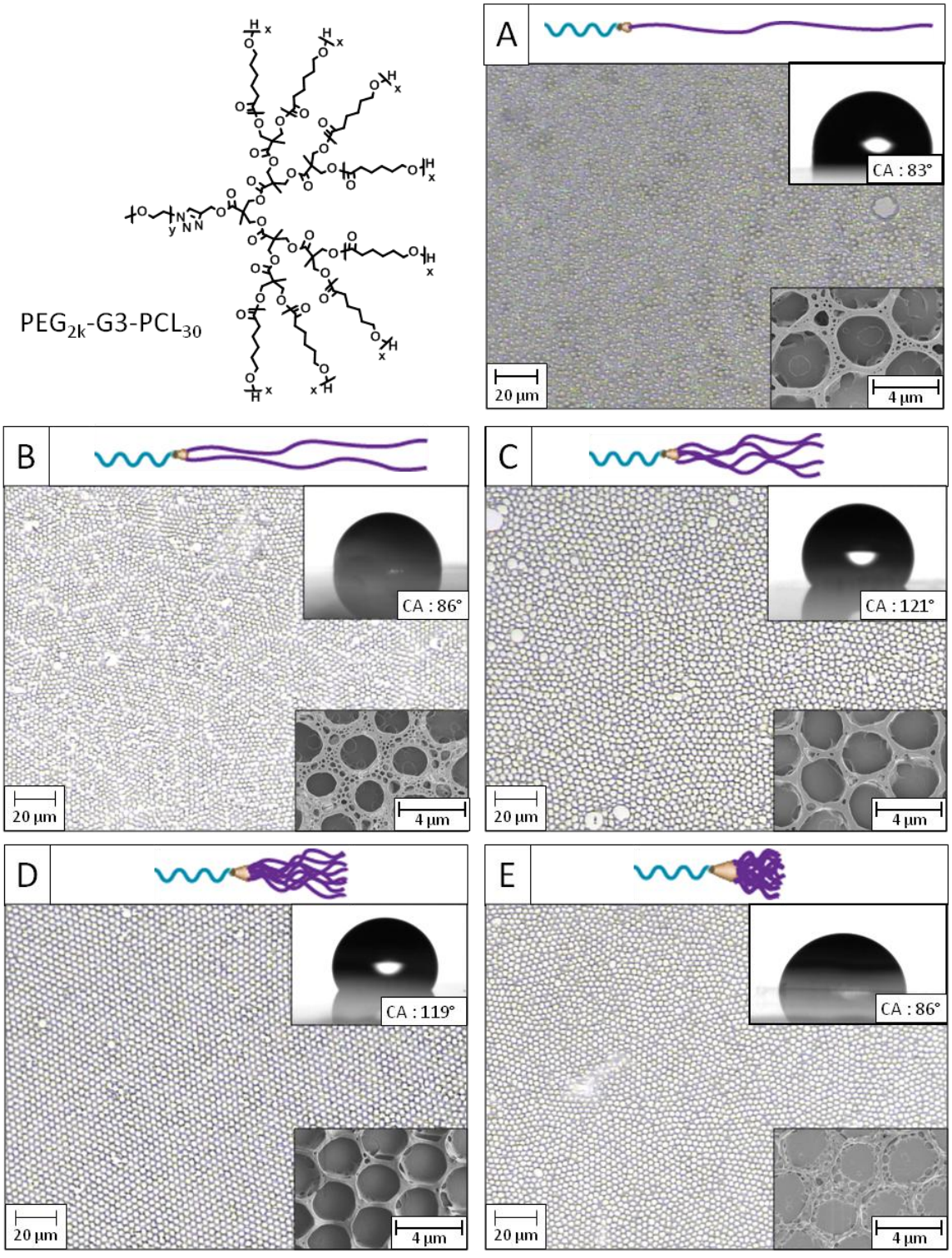

Figure 4-6. Structure of the PEG_{2k}-G3-PCL_{30} LDL hybrid (top left). Optical microscopy images of films cast from PEG_{2k}-G0-PCL_{240} (A), PEG_{2k}-G1-PCL_{120} (B), PEG_{2k}-G2-PCL_{60} (C), PEG_{2k}-G3-PCL_{30} (D) and PEG_{2k}-G4-PCL_{15} (E). Insert: image of water contact angle taken directly after deposition of a droplet (up) and SEM micrograph of the film (1.0 kV, x12k) (bottom).

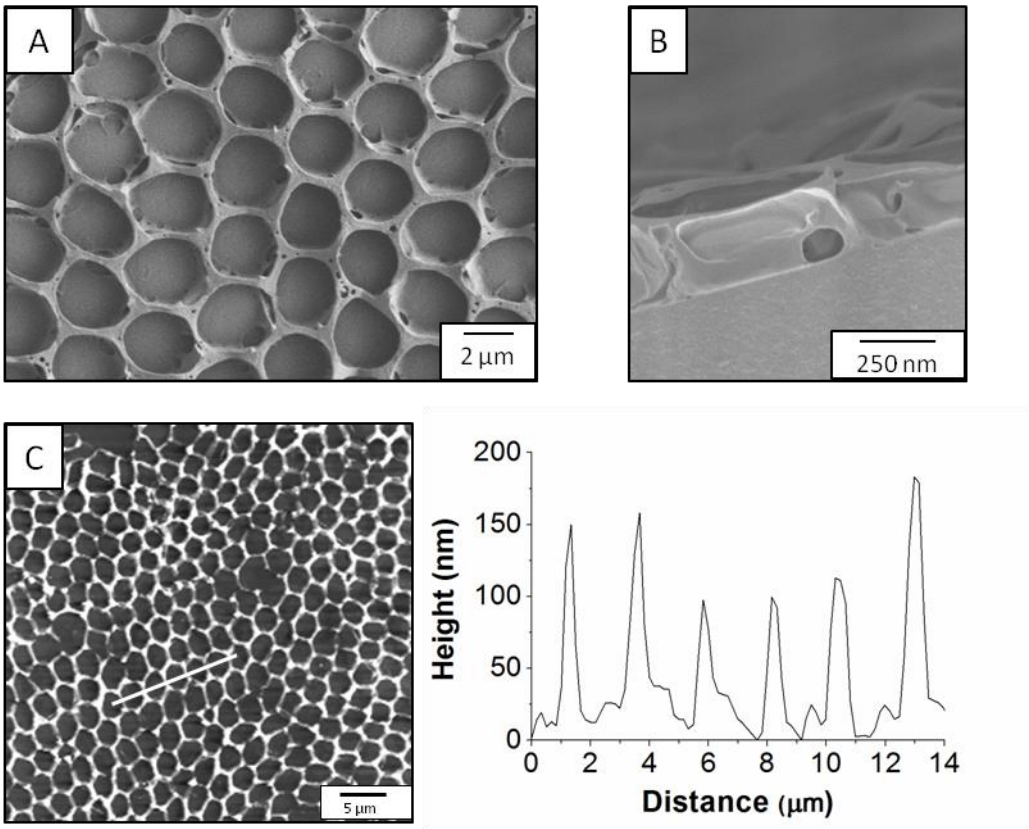

Figure 4-7. SEM micrograph of the top (A) and cross-section (B) and AFM image and profile (C) of a honeycomb film cast from PEG_{2k}-G3-PCL_{30}. The white line on the AFM image shows were the profile was extracted.

The wide opening of the pores is due to the relatively low interfacial tension of the PEG_{2k}-G3-PCL_{30} solution that does not allow the polymer to completely engulf the water droplet. The changes in surface morphology from a flat surface to an ordered porous surface significantly increased the hydrophobic nature of the film with an increase in water contact angle from 73° to 119°. Increasing the number of branches to 16 with the fourth generation dendron disrupts the ordering. This effect is probably due to the decrease in interfacial tension measured at 19.1 mN/m for the PEG_{2k}-G3-PCL_{30} and 15.8 mN/m for the PEG_{2k}-G4-PCL_{15}. This phenomenon could be related to a decrease in LDL orientation mobility as a consequence of the multiplicity of the short PCL chains.

To confirm this hypothesis, the density ρ of a unimolecular polymeric sphere in solution was evaluated using the following formula:

$$\rho = \frac{Mn/N_a}{\frac{4}{3}\,\pi\, Rg^3}$$

where Mn is the theoretical molecular weight of a molecule, N_a is the Avogadro constant and Rg is the radius of gyration of the molecule obtained by SEC in THF. A plot of the obtained density as a function of the number of PCL arms of the molecule is presented in Figure 4-8. When increasing the number of arms up to eight, corresponding to a third

generation dendron, the density of the sphere decreases. The dendritic linker separates the chains and causes this decrease in density. Introducing a fourth generation dendritic linker has the opposite effect and result in an increase in density: sixteen chains are now attached to a small core and are therefore closer to each other, making the macromolecule more compact. The less compact and thus more flexible structure observed for the third generation linker facilitates the orientation of the LDL at the water-solution interface and thus favors the formation of a well-ordered film.

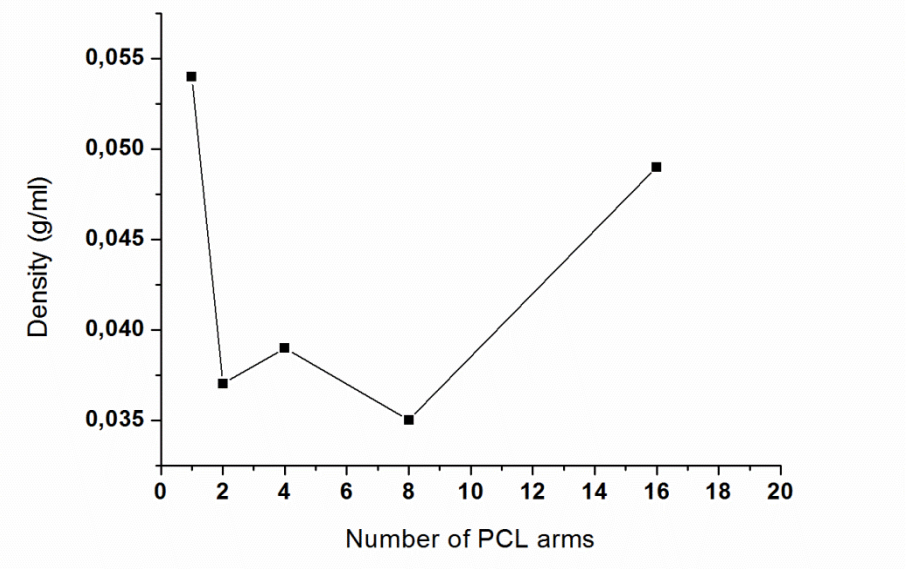

Figure 4-8. Density of a unimolecular polymeric sphere in THF as a function of the number of PCL arms. A black line connecting the datapoints was introduced to guide the eyes.

4.2.2 Thiol-ene based LDL hybrids

Considering the impact of the polymeric architecture on the film formation, a LDL based on UV-initiated TEC instead of CuAAC was synthesized. This material was designed to evaluate the impact of the coupling chemistry of the linear and dendritic blocks: in comparison to a quite stiff triazole ring, the thio-ether linkage is expected to introduce more flexibility into the structure. A hydroxyl terminated bis-MPA dendron of third generation possessing an allyl moiety at the focal point was used as initiator for the ROP of ε-CL. Consecutive coupling to a thiol-functional 2 000 g/mol PEG yielded the PEG_{2k}-S-G3-PCL_{30}.(Scheme 4-1) To allow for direct comparison with the PEG_{2k}-G3-PCL_{30} system, the length of the different blocks was kept constant.

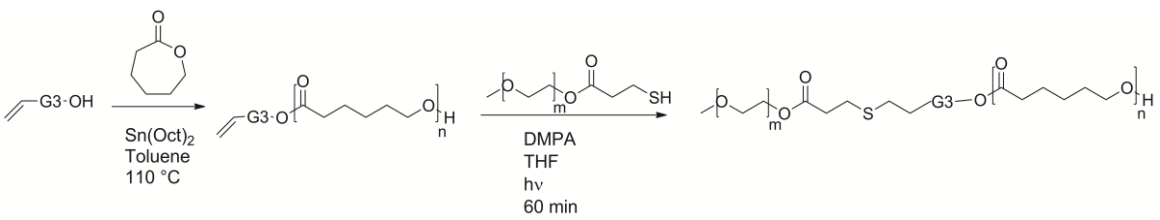

Scheme 4-1. Synthesis of a PEG_{2k}-S-G3-PCL_{30} LDL hybrid

Direct casting of the polymer at 1 mg/ml in benzene only led to the formation of an irregular film (Figure 4-9A). However, by lowering the concentration to 0.5 mg/ml, an ordered monolayer with pores of ≈3.5 μm in diameter was obtained (Figure 4-9B). This small change in morphology results in a decrease in contact angle from 110° to 92°. In this case, the higher flexibility of the material allows for better stabilization of the water condensate at lower concentration. On the opposite, at 1 mg/ml, the PEG_{2k}-S-G3-PCL_{30} hybrid accumulates at the surface of the organic solution and forms a compact layer that inhibits the stabilization of the forming droplets.[121] By decreasing the concentration, a better stabilization could be achieved, leading to a more ordered film.

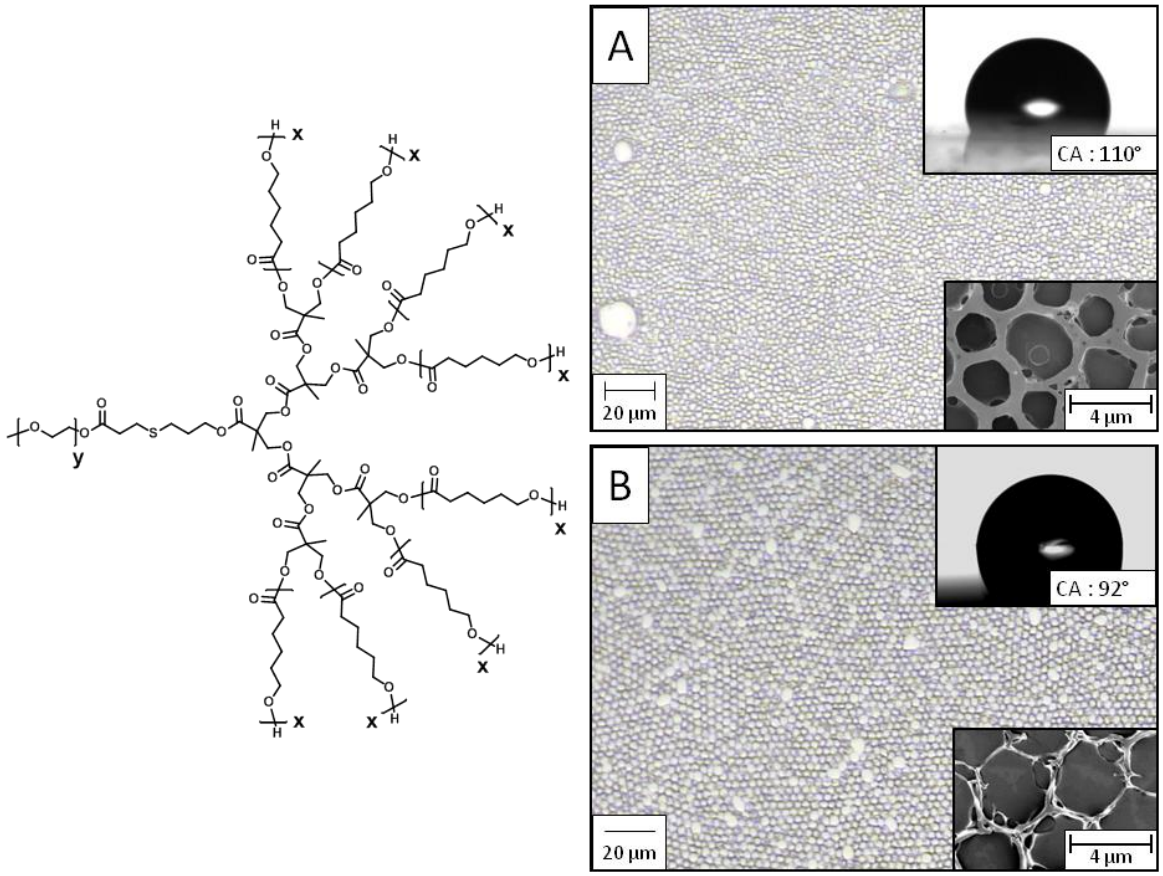

Figure 4-9. Structure of the PEG_{2k}-S-G3-PCL_{30} LDL hybrid (left). Optical microscopy images of films cast from PEG_{2k}-S-G3-PCL_{30} at 1 mg/ml (A) and 0.5 mg/ml (B). Insert: image of water contact angle taken directly after deposition of a droplet (up) and SEM micrograph of the film (1.0 kV, x12k) (bottom).

4.2.3 LDL hybrid based on amorphous PLA

So far, all the synthesized materials were exploiting semi-crystalline PCL as hydrophobic material. To extend the study, a LDL hybrid using amorphous PLA as biocompatible and hydrophobic segment was synthesized, keeping the third generation dendron as dendritic linker and aiming at a similar total molecular weight (Scheme 4-2). Similarly to the previous strategy, ROP of LA was initiated from the hydroxyl groups of a third generation alkyne-functional bis-MPA dendron. The polymerization was performed in toluene at 110°C using

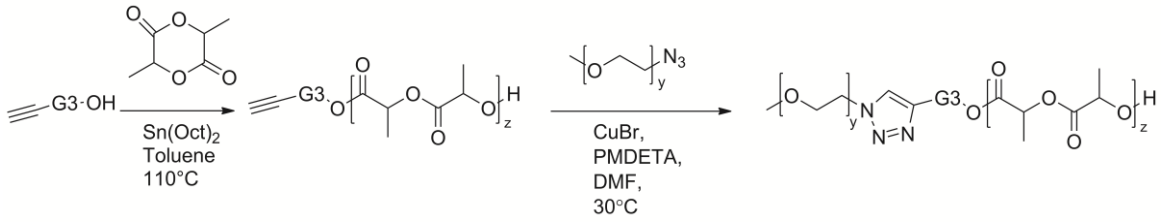

Scheme 4-2. Synthesis of a PEG_{2k}-G3-PLA_{30} LDL hybrid.

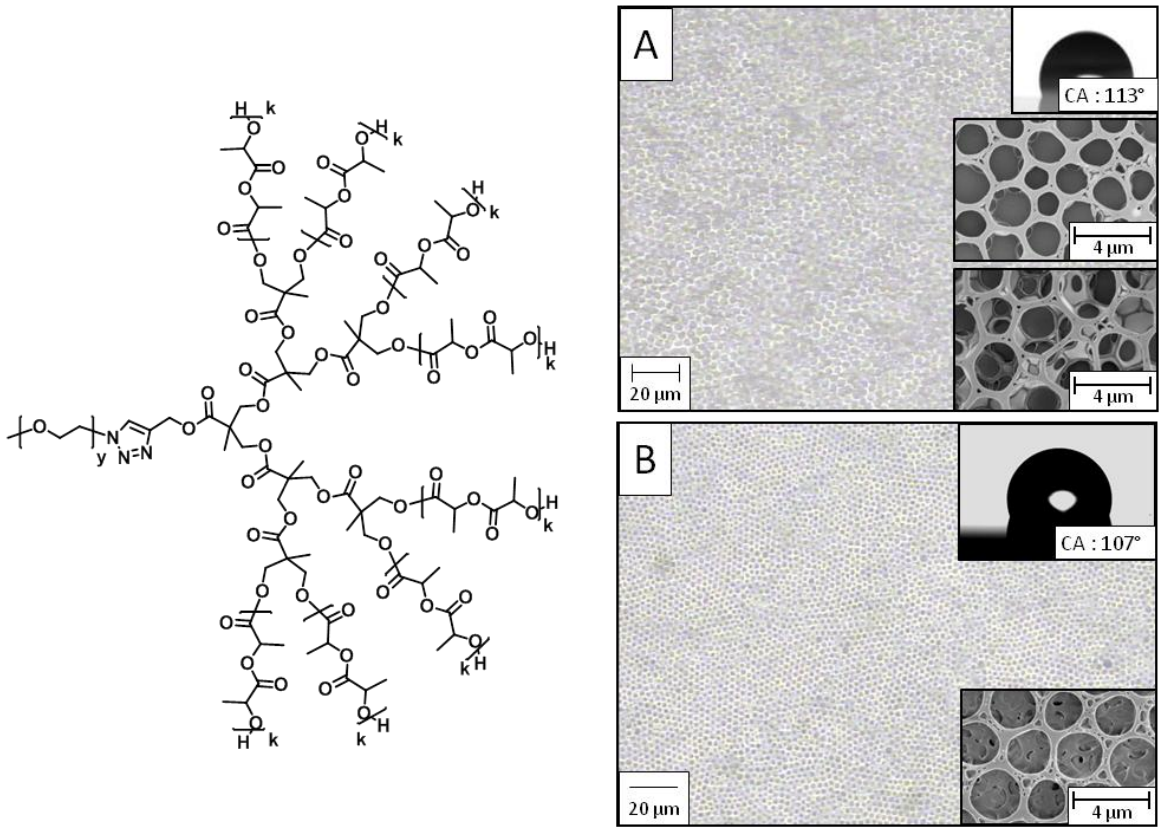

Figure 4-10. Structure of the PEG_{2k}-G3-PLA_{30} LDL hybrid (left). Optical microscopy images of films cast from PEG_{2k}-G3-PLA_{30} at 1 mg/ml (A) and 2.5 mg/ml (B). Insert: image of water contact angle taken directly after deposition of a droplet (up) and SEM micrograph of the film (1.0 kV, x12k) (bottom).

$Sn(Oct)_2$ as catalyst. After coupling with an azide-functional PEG of 2 000 g/mol, a new LDL was obtained with a narrow dispersity and a molecular weight of 37 900 g/mol. As expected, the obtained material was amorphous and presented a T_g at 36.2 °C, as measured by DSC.

Casting of a 1 mg/ml solution under 95 % RH resulted in a non homogeneous film presenting two types of structures: some parts of the film consisted of a monolayer of irregular pores while multilayers of interconnected pores were formed on other areas (Figure 4-10A). The presence of these two types of domains originates from different drying speeds. Rapid solvent evaporation, in the thinner parts of the film, causes the formation of a

monolayer of pores. On the opposite, as a longer drying time is required in the thicker parts of the film, water droplets can diffuse in the organic solution and assemble into multilayers. These disordered areas with interconnected pores suggest that poor stabilization of the film was achieved and that coalescence took place. Stabilization improved with increasing polymer concentration: films cast at 2.5 mg/ml presented an ordered array with a monolayer of open pores (Figure 4-10B).

4.2.4 Inverted PCL_{240}-G3-TEG LDL hybrid

4.2.4.1 Synthesis via ROP, CuAAC chemistry and anhydride coupling

To investigate the effect of the position of the blocks relative to the dendron, an inverted structure was devised having a single long PCL chain attached to the core of the dendron and short TEG arms at the periphery (Figure 4-4). This LDL was designed to display the same total PEG to PCL ratio as the previously synthesized materials. A third generation linker was selected since the most ordered films were generated by PEG_{2k}-G3-PCL_{30} in the preceding study. To obtain a similar architecture, an azide functionalized PCL was coupled to a TEG modified dendron (Scheme 4-3). ROP of ε-CL was initiated from benzyl alcohol with a targeted DP of 240. The terminal hydroxyl group was reacted with 6-azidohexanoic anhydride to yield N_3-PCL_{240}, which was then coupled to an alk-G3-OH dendron via CuAAC chemistry.

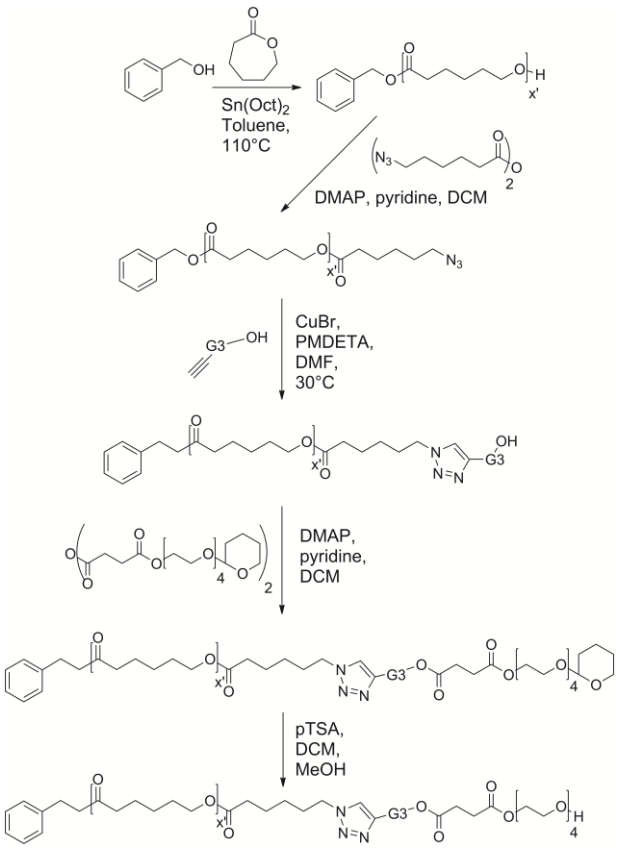

Scheme 4-3. Synthesis of the PCL_{240}-G3-TEG-OH inverted LDL hybrid.

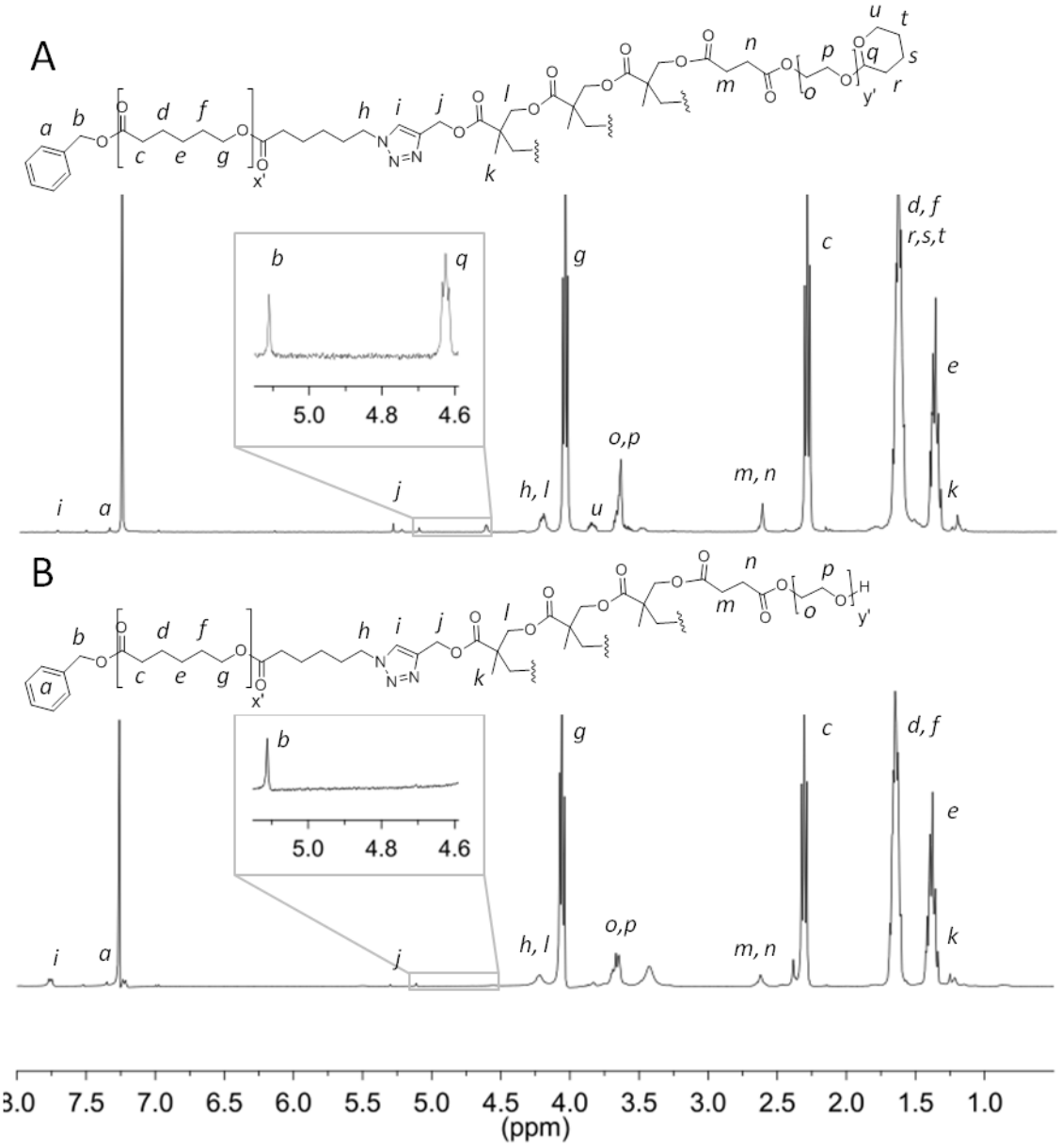

Figure 4-11. ^{1}H-NMR spectra of the PCL_{240}-G3-TEG-OH hybrid before (A) and after (B) deprotection of the THP groups.

In this case, the coupling reaction was performed in DMF at 30 °C using CuBr and PMDETA as catalytic system. Only 1.2 eq of alkynes to azide and 15 h were necessary to obtain full substitution. The hydroxyl groups of the dendron were subsequently functionalized with THP-protected TEG anhydride, generating the PCL_{240}-G3-TEG-THP LDL hybrid. Deprotection of the THP groups using p-TSA in methanol yielded the PCL_{240}-G3-TEG-OH, with eight hydrophilic hydroxyl groups. Full deprotection was confirmed by ^{1}H-NMR (Figure 4-11) with full disappearance of the triplet at 4.63 ppm (signal *q*) corresponding to the THP protective group. Characterization of the molecule by SEC gave a dispersity of 1.24 and DSC analysis indicated a semi-crystalline nature with a T_m and ΔH_m similar to the one measured for the PEG_{2k}-G3-PCL_{30} system, Table 4-1.

4.2.4.2 Formation of ordered porous films

Independently of the casting conditions (solvent, concentration, humidity), no ordered porous film could be obtained from the PCL_{240}-G3-TEG-OH system. One explanation could be the too high hydrophilicity of the molecule with 8 short hydroxyl-terminated TEG chains that could induce poor stabilization of the condensing water droplets. However, the less hydrophilic PCL_{240}-G3-TEG-THP, which has an interfacial tension of 25.7 mN/m, could produce ordered porous films when cast under suitable conditions. Casting of 50 µl of a 1 mg/ml solution in benzene under 95 % RH led to the formation of an ordered porous array with a pore diameter of ≈ 4 µm and a CA of 95 ° (Figure 4-12). Exposure of the film to *p*-TSA in methanol resulted in the regeneration of the terminal hydroxyl functionalities by deprotection of the THP groups. As a consequence the hydrophilicity of the film increases, as indicated by the decrease in contact angle from 95° to 74°. The deprotection did not affect the porosity of the film. However, the pore walls were found thinner after deprotection, suggesting a rearrangement of the polymeric chains in methanol (Figure 4-12). This hydroxyl functional porous film could potentially be used as template for further functionalization reactions.

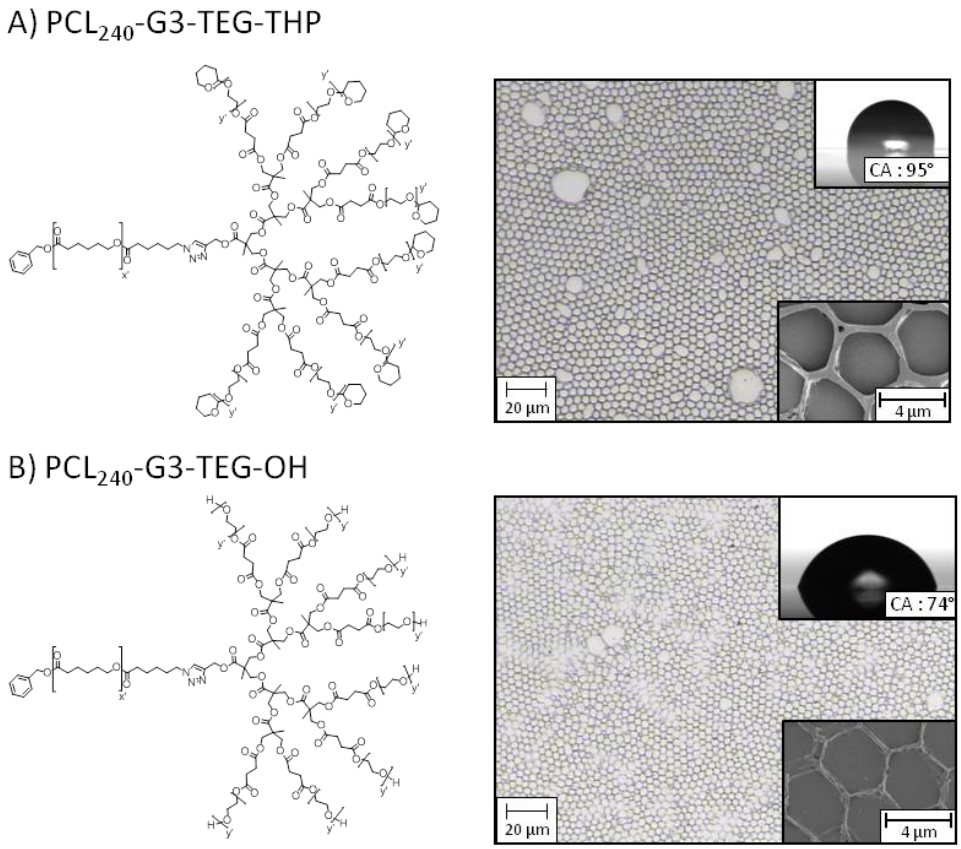

Figure 4-12. Structure and optical microscopy images of honeycomb films cast from PCL_{240}-G3-TEG-THP (A) and PCL_{240}-G3-TEG-OH (B). Insert: CA angle image taken directly after deposition of a water droplet (top) and SEM micrograph (1 kV, x12k) (bottom)

4.3 MACROTHIOLS AS VERSATILE TOOLS FOR THE PREPARATION OF DENDRITIC MATERIALS

Efficient coupling of dendrons to various polymeric cores is a simple way to access sophisticated functional dendritic structures. So far, bis-MPA dendrons functionalized with an alkyne moiety were conjugated to diverse macromolecules via CuAAC reaction. However, remaining traces of toxic copper can be a great concern for biological applications. An alternative is to exploit the copper-free and UV-initiated TEC chemistry to achieve advanced and well-defined architectures. Since thiols are highly reactive, they can couple to a wide range of molecules under mild conditions and can thus be exploited in numerous fields such as electronics, optics or for biological applications. Despite their interesting features, the commercial availability of thiols is today mainly limited to low molecular weight compounds or PEG-based structures. Therefore enlarging the collection of available large molecular weight thiols is of great interest. Hence the synthesis of high molecular weight dendritic macrothiols and their ability to efficiently couple to various core molecules via TEC chemistry were investigated (Figure 4-13).

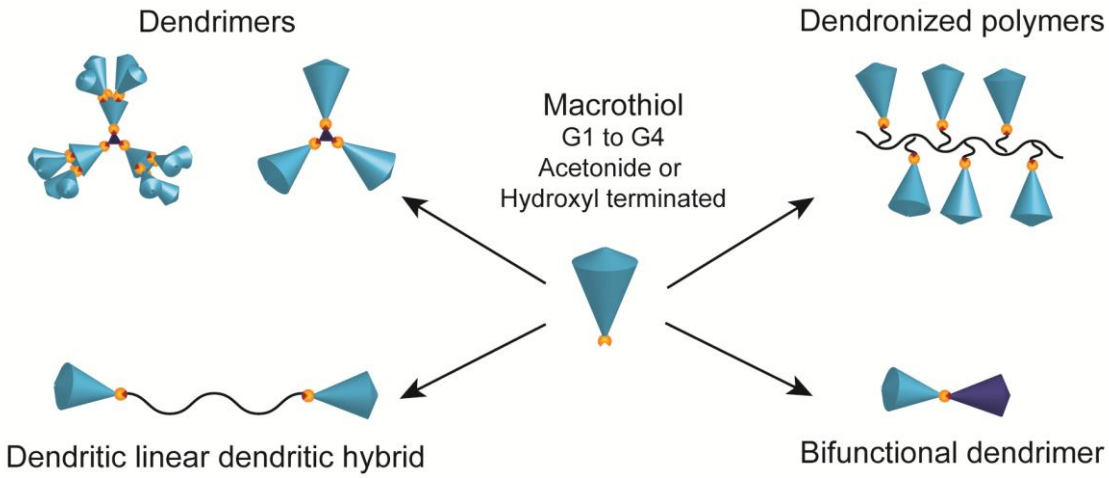

Figure 4-13. Overview of the dendritic library synthesized by coupling of macrothiols to various polymeric cores.

4.3.1 Synthesis of macrothiols

Bis-MPA dendrons of generation 1 to 4 functionalized with a thiol group at the focal point and either acetonide- or hydroxyl-terminated were prepared starting from a disulfide core (Scheme 4-4). Dendrimers up to generation four were synthesized by iterative growth and activation steps using acetonide-protected bis-MPA anhydride as monomer. Characterization of the materials by SEC confirmed the low dispersity of the structures (Figure 4-14A). Once the desired generation was reached, the disulfide bond was selectively cleaved to generate the macrothiol of identical generation. Cleavage was performed on the acetonide terminated dendrimers under inert atmosphere using DTT and TEA in an optimized disulfide:DTT:TEA molar ratio of 1:2:4. The reaction was monitored by MALDI-

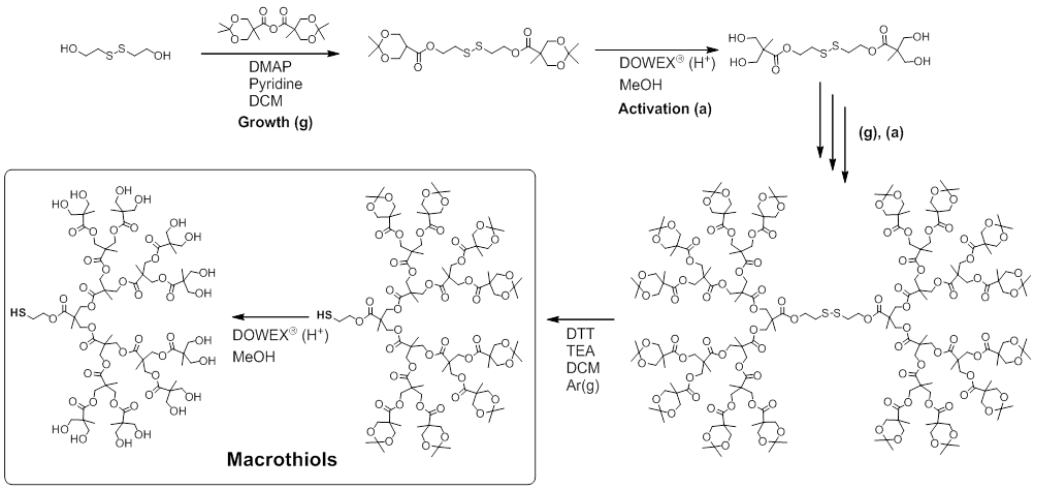

Scheme 4-4. Synthesis of the macrothiols from a disulfide core.

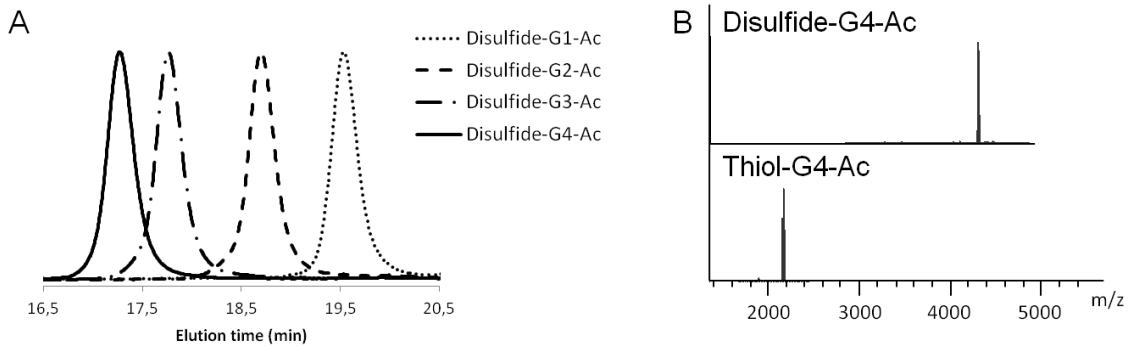

Figure 4-14. SEC traces of the acetonide-terminated dendrimers and MALDI-Tof spectra of the generation four acetonide-terminated disulfide and macrothiol.

TOF MS (Figure 4-14B) and after purification of the products by flash chromatography, pure compounds were isolated in yields above 80 % and with low dispersities. The solubility of the macrothiols could be tailored by deprotection of the acetonide groups using acidic DOWEX® resin: while the acetonide protected molecules were only soluble in organic solvents (DCM, THF, acetonitrile…), the hydroxyl terminated analogues could be dissolved in water or methanol.

Analysis of the materials by MALDI-TOF MS after one month storage under argon at room temperature revealed that the macrothiols were stable against spontaneous disulfide formation. This approach permits the facile synthesis of macrothiols having molecular weight up to 2140 g/mol (HS-G4-Ac).

4.3.2 Synthesis of advanced dendritic materials via TEC chemistry.

The ability of these macrothiols to be efficiently coupled to various polymeric cores was investigated through the synthesis of a dendritic library comprising dendrimers, bifunctional dendrimers, dendronized polymers and DLD hybrids. Initially the synthesis of monodisperse dendrimers was investigated: acetonide-terminated macrothiols of generation three (HS-G3-Ac) were reacted to a trifunctional allylic triazine core.

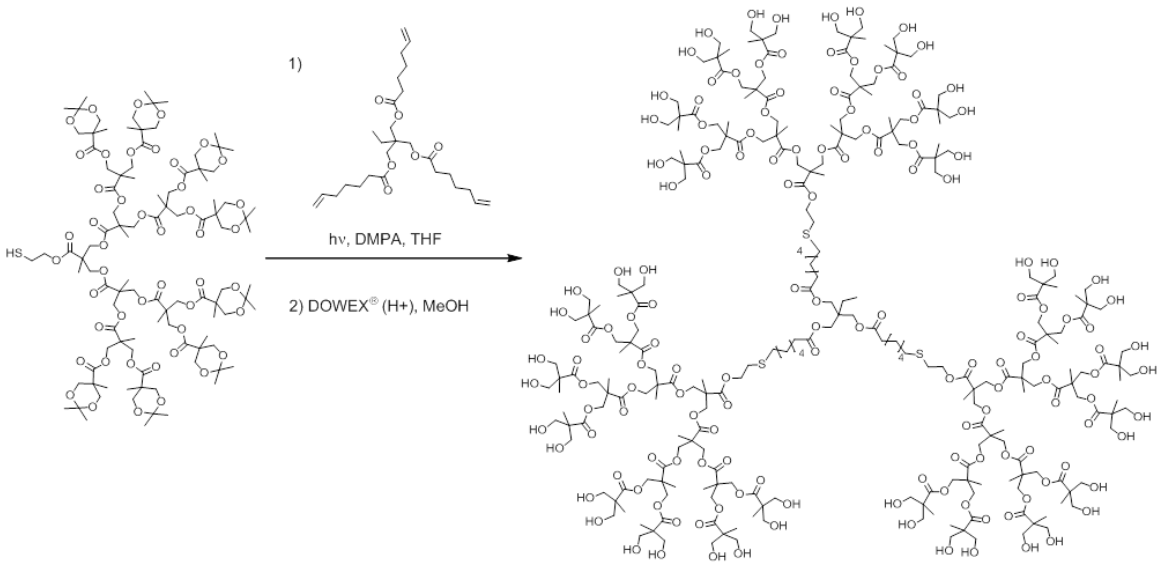

Scheme 4-5. Synthesis of a fourth generation dendrimer via TEC coupling.

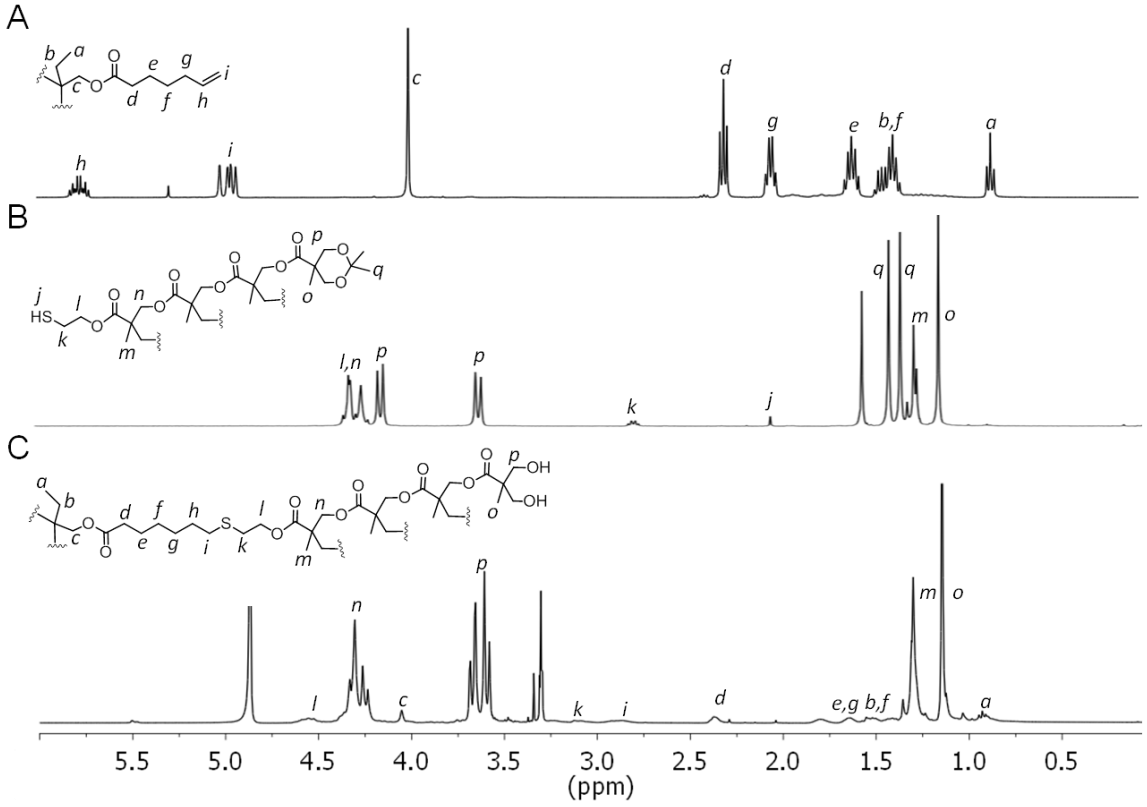

Figure 4-15. ^{1}H-NMR spectra of the trifunctional allylic TMP core recorded in $CDCl_3$ (A), the acetonide-terminated generation four macrothiol recorded in $CDCl_3$ (B) and the hydroxyl-terminated generation four dendrimer recorded in MeOD(C).

To ensure full miscibility of the starting materials with the DMPA initiator, a small amount of THF was introduced in the reaction vessel. Disulfide formation was suppressed by purging the system with argon before UV exposure. A slight excess of thiol (2 eq per alkene group) and 30 min irradiation were sufficient for the reaction to reach completion. However, reaction of HS-G4-Ac with the triazine core yielded only the disubstituted product, regardless of the irradiation time or excess of thiol used. This is related to the limited accessibility of the triazine core after attachment of the first two dendrons due to steric hindrance. To circumvent this problem the use of a more extended core was envisioned: a twofold excess of HS-G4-Ac macrothiols were reacted with a triallylic core derived from TMP(Scheme 4-5). After acidic deprotection of the isolated product, a fourth generation bis-MPA dendrimer was obtained in a total yield of 58 %. The reaction was followed by MALDI-TOF MS and ^{1}H-NMR (Figure 4-15). The absence of signals at 4.97 ppm and 5.78 ppm corresponding to the allylic protons as well as the disappearance of signal at 2.80 ppm related to the protons in alpha position to the thiol group confirm that full substitution of the core material has been obtained and that excess thiol has been efficiently removed. Moreover, the shift of the two doublets at 3.64 ppm and 4.14 ppm into a new signal at 3.62 ppm indicates that full removal of the ketal groups has been achieved.

Given the successful preparation of the fourth generation dendrimer, the synthesis of more complex bifunctional dendrimers was explored. Due to their nature, bifunctional dendrimers can easily be functionalized to include dual features, such as fluorescence and targeting moieties.[122] Therefore, such structures are elegant candidates for application driven research. Bifunctional dendrimers were achieved by TEC coupling of an acetonide-protected macrothiol with a complementary hydroxyl functionalized bis-MPA dendron having an allyl group at the focal point (Scheme 4-6A). Coupling of generation three materials generated the bifunctional third generation dendrimer in 76 % yield after simple purification by precipitation. A fivefold excess of thiol and 1 h of irradiation were necessary to obtain full conversion of the alkene groups.

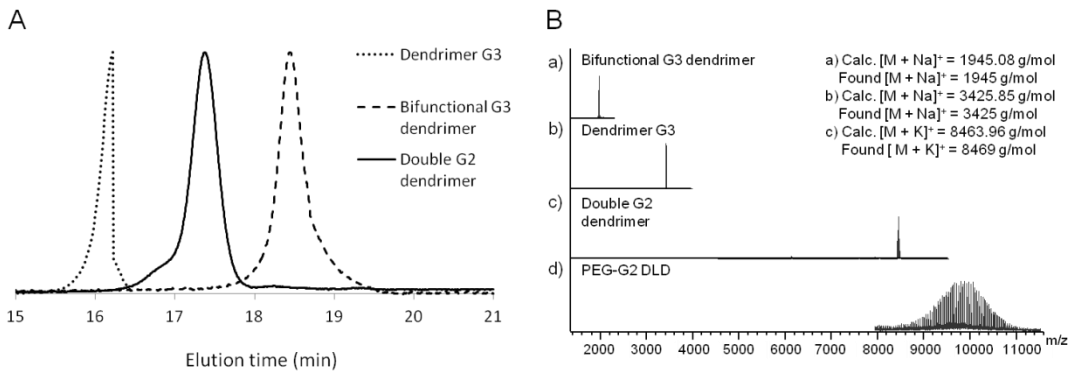

Figure 4-16. SEC traces (A) and MALDI-TOF spectra (B) of various macromolecules obtained via TEC reaction of macrothiols.

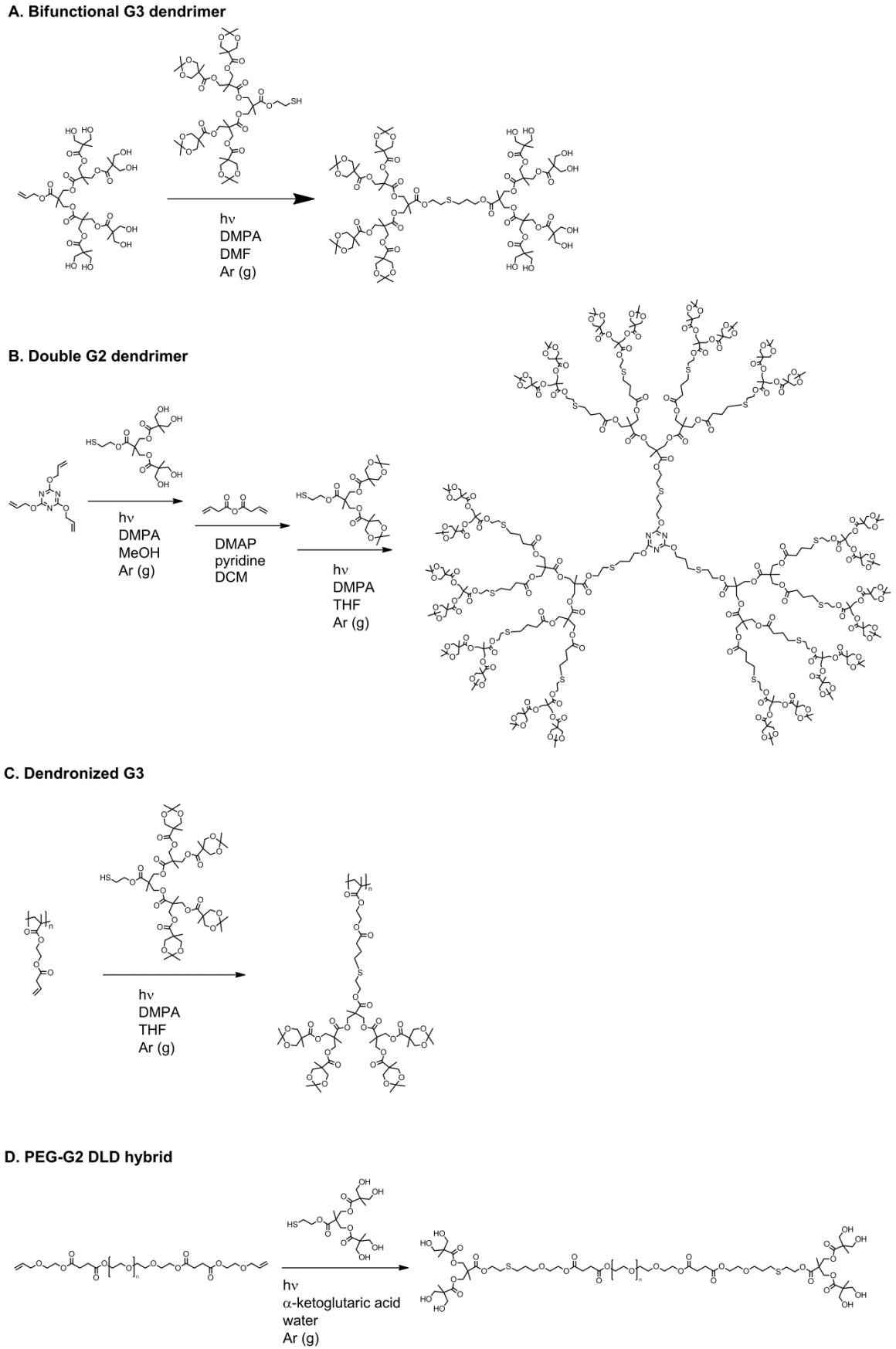

Scheme 4-6. Synthesis of a bifunctional dendrimer of third generation (A), a double generation two dendrimer (B), a dendronized polymer (C) and a DLD hybrid based on PEG and second generation dendrons (D).

The ability of the macrothiols to generate sophisticated molecules was further evaluated via the double convergent approach (Scheme 4-6B). Starting from a trifunctional allylic core, TEC of HS-G2-OH followed by post-functionalization of the hydroxyl groups with but-3-enoic anhydride yielded a second generation dendrimer decorated with 12 alkenes. 40 min of irradiation and 1.5 eq of thiol per alkene groups were sufficient to achieve full conversion. In the next step, the alkene functionalities were coupled to HS-G2-Ac and, after 30 min of UV exposure and consecutive purification, a fully substituted dendrimer with 24 acetonide groups was obtained in 74 % yield. Characterization by SEC and MALDI-TOF MS confirmed the synthesis of a flawless structure (Figure 4-16).

The library was extended with the synthesis of dendronized polymers via a "grafting to" approach: dendritic wedges were coupled to a linear polymer possessing allylic pendant groups (Scheme 4-6C). A fully allylated poly(HEMA) was obtained by coupling of but-3-enoic anhydride to the hydroxyl groups of the repeating unit using DMAP and pyridine. The polymer was then reacted with macrothiols of generation 1 to 3 with either hydroxyl or acetonide terminal groups. Increasing amount of macrothiols and longer reaction times were required with increasing dendron generation (Table 4-2), due to steric hindrance. After selection of an appropriate solvent, the reaction could be performed with both acetonide or hydroxyl terminated macrothiols.

Table 4-2. Overview of the synthesized dendronized polymers

Dendron generation	End-groups	Allyl:thiol ratio	Irradiation time (min)	Yield
G1	Acetonide	1:1.5	20	80 %
G1	Hydroxyl	1:1.5	15	76 %
G2	Acetonide	1:3	60	68 %
G3	Acetonide	1:4	90	61 %

Finally, exploiting the versatility of the TEC chemistry that can be performed in both organic solvent and water, the synthesis of a water-soluble DLD was explored. Reaction of a PEG-diallyl with HS-G2-OH macrothiols in water using α-ketoglutaric acid as initiator yielded the fully substituted DLD (Scheme 4-6D). Given the high molecular weight of the PEG (8 000 g/mol) a fivefold excess of thiols per allyl group and 30 min UV irradiation were required to complete the reaction. SEC and MALDI-TOF MS characterizations of the synthesized products are presented in Figure 4-16 and confirmed the monodisperse nature and purity of the materials.

4.4 PREPARATION OF HIGHLY FUNCTIONAL AND THERMALLY STABLE POROUS FILMS

The previous studies revealed that ordered porous films could be formed from linear-dendritic linear hybrids for which the introduction of the dendritic linker favored the pore formation. By casting and subsequent activation of the film, a functional surface presenting hydroxyl groups could be obtained. A new set of LD materials was therefore developed using the newly synthesized macrothiols as dendritic components. In this case, the dendritic wedge was exploited to introduce multifunctionality inside the pores of the film. Moreover the linear block could be modified to introduce cross-linkable groups that could be utilized to improve the thermal stability of the films.

4.4.1 Synthesis of alkyne functional LD hybrids and porous film formation

The overall synthesis of the LD hybrid relies on ATRP of a HEMA derivative, TEC chemistry and anhydride reactions (Scheme 4-7). ATRP was chosen as controlled polymerization method due to its versatility towards solvents and monomers as well as tolerance to various functional groups. The linear block of the hybrid was designed to introduce hydrophobicity into the structure, hence HEMA was modified with benzylidene-protected bis-MPA anhydride and subsequently polymerized from HO-EBiB using CuCl, $CuCl_2$ and bipyridyl in anisole aiming at a molecular weight of 22 000 g/mol. ([HEMA]/[HO-EBiB]/[CuCl]/[$CuCl_2$]/[Bipy] = 2*DPtarget:1:1:0.1:2). The available hydroxyl group of the initiator was functionalized with 4-pentenoic anhydride allowing for TEC with a HS-G2-OH. Due to the high molecular weight of the linear block, a 1:10 allyl to thiol ratio was required to ensure full conversion of the alkene groups within 30 min. The hydroxyl groups of the dendritic wedge were further reacted with alkyne-TEG anhydride to yield poly(HEMA-Bz)$_{22k}$-G2-TEG-Alk. In addition to introducing hydrophilicity to the molecule, the TEG spacer also helps to direct the alkyne groups inside the pores, making them available for postfunctionalization reactions.

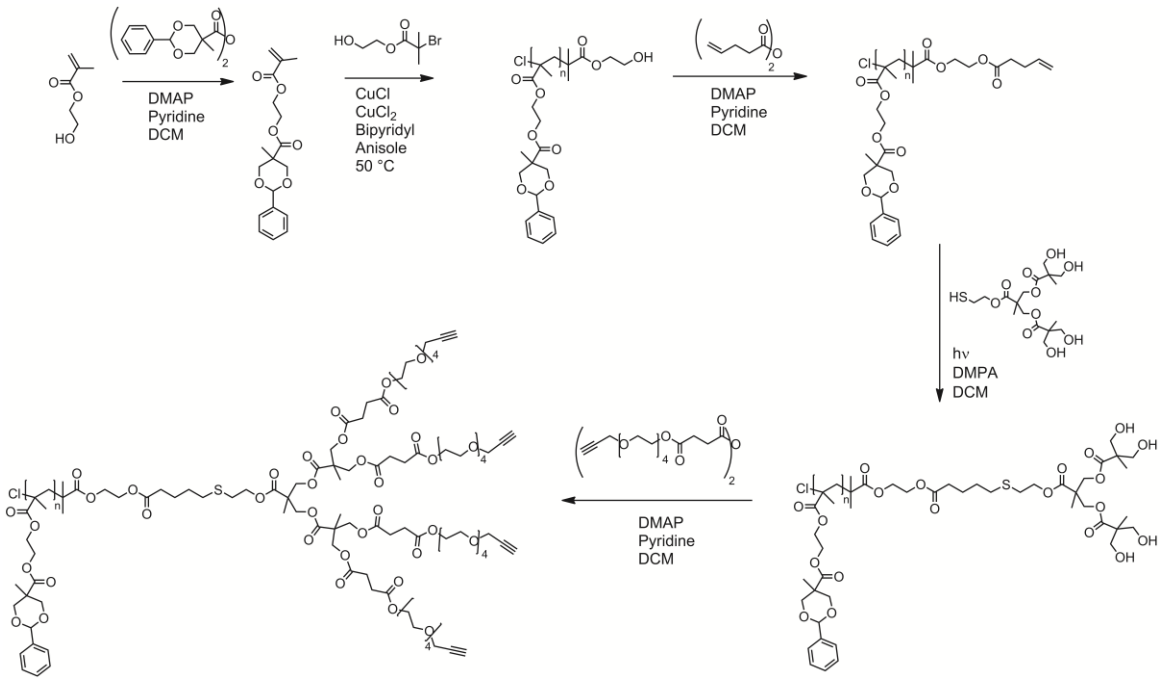

Scheme 4-7. Synthesis of a poly(HEMA-Bz)$_{22k}$-G2-TEG-Alk.

The aptitude of this polymer to form porous films via BF was later evaluated by casting a polymer solution under different casting conditions. Interestingly, different topographies could be obtained at different concentrations. When cast on a glass substrate at a concentration of 20 mg/ml in chloroform under 95 % RH at room temperature, the polymer formed films with narrow surface holes (≈ 800 nm in diameter) and large underlying cavities (≈ 2.5 μm in diameter) (Figure 4-17A). In contrast, films cast at 2.5 mg/ml in chloroform on a glass substrate cooled down to 0 °C under 80 % RH presented multilayers of wide open pores (1.7 μm in diameter) (Figure 4-17B). The differences in morphology are related to differences in kinetics during the pore formation: at low polymer concentration and low temperature, water condenses relatively fast on the surface of the film while the organic solvent needs long time to evaporate. Therefore the water droplets have time to diffuse into the organic solution and several porous layers can form. Moreover, the low polymer concentration does not permit an encapsulation of the droplets of the top layer during the last stage of drying and consequently the film presents an open structure.

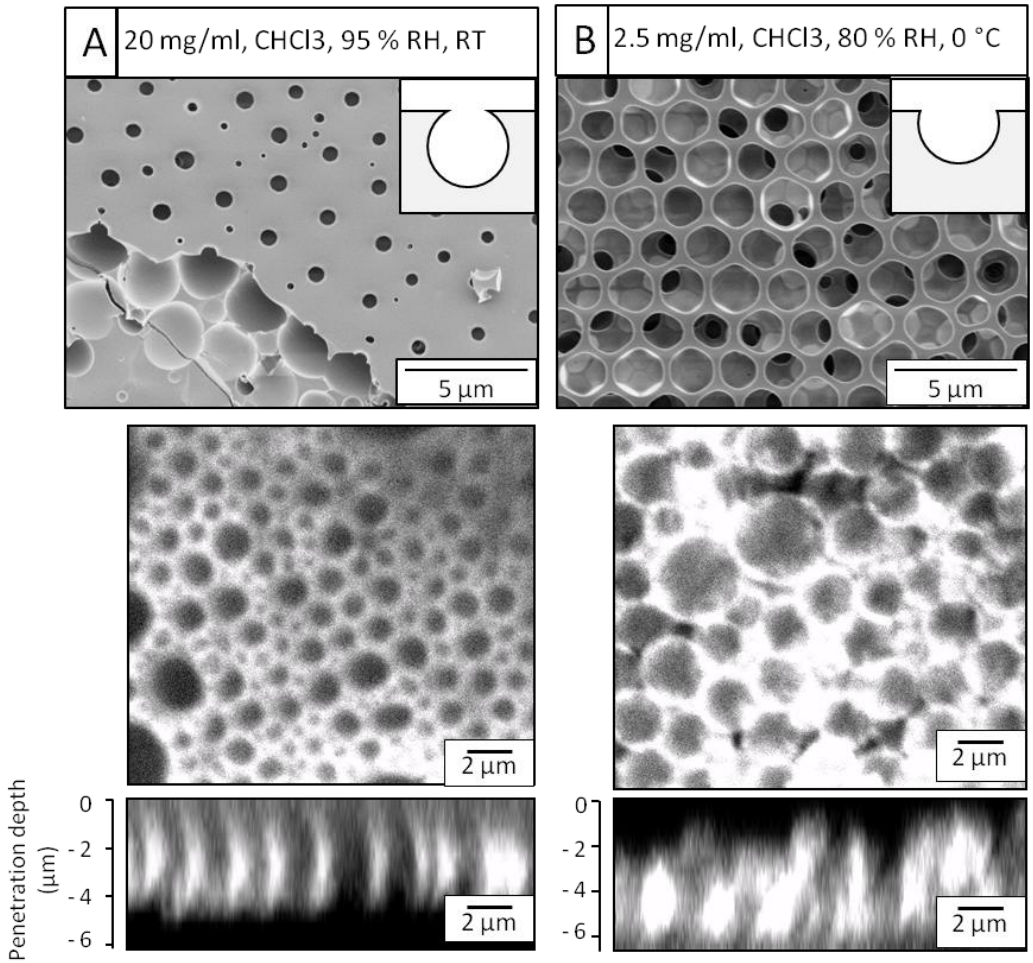

Figure 4-17. SEM (1kv, x6k) micrographs (top) and confocal fuorescence micrographs (middle) and depth profile (bottom) of porous films cast from poly(HEMA-Bz)$_{22k}$-G2-TEG-Alk at 20 mg/ml in $CHCl_3$ under 95% RH (A) and at 2.5 mg/ml in $CHCl_3$ under 80 % RH at 0°C (B). Fluorescence is visualized in white and the micrographs were taken at 1.6 µm (A) and 2.4 µm (B) under the surface.

To evaluate the availability of the alkyne groups, the cast films were labeled with fluorescent Rhodamine-B via CuAAC chemistry. The reaction was performed in water to preserve the structure of the film. A large excess of fluorophores (≥ 4 eq azide per alkyne) was used to ensure full conversion of the alkyne groups. Confocal fluorescence analysis was performed by recording the fluorophore emission within optical slices with 0.4 µm FWHM thickness and a depth profile was acquired by scanning sequential slices in the sample from top to bottom until no more fluorescence was detected. Fluorophores could be found on each film confirming the availability of the alkyne groups for CuAAC reaction (Figure 4-17). The slight changes in morphology observed as compared to the SEM images could originate from rearrangement of the polymers during labeling. Fluorescence could be measured over a thickness of ≈ 5 µm suggesting that the different surface topographies of the films did not affect the functionalization. The absence of fluorescence within the pores (appearing in black on the micrographs and depth profiles) indicates that excess of Rhodamine-B has successfully been removed.

4.4.2 Preparation of thermally stable honeycomb films

Even though the previously formed films can be activated in water at room temperature, improving their thermal stability would widen their range of possible functionalizations and applications. Thus the introduction of cross-linkable groups on the linear polymeric backbone was envisioned. Azide substituted poly(para phenyleneethynylene)groups are known to undergo thermal cross-linking at 300 °C, turning solvent-soluble films into free-standing insoluble films while maintaining the film morphology.[123] However the use of elevated temperature requires the use of initially stable films and we thus preferred UV as a milder cross-linking source. The easily functionalized HEMA allowed for random introduction of cross-linkable azide groups and hydrophobic benzylidene groups along the linear backbone. Poly(HEMA)$_{8k}$ was synthesized by ATRP in a water/methanol 50/50 solvent at 0 °C using CuCl, $CuCl_2$ and bipyridyl as catalytic system. The reaction was performed aiming at a DP of 65 reached at 80 % monomer conversion, identical to the one of the poly(HEMA-Bz)$_{22k}$-G2-TEG-Alk system. The functionalization of poly(HEMA)$_{8k}$ was performed as a pseudo one-pot anhydride reaction: benzylidene-protected bis-MPA anhydride was first reacted to a limited number of hydroxyl groups of the poly(HEMA) backbone after which an excess of 6-azidohexanoic anhydride was added to the reaction vessel to convert the unreacted hydroxyl groups. To maintain the hydrophobic character of the linear polymer, the benzylidene groups were targeted to cover 90 % of the hydroxyl groups. However, analysis of the ^{1}H-NMR spectrum of the polymer and comparison of the integrals of the signal at 3,2 ppm and 5.4 ppm corresponding to the azide and benzylidene

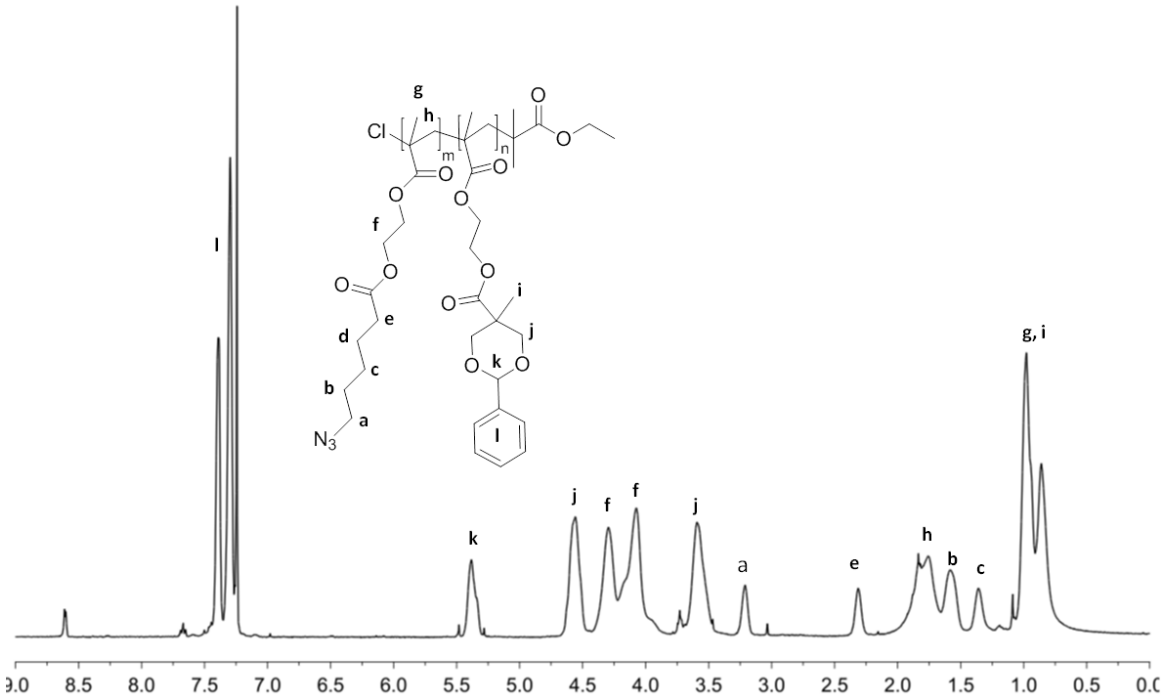

Figure 4-18. ^{1}H-NMR spectrum of the poly(HEMA-Bz-*ran*-HEMA-N_3) acquired in chloroform.

groups respectively revealed an actual azide to benzylidene ratio of 80/20 (Figure 4-18). This difference is probably due to traces of MeOH or water in the system that opened the benzylidene anhydride.

The pure poly(HEMA-Bz-*ran*-HEMA-N_3) was then cast on a glass substrate and its ability to cross-link into a thermally stable film was evaluated. After optimization of the casting conditions, a honeycomb film was obtained from a 10 mg/ml solution in chloroform cast at 75 % RH. The film presented 1 μm wide surface openings with underlying spherical cavities of 2.5 μm in diameter (Figure 4-19 left). Cross-linking of the film was subsequently performed by placing the as-cast film on the conveyor belt of a UV fusion lamp and exposing it to a total dose of 387 mJ/cm^2, without addition of initiator. The stability of the film was assessed by heating the film with 10 °C increments every 5 min. In comparison to a non-cross-linked film which started to lose its morphology at 50 °C (4 degrees above its T_g), the cross-linked film kept its morphology upon heating up to 200 °C (Figure 4-19 right).

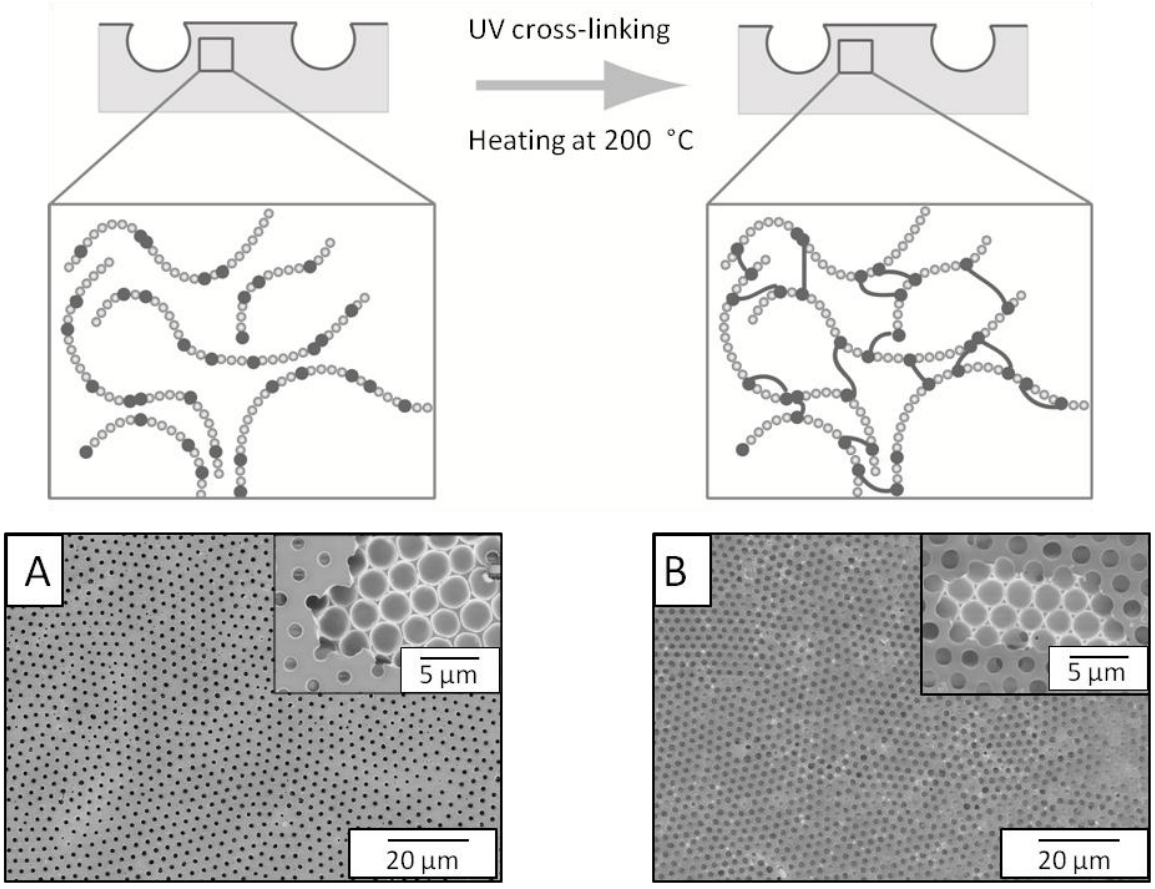

Figure 4-19. Schematic representation and SEM micrographs (1kV, x1k) of the poly(HEMA-Bz-ran-HEMA-N_3) honeycomb film before cross-linking (left) and after cross-linking and heating at 200 °C for 5 min (right). The inserts were taken after pealing of the top layer of the film with adhesive tape (1kV, x6k).

5. CONCLUSIONS

Ordered porous films were generated from a library of LDLs exploiting multifunctional bis-MPA dendrons as dendritic linker and using efficient CuAAC and TEC chemistries. The introduction of alkyne groups on the dendritic wedge allowed for an efficient postfunctionalization of the film, thus extending the scaffolding ability of the material. The achieved functional surfaces could find use in multiple applications for instance as sensors or in catalysis.

Prior to utilizing new materials in biological applications, their biocompatibility needed to be addressed. Hence, a degradation and toxicity study was performed on well-established bis-MPA dendrimers to confirm their biocompatibility. Evaluation of the degradation profile of a TMP-G4-OH dendrimer under physiological conditions, pHs ranging from 4.5 to 7.5 and temperature of 37 °C, revealed that the dendrimer undergo fast degradation via a depolymerization mechanism in alkaline conditions. Further, an MTT assay of immune competent cells exposed to the dendrimer or its structural components showed the non-cytotoxic nature of the materials. This study confirms the biocompatibility of these materials and supports their use in biological applications.

A library of amphiphilic LDL hybrids issued from biocompatible building blocks was later produced and utilized to evaluate the effect of the polymeric architecture of the formation of porous films via the BF method. Well-defined structures were achieved by combination of controlled ROP and efficient CuAAC and TEC reactions. ROP of hydrophobic ε-CL from the peripheral hydroxyl groups of bis-MPA dendrons followed by CuAAC between the alkyne groups located at the focal point of the dendron and a azide-functional PEG yielded amphiphilic semi-crystalline LDLs. Investigation of the effect of branching on the film formation by comparison of a library of materials having a constant total molecular weight but including dendrons of various generations, and thus different lengths of the PCL arms, revealed that the PEG_{2k}-G3-PCL_{30} material was best suited to form highly ordered films. This property was related to the low density of the polymer in solution which results in a higher flexibility of the chains and better stabilization of the condensing droplets. Interestingly, replacing the relatively stiff triazole linkage by a more flexible thioether bound in the structure led to formation of ordered films at lower polymer concentration, probably resulting from an enhanced stabilization of the water droplets. Ordered porous arrays could additionally be obtained from the fully amorphous PEG_{2k}-G3-PLA_{30}. Finally, the relative position of the linear blocks in the LDL was proven to be insignificant: highly ordered films could be generated from an inverted PCL_{240}-G3-TEG-THP structure. Deprotection of the THP under mild conditions in water regenerated the hydroxyl groups while preserving the

porous structure. This last approach permits the synthesis of activated porous film suitable for further functionalization reactions.

Efficient coupling of dendrons to other polymeric materials is a simple way to access dendritic linear hybrids. To further extend the range of achievable structures, bis-MPA dendrons functionalized with a thiol moiety at the focal point were synthesized and their ability to react with different allyl-functional cores was evaluated. Macrothiols of generation 1 to 4, either hydroxyl or acetonide terminated, were produced by divergent dendrimer growth initiated from a dihydroxyl-functional disulfide core followed by disulfide cleavage using DTT. The dendritic thiols were achieved in high yields and with molecular weight up to 2140 g/mol. Coupling of these macrothiols, to allylic cores via TEC reaction generated a comprehensive dendritic library that includes dendrimers, asymmetrical dendrimers, dendronized polymers and DLD hybrids. All the dendritic hybrids could be obtained in relatively good yields and high purity as confirmed by SEC and MALDI-TOF analyses. By appropriately tailoring the nature of the end-groups, hydrophilic macrothiols were obtained, allowing for construction of dendritic hybrids in water. The high reactivity of the thiols and versatility of the method renders the macrothiols attractive for a broad range of applications.

Finally a new set of LDs was synthesized capitalizing on the efficient coupling of macrothiols to allylic cores as well as on the effect of dendritic linkers on porous film formation. In this case, the dendritic wedge was used to introduce multifunctionality inside the pores of the film thereby allowing for further functionalization. An alkyne functional LD hybrid was synthesized by successive ATRP of a benzylidene-modified HEMA monomer, TEC reaction with a HS-G2-OH and activation with alkyne-functional TEG anhydride. Casting of the polymer under humid conditions followed by labeling with Rhodamine-B via CuAAC confirmed the availability of the alkyne groups for further post-functionalizations. In parallel, exploiting the facile modification of HEMA by anhydride coupling, cross-linkable azide groups and hydrophobic benzylidene units were randomly introduce along the linear HEMA backbone. Highly ordered porous films were successfully generated by BF on the random polymer. After exposure of the porous films to UV irradiation, the stability of the films could be increased by 150 °C. Combination of these two approaches could lead to highly stable and functional films with unlimited potential applications.

6. FUTURE WORK

Highly ordered micro- or nanoporous surfaces have the potential to be used in a myriad of applications due to their large surface area and high porosity. Since the BF method is a simple way to fabricate such surfaces, a better understanding of the parameters governing the pore formation would be of significant interest. Ideally, one would like to be able to select a specific morphology and know how to design a suitable polymer to obtain such morphology. Our studies have revealed that the density of the amphiphilic polymer is an important parameter for the formation of ordered structures. One interesting study would be the comparison of the densities of polymers issued from different monomers but having a similar architecture.

The development of highly functional and stable films is a promising concept. Combining the linear cross-linkable block with the dendron multivalency could lead to very interesting surfaces that could be used as sensors. One limitation of our system is the use of CuAAC chemistry to activate the functional surfaces since the toxicity of copper can be an obstacle when aiming at biological applications. Therefore, the use of the mild and biocompatible thiol-maleimide reaction could be a major advantage. This requires the development of a new set of materials functionalized with maleimides. Since thiols can be present in various proteins such as antibodies and enzymes, this would allow for coupling of these biological entities to the porous surface and hence would make their use as sensors possible.

Finally, even though the biocompatibility of the different building blocks is now established, a thorough degradation and biocompatibility study on materials built via CuAAC or TEC chemistry should be performed. These materials contain triazole and thioether linkages that could be cytotoxic. Moreover the addition of polymeric chains at the edges of the dendrons could significantly affect the degradation profile and thus the excretion of the products.

7. ACKNOWLEDGEMENTS

First of all, I would like to express my sincere gratitude to my main supervisor, Associate Professor Michael Malkoch for your help and guidance during these years. I have really learnt a lot working with you. Your many ideas and passion about research have been really inspiring. I also would like to thank my co-supervisor, Professor Anders Hult for accepting me as PhD student in the coating group. You have created a really good research group and a nice place to work at.

I also want to express my gratitude to the other seniors at the coating division. Professor Mats Johansson is thanked for all his help and interesting discussion during these years and for always being helpful with lab-related questions. Professor Eva Malmström is thanked for all her positive energy and for being an incredible person: how can you manage to be both professor and deputy president and still find time for your students? Assistant Professor Anna Carlmark-Malkoch is thanked for being such a nice and positive person to work with.

I would like to thank all the seniors at the department of Fiber and Polymer Technology for making it such a great research place. A special thank goes to Professor Lars Berglund for giving me nice recommendations and for all our interesting discussions. I am also grateful to all the administrative personal and particularly Inger, Inga, Mia, Vera and Barbara for all the help during these years. I also want to acknowledge the technical staff, Karin and Kjell for solving computer-related issues, Bosse for always fixing lab-related problems, and Ulla for helping me with the printing of this thesis.

The Swedish research council (Vetenskapsrådet) and Wilhelm Beckers Jubileumsfond are greatly acknowledged for financial support. KTH travel-grants are thanked for financial contributions to conferences.

I would like to thank all my co-authors for nice and fruitful collaborations. In particular, I want to express my gratitude to Professor Amir Fahmi for accepting me in his lab in Nottingham. Nicolas is greatly acknowledged for all his help during my stay in England: I would not have made it without you. I am grateful to Professor Bengt Fadeel and Associate Professor Andreas Nyström for their help and guidance in the toxicity project. A special "thank you" goes to Neus for always being so positive and a great friend: it was a pleasure to work with you. Finally I would like to thank Professor Hjalmar Brismar for his help with fluorescence microscopy and for always finding time for me when I needed it.

All the present and formers members of Ytgruppen are sincerely acknowledged for making it such a great place to work at. It has been a real pleasure to work with all of you during these years and it felt like home at the division. I really appreciated to work with so many friends around. Thank you Jan, Susanne, Emelie, Martin, Christian, Mauro, Linn, Yvonne, Carl, Markus, Assya, Kim, Kristina, Linda, Susana, Sam, Oliver, Carmen, Hui,

Emma L., Sara O., Viktor, David, Andrea, Vilhelm, Daniel, Sara K., Petra, Alireza, Ting, Pontus, Maribel, Stacy, Camilla, Robert, Niklas, Hanna Lö., Lina, Bella, Hanna L., Axel, Sandra, Ynhi and all the others that have spent some time with us. A special "thank you" goes to my wonderful roommates Yvonne, Emelie, Carl, Christian, Susana, Sam, Camilla and Niklas for all our nice discussions, work-related or not. Yvonne, it was so nice and fun to work next to you in the lab. You taught me a lot, I really enjoyed it. Oliver, you were a great student. Thank you for trying to teach me to delegate work and for keeping me away from the lab when I was supposed to write. Thank you Pontus for all your help in the lab and for always answering all my questions, I appreciated it a lot. Jan, thank you for nice collaborations and for always trusting me in the lab. Your constant happiness makes it so easy to work with you. Maribel, I want to thank you for being so kind and helpful when I started in the lab. Thank you Ynhi for being such a nice and happy person. I really appreciated working with you. Thank you to all of you who have helped me with the writing of this thesis and particularly Linn and Oliver who corrected my "sammanfattning" in swenglish. I also would like to thank all the present and former members of Polymer Factory, Jonas, Shams, Mason, Pelle, Kristin, Bella, Robert, Suba, Cindy and all the others. You were really great colleagues and friends and it was a pleasure to share the lab with you. All the other members of Fiber and Polymer are also greatly acknowledged. It was such a nice place to work at with so many helpful students all around. A special "thank you" goes to Michaela for always being available when I needed help with the SEM.

I also would like to thank all my friends, at KTH and outside, for their support during these years and for all the nice moments we have spent together.

Je souhaite aussi remercier toute ma famille. Papa, Maman, vous m'avez toujours fais confiance et avez toujours cru en moi et cela m'a beaucoup aidé. Même si vous auriez peut-être préféré que je reste en France, vous m'avez soutenu quand j'ai voulu partir en Suède et avez accepté de ne me voir que quelques semaines par an. Je sais que même si vous n'êtes pas à Stockholm, je peux toujours compter sur vous. Aurore, Pierre, Martial, Carine, Clémence, Agathe et Mathilde, merci pour votre soutien et votre disponibilité à chaque fois que je rentre en France. Merci à tous pour tous les bons moments que nous avons partagés.

Jag vill också tacka familjen Syren för deras stöd under hela min doktorandtid. Jag vet att ni ser mig som en del av familjen och det betyder mycket för mig.

Till sist vill jag tacka min underbar Per-Olof för alt din kärlek och ditt stöd. Dt är så skönt att veta att du finns och att du alltid ställer upp när jag behöver dig. Stor tack.

8. REFERENCES

1. G. Peatterson, *A Prehistory of Polymer Science*, Springer, 2012.
2. J. M. J. Frechet and D. A. Tomalia, *Dendrimers and other dendritic polymers*, Wiley, 2001.
3. P. Antoni, Y. Hed, A. Nordberg, D. Nystrom, H. von Holst, A. Hult and M. Malkoch, *Angew Chem Int Edit*, 2009, **48**, 2126-2130.
4. A. Carlmark, C. J. Hawker, A. Hult and M. Malkoch, *Chemical Society Reviews*, 2009, **38**, 352-362.
5. E. Buhleier, W. Wehner and F. Vogtle, *Synthesis-Stuttgart*, 1978, 155-158.
6. D. A. Tomalia, H. Baker, J. Dewald, M. Hall, G. Kallos, S. Martin, J. Roeck, J. Ryder and P. Smith, *Polym J*, 1985, **17**, 117-132.
7. G. R. Newkome, Z. Q. Yao, G. R. Baker and V. K. Gupta, *J Org Chem*, 1985, **50**, 2003-2004.
8. C. J. Hawker and J. M. J. Frechet, *Journal of the American Chemical Society*, 1990, **112**, 7638-7647.
9. M. V. Walter and M. Malkoch, *Chemical Society Reviews*, 2012, **41**, 4593-4609.
10. S. M. Grayson and J. M. J. Frechet, *Chemical Reviews*, 2001, **101**, 3819-3867.
11. Dendritech Inc., www.dendritech.com.
12. Dendritic Nanotechnologies, Inc., www.dnanotech.com.
13. Polymer Factory Sweden AB, www.polymerfactory.com.
14. SyMO-Chem, www.symo-chem.nl.
15. I. Gitsov and J. M. J. Frechet, *Macromolecules*, 1993, **26**, 6536-6546.
16. I. Gitsov, *J. Polym. Sci., Part A: Polym. Chem.*, 2008, **46**, 5295-5314.
17. C. M. Dong and G. Liu, *Polym. Chem.*, 2013, **4**, 46-52.
18. D. Astruc, E. Boisselier and C. Ornelas, *Chemical Reviews*, 2010, **110**, 1857-1959.
19. Y. Y. Cheng, L. B. Zhao, Y. W. Li and T. W. Xu, *Chemical Society Reviews*, 2011, **40**, 2673-2703.
20. B. K. Nanjwade, H. M. Bechra, G. K. Derkar, F. V. Manvi and V. K. Nanjwade, *Eur. J. Pharm. Sci.*, 2009, **38**, 185-196.
21. A. Patidar and D. S. Thakur, *Int. J. Pharm. Sci. Nanotechnol.*, 2011, **4**, 1383-1389, 1387 pp.
22. A. Felczak, N. Wronska, A. Janaszewska, B. Klajnert, M. Bryszewska, D. Appelhans, B. Voit, S. Rozalska and K. Lisowska, *New J. Chem.*, 2012, **36**, 2215-2222.
23. K. Jain, P. Kesharwani, U. Gupta and N. K. Jain, *International Journal of Pharmaceutics*, 2010, **394**, 122-142.
24. O. L. P. De Jesus, H. R. Ihre, L. Gagne, J. M. J. Frechet and F. C. Szoka, *Bioconjugate Chemistry*, 2002, **13**, 453-461.
25. E. R. Gillies, E. Dy, J. M. J. Frechet and F. C. Szoka, *Molecular Pharmaceutics*, 2005, **2**, 129-138.
26. H. C. Kolb, M. G. Finn and K. B. Sharpless, *Angewandte Chemie-International Edition*, 2001, **40**, 2004-2021.

27. B. J. Adzima and C. N. Bowman, *Aiche J.*, 2012, **58**, 2952-2965.
28. J. L. Hou, X. F. Liu, J. Shen, G. L. Zhao and P. G. Wang, *Expert Opinion on Drug Discovery*, 2012, **7**, 489-501.
29. S. Hvilsted, *Polymer International*, 2012, **61**, 485-494.
30. G. K. Such, A. P. R. Johnston, K. Liang and F. Caruso, *Prog. Polym. Sci.*, 2012, **37**, 985-1003.
31. K. Kempe, A. Krieg, C. R. Becer and U. S. Schubert, *Chemical Society Reviews*, 2012, **41**, 176-191.
32. E. Lallana, F. Fernandez-Trillo, A. Sousa-Herves, R. Riguera and E. Fernandez-Megia, *Pharmaceutical Research*, 2012, **29**, 902-921.
33. C. Barner-Kowollik, F. E. Du Prez, P. Espeel, C. J. Hawker, T. Junkers, H. Schlaad and W. Van Camp, *Angewandte Chemie International Edition*, 2011, **50**, 60-62.
34. A. Michael, *Journal für Praktische Chemie*, 1893, **48**, 94-95.
35. R. Huisgen, *Angew. Chem.*, 1963, **75**, 604-637.
36. V. V. Rostovtsev, L. G. Green, V. V. Fokin and K. B. Sharpless, *Angew Chem Int Edit*, 2002, **41**, 2596-+.
37. C. W. Tornoe, C. Christensen and M. Meldal, *J Org Chem*, 2002, **67**, 3057-3064.
38. L. Y. Liang and D. Astruc, *Coord. Chem. Rev.*, 2011, **255**, 2933-2945.
39. V. O. Rodionov, S. I. Presolski, D. D. Diaz, V. V. Fokin and M. G. Finn, *Journal of the American Chemical Society*, 2007, **129**, 12705-12712.
40. J. C. Jewett and C. R. Bertozzi, *Chemical Society Reviews*, 2010, **39**, 1272-1279.
41. C. Ornelas, J. Broichhagen and M. Weck, *Journal of the American Chemical Society*, 2010, **132**, 3923-3931.
42. V. D. Bock, H. Hiemstra and J. H. van Maarseveen, *Eur. J. Org. Chem.*, 2006, 51-68.
43. D. Astruc, L. Y. Liang, A. Rapakousiou and J. Ruiz, *Accounts of Chemical Research*, 2012, **45**, 630-640.
44. J. E. Hein and V. V. Fokin, *Chemical Society Reviews*, 2010, **39**, 1302-1315.
45. J. A. Johnson, M. G. Finn, J. T. Koberstein and N. J. Turro, *Macromol. Rapid Commun.*, 2008, **29**, 1052-1072.
46. T. Posner, *Ber. Dtsch. chem. Ges.*, 1905, **38**, 646-657.
47. J. V. Braun and R. Murjahn, *Ber. Dtsch. Chem. Ges. B*, 1926, **59B**, 1202-1209.
48. C. E. Hoyle and C. N. Bowman, *Angew Chem Int Edit*, 2010, **49**, 1540-1573.
49. C. E. Hoyle, T. Y. Lee and T. Roper, *Journal of Polymer Science Part a-Polymer Chemistry*, 2004, **42**, 5301-5338.
50. C. E. Hoyle, A. B. Lowe and C. N. Bowman, *Chemical Society Reviews*, 2010, **39**, 1355-1387.
51. K. Griesbaum, *Angew. Chem., Int. Ed. Engl.*, 1970, **9**, 273-287.
52. A. Dondoni, *Angew Chem Int Edit*, 2008, **47**, 8995-8997.
53. A. Dondoni and A. Marra, *Chemical Society Reviews*, 2012, **41**, 573-586.
54. S. Penczek, M. Cypryk, A. Duda, P. Kubisa and S. Slomkowski, *Prog. Polym. Sci.*, 2007, **32**, 247-282.
55. D. A. Shipp, *Polymer Reviews*, 2011, **51**, 99-103.
56. D. Bertin, D. Gigmes, S. R. A. Marque and P. Tordo, *Chem. Soc. Rev.*, 2011, **40**, 2189-2198.
57. E. Rizzardo and D. H. Solomon, *Aust. J. Chem.*, 2012, **65**, 945-969.
58. M. K. Georges, R. P. N. Veregin, P. M. Kazmaier and G. K. Hamer, *Macromolecules*, 1993, **26**, 2987-2988.
59. K. Matyjaszewski, *Isr. J. Chem.*, 2012, **52**, 206-220.
60. J. Chiefari, Y. K. Chong, F. Ercole, J. Krstina, J. Jeffery, T. P. T. Le, R. T. A. Mayadunne, G. F. Meijs, C. L. Moad, G. Moad, E. Rizzardo and S. H. Thang, *Macromolecules*, 1998, **31**, 5559-5562.

61. G. Moad, E. Rizzardo and S. H. Thang, *Aust. J. Chem.*, 2012, **65**, 985-1076.
62. A. C. Albertsson and I. K. Varma, *Biomacromolecules*, 2003, **4**, 1466-1486.
63. H. R. Kricheldorf, I. Kreisersaunders and C. Boettcher, *Polymer*, 1995, **36**, 1253-1259.
64. N. E. Kamber, W. Jeong, R. M. Waymouth, R. C. Pratt, B. G. G. Lohmeijer and J. L. Hedrick, *Chem. Rev. (Washington, DC, U. S.)*, 2007, **107**, 5813-5840.
65. H. Y. Tian, Z. H. Tang, X. L. Zhuang, X. S. Chen and X. B. Jing, *Prog. Polym. Sci.*, 2012, **37**, 237-280.
66. Y. Wang and S. M. Grayson, *Adv. Drug Deliv. Rev.*, 2012, **64**, 852-865.
67. M. Kato, M. Kamigaito, M. Sawamoto and T. Higashimura, *Macromolecules*, 1995, **28**, 1721-1723.
68. J. S. Wang and K. Matyjaszewski, *Journal of the American Chemical Society*, 1995, **117**, 5614-5615.
69. V. Percec and B. Barboiu, *Macromolecules*, 1995, **28**, 7970-7972.
70. M. S. Kharasch, E. V. Jensen and W. H. Urry, *Science*, 1945, **102**, 128.
71. K. Matyjaszewski, *Macromolecules (Washington, DC, U. S.)*, 2012, **45**, 4015-4039.
72. D. J. Siegwart, J. K. Oh and K. Matyjaszewski, *Prog. Polym. Sci.*, 2012, **37**, 18-37.
73. M. S. Park, Y. Lee and J. K. Kim, *Chem. Mat.*, 2005, **17**, 3944-3950.
74. V. Torres-Costa and R. J. Martin-Palma, *Journal of Materials Science*, 2010, **45**, 2823-2838.
75. M. A. Chari, D. Shobha, E. R. Kenawy, S. S. Al-Deyab, B. V. S. Reddy and A. Vinu, *Tetrahedron Lett.*, 2010, **51**, 5195-5199.
76. P. Pilla, A. Cusano, A. Cutolo, M. Giordano, G. Mensitieri, P. Rizzo, L. Sanguigno, V. Venditto and G. Guerra, *Sensors*, 2009, **9**, 9816-9857.
77. G. Korotcenkov and B. K. Cho, *Critical Reviews in Solid State and Materials Sciences*, 2010, **35**, 1-37.
78. B. J. Melde and B. J. Johnson, *Analytical and Bioanalytical Chemistry*, 2010, **398**, 1565-1573.
79. S. P. Adiga, C. M. Jin, L. A. Curtiss, N. A. Monteiro-Riviere and R. J. Narayan, *Wiley Interdiscip. Rev.-Nanomed. Nanobiotechnol.*, 2009, **1**, 568-581.
80. D. A. Bernards and T. A. Desai, *Soft Matter*, 2010, **6**, 1621-1631.
81. D. Nystrom, E. Malmstrom, A. Hult, I. Blakey, C. Boyer, T. P. Davis and M. R. Whittaker, *Langmuir*, 2010, **26**, 12748-12754.
82. G. Widawski, M. Rawiso and B. Francois, *Nature*, 1994, **369**, 387-389.
83. U. H. F. Bunz, *Advanced Materials*, 2006, **18**, 973-989.
84. H. Sun and L. X. Wu, *Prog. Chem.*, 2010, **22**, 1784-1798.
85. L. Rayleigh, *Nature*, 1911, 416-417.
86. L. Rayleigh, *Nature*, 1912, 436-438.
87. D. Fritter, C. M. Knobler and D. A. Beysens, *Phys. Rev. A*, 1991, **43**, 2858-2869.
88. A. Steyer, P. Guenoun, D. Beysens, D. Fritter and C. M. Knobler, *Europhys. Lett.*, 1990, **12**, 211-215.
89. J. L. Viovy, D. Beysens and C. M. Knobler, *Phys. Rev. A: Gen. Phys.*, 1988, **37**, 4965-4970.
90. M. Hernandez-Guerrero, T. P. Davis, C. Barner-Kowollik and M. H. Stenzel, *Eur. Polym. J.*, 2005, **41**, 2264-2277.
91. J. Li, J. Peng, W. H. Huang, Y. Wu, J. Fu, Y. Cong, L. J. Xue and Y. C. Han, *Langmuir*, 2005, **21**, 2017-2021.
92. M. Srinivasarao, D. Collings, A. Philips and S. Patel, *Science*, 2001, **292**, 79-83.
93. P. Escale, L. Rubatat, L. Billon and M. Save, *Eur. Polym. J.*, 2012, **48**, 1001-1025.
94. M. Hernandez-Guerrero and M. H. Stenzel, *Polym. Chem.*, 2012, **3**, 563-577.
95. M. H. Stenzel-Rosenbaum, T. P. Davis, A. G. Fane and V. Chen, *Angew. Chem., Int. Ed.*, 2001, **40**, 3428-3432.

96. L. Li, Y. W. Zhong, J. Li, C. K. Chen, A. J. Zhang, J. Xu and Z. Ma, *Journal of Materials Chemistry*, 2009, **19**, 7222-7227.
97. B. H. Zhao, J. Zhang, X. D. Wang and C. X. Li, *Journal of Materials Chemistry*, 2006, **16**, 509-513.
98. W. Y. Dong, Y. F. Zhou, D. Y. Yan, Y. Y. Mai, L. He and C. Y. Jin, *Langmuir*, 2009, **25**, 173-178.
99. Y. F. Zhou and D. Y. Yan, *Chemical Communications*, 2009, 1172-1188.
100. B. Francois, O. Pitois and J. Francois, *Advanced Materials*, 1995, **7**, 1041-&.
101. B. Francois, G. Widawski, M. Rawiso and B. Cesar, *Synthetic Metals*, 1995, **69**, 463-466.
102. C. X. Cheng, Y. Tian, Y. Q. Shi, R. P. Tang and F. Xi, *Langmuir*, 2005, **21**, 6576-6581.
103. K. H. Wong, T. P. Davis, C. Bamer-Kowollik and M. H. Stenzel, *Polymer*, 2007, **48**, 4950-4965.
104. M. H. Stenzel, T. P. Davis and A. G. Fane, *Journal of Materials Chemistry*, 2003, **13**, 2090-2097.
105. B. Francois, Y. Ederle and C. Mathis, *Synthetic Metals*, 1999, **103**, 2362-2363.
106. J. Peng, Y. C. Han, Y. M. Yang and B. Y. Li, *Polymer*, 2004, **45**, 447-452.
107. Y. Fukuhira, H. Yabu, K. Ijiro and M. Shimomura, *Soft Matter*, 2009, **5**, 2037-2041.
108. M. H. Stenzel-Rosenbaum, T. P. Davis, A. G. Fane and V. Chen, *Angew Chem Int Edit*, 2001, **40**, 3428-+.
109. L. A. Connal, R. Vestberg, C. J. Hawker and G. G. Qiao, *Adv. Funct. Mater.*, 2008, **18**, 3706-3714.
110. O. Pitois and B. Francois, *Colloid and Polymer Science*, 1999, **277**, 574-578.
111. N. Maruyama, T. Koito, J. Nishida, T. Sawadaishi, X. Cieren, K. Ijiro, O. Karthaus and M. Shimomura, *Thin Solid Films*, 1998, **327**, 854-856.
112. A. Nygard, T. P. Davis, C. Barner-Kowollik and M. H. Stenzel, *Australian Journal of Chemistry*, 2005, **58**, 595-599.
113. S. R. S. Ting, E. H. Min, P. Escale, M. Save, L. Billon and M. H. Stenzel, *Macromolecules*, 2009, **42**, 9422-9434.
114. F. Galeotti, V. Calabrese, M. Cavazzini, S. Quici, C. Poleunis, S. Yunus and A. Bolognesi, *Chem. Mat.*, 2010, **22**, 2764-2769.
115. A. Munoz-Bonilla, E. Ibarboure, V. Bordege, M. Fernandez-Garcia and J. Rodriguez-Hernandez, *Langmuir*, 2010, **26**, 8552-8558.
116. H. Ihre, d. J. O. L. Padilla and J. M. J. Frechet, *J. Am. Chem. Soc.*, 2001, **123**, 5908-5917.
117. P. Antoni, D. Nystroem, C. J. Hawker, A. Hult and M. Malkoch, *Chem. Commun. (Cambridge, U. K.)*, 2007, 2249-2251.
118. R.-V. Ostaci, D. Damiron, S. Capponi, G. Vignaud, L. Leger, Y. Grohens and E. Drockenmuller, *Langmuir*, 2008, **24**, 2732-2739.
119. M. C. Parrott, S. R. Benhabbour, C. Saab, J. A. Lemon, S. Parker, J. F. Valliant and A. Adronov, *J. Am. Chem. Soc.*, 2009, **131**, 2906-2916.
120. C. C. Lee, J. A. MacKay, J. M. J. Frechet and F. C. Szoka, *Nat. Biotechnol.*, 2005, **23**, 1517-1526.
121. Y. Tian, C. Dai, H. Y. Ding, Q. Z. Jiao, L. H. Wang, Y. Q. Shi and B. Q. Liu, *Polymer International*, 2007, **56**, 834-839.
122. P. Wu, M. Malkoch, J. N. Hunt, R. Vestberg, E. Kaltgrad, M. G. Finn, V. V. Fokin, K. B. Sharpless and C. J. Hawker, *Chem. Commun. (Cambridge, U. K.)*, 2005, 5775-5777.
123. B. Erdogan, L. Song, J. N. Wilson, J. O. Park, M. Srinivasarao and U. H. F. Bunz, *J. Am. Chem. Soc.*, 2004, **126**, 3678-3679.